STRUCTURED CATALYSTS FOR LOW TEMPERATURE COS HYDROLYSIS PROCESS INTENSIFICATION

Simona Renda

UNIVERSITY OF SALERNO

DEPARTMENT OF INDUSTRIAL ENGINEERING

Ph.D. Course in Industrial Engineering
Curriculum in Chemical Engineering - XXXV Cycle

STRUCTURED CATALYSTS FOR LOW TEMPERATURE COS HYDROLYSIS PROCESS INTENSIFICATION

Supervisor
Prof. Vincenzo Palma

Ph.D. student
Simona Renda

Scientific Referees
Emma Palo, Ph.D.
Ing. Michele Colozzi

Ph.D. Course Coordinator
Prof. Francesco Donsì

«Tout commence par une interruption.»

Acknowledgments

Mettono ansia, le cose che finiscono. Ed è per questo che l'intestazione di questa tesi è un monito, e mi aiuta a ricordare che quello che veramente conta, più del traguardo, è il trascorso.

Nel mio, di trascorso, ho avuto la gioia di avere al mio fianco persone eccezionali, che mi sembra più che doveroso ringraziare, nonostante tirare le somme dopo quattro anni in cui il laboratorio T1 è stata la mia seconda casa (quasi prima, scusa mamma) è un po' difficile.

Il primo, fondamentale, ringraziamento, va al prof. Palma. La sua passione rispetto a quello che fa è sempre stata di ispirazione e di stimolo, e se c'è questa terza tesi a ribadire il concetto è sicuramente merito suo. Grazie per essere stato una presenza costante, per l'aiuto a risolvere i problemi, per il guizzo di genialità davanti a risultati che sembrano insensati che solo "il prof." può avere. Ho cercato di assorbire quanto più possibile, e tutto ciò farà per sempre parte del mio bagaglio. Grazie, infine, per la fiducia che mi ha dato in questi anni, per avermi dato voce nelle discussioni "da grandi", per aver sempre dato alla mia opinione un peso. Nel mio percorso, è sempre stato molto importante.

Grazie agli Ing. Emma Palo e Michele Colozzi, senza i quali questo progetto di dottorato non sarebbe esistito. Mi avete permesso di infilarmi in una materia complessa, che ha posto più sfide e difficoltà di quante me ne sarei potuta aspettare, ma che ha portato enormi soddisfazioni. Grazie sempre, per la vostra disponibilità e gli incoraggiamenti, per i consigli e gli spunti di discussione.

Grazie ai colleghi tutti, presenti e passati. Questo lavoro, si sa, dà la possibilità di conoscere tante persone, e nello stesso tempo detemina talvolta che la strada percorsa insieme sia breve. Non importa quanto tempo possiamo aver condiviso, siete stati tutti importanti. Grazie a Concetta, per essere stata sempre un punto di riferimento costante, e per essere stata, soprattutto in questo ultimo anno, amica e confidente. Grazie ad Olga, per essere stata di sollievo nelle lunghe giornate, e compagna di avventure nei viaggi di lavoro. Avrei voluto che ce ne fossero di più. Grazie ad Eugenio, che ha condiviso con me questo percorso. Avere al mio fianco una persona con più esperienza ha sicuramente facilitato tante cose. Grazie a tutti i colleghi nuovi, Emilia, Liberato, Nicola e Laura, siete stati una ventata di aria fresca quando più ce n'era bisogno. Spero di avervi incoraggiato a sufficienza, in bocca al lupo per ogni cosa. Un grazie di cuore sicuramente va a Giusy. In questi anni sei stata d'esempio, coi tuoi sorrisi anche quando stanca, per la tenacia e l'intraprendenza con cui hai affrontato qualsiasi sfida. Grazie a Vincenzo, per la simpatia e per tutte le perle di saggezza, ma prima di ogni altra cosa per

l'enorme disponibilità che dimostri ogni giorno. Sono sicura che sia un dono non da poco. Grazie ad Antonella, per avermi aiutato a tenere a mente scadenze, corsi, documenti da compilare, per aver condiviso i momenti di ansia sotto sotto agli "eventi" più importanti.

Grazie a Marco, per avermi guidata nelle asperità di questo mondo nei momenti in cui ce n'era più bisogno, per la sincerità che mi hai promesso dal primo giorno, e per le opinioni che hanno saputo indirizzarmi.

Grazie a Daniela, per essermi stata accanto nella fase iniziale di questo percorso. Hai reso semplici cose che mi hanno messo in difficoltà; senza la tua esperienza, sarebbe di certo stato tutto molto più complicato.

Infine, grazie, grazie, grazie ad Antonio. Se non ci fossimo incontrati il primo giorno che ho messo piede in laboratorio, nell'ormai un po' lontano 2015, non so se sarei mai arrivata a scegliere questo percorso. Ti devo tanto. Sei stato una parte fondamentale nella mia formazione, e guardarti all'opera tante volte mi hai fatto capire cosa volevo essere. E nonostante non ce l'abbiamo fatta a condividere il T1 da colleghi nemmeno per un giorno (non penso di avertelo ancora perdonato), hai continuato ad essere un punto di riferimento costante. Le persone di spessore lasciano sempre traccia del loro passaggio.

Grazie a tutti i miei tesisti: Mariateresa, Luca, Ferdinando, Daniela, Salvatore, Adeliapia, Gianmarco, Riccardo, Maria. Un grazie un po' più speciale a Roberta e a Nicole, il cui lavoro è contenuto in questa tesi: grazie per la cura, l'attenzione e l'interesse che avete dimostrato e con cui avete portato avanti le vostre attività, poter riporre in voi la mia fiducia mi ha spesso alleggerito. Mariateresa, la tua dolcezza ha reso il compito arduo e pieno di responsabilità di una correlatrice alla sua prima volta un po' più semplice. Nicole, oltre che "la prima e l'ultima tesista del mio dottorato" sei stata anche amica e confidente, mi sento fortunata ad averti incontrata.

Grazie infinite ad Antonio e Giacinto. Non posso scindere questo ringraziamento, perdonatemi. Il vostro arrivo nella mia vita è stato inaspettato, ma una rivelazione. Grazie per i pomeriggi in laboratorio, per le serate in cui non sono riuscita a respirare dal ridere, ma grazie soprattutto per aver reso il mio terzo anno una gita in montagna, più che una salita. Lavorare con voi mi mancherà.

Grazie a Mariangela, per le serate, le chiacchiere, gli sfoghi. Grazie per la tua gentilezza infinita e anche solo semplicemente per esserci stata, per essere stato il viso familiare verso cui girarmi in questi corridoi.

Muchisimas gracias a mi querido amigo Pedro. Siempre me recuerdaré de tu tiempo aquí, de las cervezas juntos después del trabajo, de "you italians should eat less and drink more!". Ha sido una experiencia tenerte aquí. Espero que nos veremos quanto antes.

Grazie agli amici di sempre: a Giovanni e Mario per essere da anni un punto fisso e di ritrovo, a Marta per avermi tanto sostenuto e accompagnato mentre muovevo i miei primi passi in mezzo a tutto questo, a Marco perché il

tuo sorriso e le tue parole sono sempre state di conforto nelle serate dei giorni che sembravano non finire mai, in cui la stanchezza si faceva sentire.

Un grazie infinito alla mia famiglia. Più che nelle scelte universitarie, adesso sentirmi sostenuta nelle scelte lavorative e di vita è stato fondamentale. Dite sempre che io sono imprevedibile, ma forse è solo che mi sento di poter scegliere a cuor leggero, sapendo che vi avrò al mio fianco.

Mamma e papà, grazie per essere sempre stati di esempio e punti di riferimento, per aver condiviso con me le mie soddisfazioni come se fossero le vostre.

Martina e Francesco, avere dei fratelli non è sempre la cosa più facile del mondo, ma è senz'altro la compagnia più solida che si può avere nella vita. Grazie per non avermene mai fatto dubitare, nemmeno per un secondo.

Grazie a zia Annalisa, per essere stata sempre presente anche se a distanza, e a zia Sirella per essere stata sempre la mia confidente.

Grazie ai miei nonni, che per me ci sono tutti sempre. Passerò la vita a volervi rendere orgogliosi, e sono sicura che porterà a fare sempre cose buone.

Grazie a Paola ed Olimpia, ad Antonio, Matteo e Piero, per aver dimostrato che si può essere famiglia in tanti modi, e non ce n'è uno migliore di un altro. Grazie ad Olimpia in particolare per essere stata una seconda sorella, per l'appoggio che mi hai dato durante questo percorso, ma soprattutto per quello che mi hai dato nella vita. Non so cosa farei senza quei vocali da 10 minuti!

Infine, ci tengo a ringraziare in particolare una persona, la cui presenza nella mia vita privata si è intrecciata con quella professionale, mettendo tutto in discussione. Christian, sei prima stato d'esempio, di conforto, di confronto. E poi un rifugio, un posto a cui tornare, una meta a cui tendere; una condivisione di scelte, esperienze, soddisfazioni. Sappiamo entrambi che sarebbe bastato tanto così a non incontrarsi mai. Grazie per aver creduto con me che fosse possibile. *Son qui perché se mi arrendo questa volta, mi arrenderò per tutta la vita.*

Publication List

Research paper

[†]***Renda S***., Ricca A., Palma V. (2023). Insights in the application of highly conductive structured catalysts to CO_2 methanation: Computational study. *International Journal of Hydrogen Energy*, *in press*. 10.1016/j.ijhydene.2023.01.338

Renda S., Cortese M., Iervolino G., Palma V., Martino M., Meloni E. (2022). Electrically driven SiC-based structured catalysts for intensified reforming processes. *Catalysis Today*, 318, 31. 10.1016/j.cattod.2020.11.020

[†]***Renda S***., Di Stasi C., Manyà J.J., Palma V. (2021). Biochar as support in catalytic CO_2 methanation: Enhancing effect of CeO_2 addition. *Journal of CO_2 Utilization*, 53, 101740. 10.1016/j.jcou.2021.101740

[†]***Renda S***., Ricca A., Palma V. (2021). Study of the effect of noble metal promotion in Ni-based catalyst for the Sabatier reaction. *International Journal of Hydrogen Energy*, 46 (22), 12117. 10.1016/j.ijhydene.2020.05.093

[†]***Renda S***., Tommasino F., Palma V., Miccio M., Okasha F. (2021). Design and setup activities for the development of methane autothermal reforming in a Jet Fountain Fluidized Bed Reactor. *Chemical Engineering Transactions*, 86, 1435. 10.3303/CET2186240

[†]***Renda S***., Ricca A., Palma V. (2020). Precursor salts influence in Ruthenium catalysts for CO_2 hydrogenation to methane. *Applied Energy*, 279, 115767. 10.1016/j.apenergy.2020.115767

Di Stasi C., ***Renda S***., Greco G., González B., Palma V., Manyà J.J. (2021). Wheat-straw-derived activated biochar as a renewable support of Ni-CeO_2 catalysts for CO_2 methanation. *Sustainability*, 13(16), 8939. 10.3390/su13168939

Pio G., ***Renda S***., Palma V., Salzano E. (2020). Safety parameters for oxygen-enriched flames. *Journal of Loss Prevention in the Process Industries*, 65, 104151. 10.1016/j.jlp.2020.104151

Meloni E., Martino M., ***Renda S.***, Muccioli O., Pullumbi P., Brandani F., Palma V. (2022). Development of Innovative Structured Catalysts for the

---

[†] *Corresponding author*

Catalytic Decomposition of N_2O at Low Temperatures. *Catalysts*, 12, 1405. 10.3390/catal12111405

Palma V., Meloni E., ***Renda S.***, Martino M. (2020). Catalysts for Methane Steam Reforming Reaction: Evaluation of CeO_2 Addition to Alumina-Based Washcoat Slurry Formulation. *C – Journal of Carbon Research*, 6, 52. 10.3390/c6030052

Muccioli O., Meloni E., Martino M., ***Renda S.***, Pullumbi P., Brandani F., Palma V. (2022). 19. Decomposition of N2O over NixCo3-xO4 Catalyst. *Chem. Eng. Trans.*, 96, 283. 10.3303/CET2296048

Di Stasi C., Cortese M., Greco G., ***Renda S.***, González B., Palma V., Manyà J.J. (2021). Optimization of the operating conditions for steam reforming of slow pyrolysis oil over an activated biochar-supported Ni-Co catalyst. *International Journal of Hydrogen Energy*, 46 (53), 26915. 10.1016/j.ijhydene.2021.05.193

Palma V., Goodall R., Thompson A., Ruocco C., ***Renda S.***, Leach R., Martino M. (2021). Ceria-coated Replicated Aluminium Sponges as Catalysts for the CO-Water Gas Shift Process. *International Journal of Hydrogen Energy*, 46(22), 12158. 10.1016/j.ijhydene.2020.04.065

Review paper

[†]***Renda S.***, Barba D., Palma V. (2022). Recent solutions for efficient carbonyl sulfide hydrolysis: a review. *I&EC Research*, 61, 5685. 10.1021/acs.iecr.2c00649

Palma V., Cortese M., ***Renda S.***, Ruocco C., (2020). A Review about the Recent Advances in Selected NonThermal Plasma Assisted Solid–Gas Phase Chemical Processes. Nanomaterials, 10, 1596. 10.3390/nano10081596

Meloni E., Iervolino G., Ruocco C., ***Renda S.***, Festa G., Martino M., Palma V. (2022). Electrified Hydrogen Production from Methane for PEM Fuel Cells Feeding: A Review. *Energies*, 15, 3588. 10.3390/en15103588

Palma V., Ruocco C., Cortese M., ***Renda S.***, Meloni E., Festa G., Martino M. (2020). Platinum Based Catalysts in the Water Gas Shift Reaction: Recent Advances. *Metals*, 10, 866. 10.3390/met10070866

Meloni E., Martino M., Iervolino G., Ruocco C., ***Renda S.***, Festa G., Palma V. (2022) The route from green H_2 production through bioethanol

---

[†] *Corresponding author*

reforming to CO_2 catalytic conversion: a review. *Energies*, 15(7), 2383. 10.3390/en15072383

Palma V., Barba D., Cortese M., Martino M., ***Renda S***., Meloni E. (2020). Microwaves and Heterogeneous Catalysis: A Review on Selected Catalytic Processes. *Catalysts*, 10, 246. 10.3390/catal10020246

Under-review paper

[†]***Renda S***., Palo E., Colozzi M., Palma V. Competitive adsorption phenomena influence on COS hydrolysis kinetics: a Langmuir-Hinshelwood comprehensive expression. *Under review in Chem. Eng. J.*

Meloni E., Cafiero L., ***Renda S.***, Martino M., Pierro M., Palma V. (2023). Ru- and Rh-based Catalysts for CO_2 Methanation Assisted by Non-Thermal Plasma. *Under review in Catalysts*

De Liso B., Palma V., Pio G., ***Renda S***., Salzano E. (2023). Extremely Low Temperatures for the Synthesis of Ethylene Oxide. *Under review in I&EC Research*[3]

Book chapters

Palma V., Barba D., Meloni E., ***Renda S.***, Ruocco C. Ultra-compact Bio-fuels catalytic reforming processes for distributed renewable hydrogen production. *Studies in Surface Science and Catalysis* **2019**, 179, 317. 10.1016/B978-0-444-64337-7.00017-3

[†] *Corresponding author*

Table of Contents

Index of Figures

Index of Tables

Abstract

This PhD project has been focused on the process intensification of COS hydrolysis, a reaction which stays in the framework of acid gas cleaning and that nowadays drives increasing attention by the petrochemical industry.

The rising economy, the increase of the demand for energy and fuels, and the consequent increase in exploitation of natural resources, have originated growing environmental concerns. Among these, the attention to sulfur contents in fossil fuels has recently received a deep focus. It is well known that most of the sulfur-derived compounds are toxic for human health, and their presence in the atmosphere could be related to the acid rains. The topic plays a key role in modern energy scenario, and it has become an incentive in improving the existent desulfurization technologies. The sulfur compounds are conventionally distinguished in organic and inorganic. Carbonyl sulfide is an organic sulfur compound, whose emissions in the atmosphere have anthropogenic roots in desulfurization processes.

In this PhD project, the problematic of carbonyl sulfide abatement has been addressed, and the existent removal technologies have been discussed, highlighting the limitations of the nowadays processes. The core of this three-years project has been the proposal and investigation of some innovative solutions to overcome the most relevant issues. Considering the present state-of-the-art, the research could provide a noteworthy improvement to the existent technologies. Hence, the shared opinion of the scientific committee of this thesis was to address the aims in two main directions: the development of a catalyst to efficiently conduct this reaction, and the development of a process technology to provide a potentially competitive industrial solution.

Once reached the milestones of finding a low-temperature active formulation, enumerating the criticalities of the process, it was offered a solution to enhance the reaction performances while demonstrating the potentiality of a coupled configuration. An open architecture configuration constituted by a closed box in with the hydrolysis reactor and the absorber were able to work at the same temperature condition was tested, assessing the feasibility of the process integration.

Then, the process intensification of COS hydrolysis was addressed following two different approaches.

On one hand, the optimized formulation was transferred on a structured catalyst, and the advantages that this solution provided to the process were highlighted, demonstrating how the micrometric layer of active phase deposited on the carrier reduces the diffusion limitation typical of this system. Then, the activity of the structured catalyst was investigated in a remarkably wide range of operating conditions, considered the extreme variability of a

real tail gas composition. Once the complete overview of the behavior of the catalyst was achieved, the collected data were employed to develop a kinetic model able to predict the performances of the process in a furtherly broad condition spectrum. In addition, the stability of the catalyst was evaluated, pointing out its ability of keeping unvaried performances, despite the formation of sulfates species on the surface due to critical reaction conditions.

Afterwards, the study of COS removal was conducted in liquid phase in presence of an aqueous solution of a customized tertiary amine. The evaluation of the effect of the presence of different packing materials with different shapes was performed. Then, the aging of the amine solution was evaluated in presence of COS and H_2S, and the experimental campaign allowed to observe that the removal in liquid phase goes through an aliquot of physical absorption and a sensible extent of reaction in liquid phase, with the portion of liquid water present in the solution.

Finally, a new experimental setup was designed for evaluating an unexplored technology: a three-phase system for the performance of COS hydrolysis. The system was composed of the structured catalyst – for a fast and efficient conversion of the COS present in a gaseous stream – and the amine solution, in which the catalyst was completely immersed, to continuously subtract the produced H_2S. The feasibility of this application was demonstrated with an outstanding success in the experiments: the three-phase system allowed to completely remove the COS – together with the produced H_2S – obtaining a clean outlet gas in a single room-temperature operating unit, excellently dwarfing the performances of both the constituting processes.

Introduction

The rising economy, the demand of energy and fuel which is intensifying, and the consequent increase in exploitation of natural resources, have originated growing environmental concerns. Among these, the attention to sulfur contents in fossil fuels has recently received a deep focus. It is well known that most of the sulfur-derived compounds are toxic for human health, and their presence in the atmosphere is dangerous; indeed, they can be addressed as the main responsible for acid rains. Despite the undeniable interest of the modern world toward the renewable energies, the increase in exploitation of less precious fossil fuels, such as coal, cannot be neglected. These sources contain a remarkably higher concentration of sulfur-based compounds compared to oil and natural gas, hence this phenomenon amplifies the general attention to the environmental issues and the volumetric growth of harmful substances in atmosphere. The topic plays a key role in modern desulfurization scenario, and it has become an incentive in improving the existent desulfurization technologies.

It is commonly accepted to classify the sulfur-containing compounds as organics and inorganics. Carbonyl sulfide is an organic sulfur compound, and it is the most long-lived reduced sulfide which can be present in the atmosphere. Although its concentration in air is determined also by volcanic activity, most of the carbonyl sulfide is produced anthropogenically in desulfurization processes. In this Ph.D. thesis, the problematic of carbonyl sulfide abatement will be addressed, and the existent removal technologies will be discussed, highlighting the limitations of the nowadays processes. The core of this three-years project has been the proposal and investigation of some innovative solutions to overcome the most relevant issues. The results achieved to this aim will be discussed in this dissertation.

Chapter I.
COS removal: general issues and present technologies

I.1 Carbonyl sulfide: chemistry and properties

Carbonyl sulfide (COS or S=C=O), also known as carbon oxide sulfide or carbon oxysulfide, is a colorless gas at ambient conditions and it is classified as dangerous for human health and a pollutant for the environment. Before 1867, COS was erroneously observed as a mixture of carbon dioxide and hydrogen sulfide, until it was synthetized (Ferm, 1957). Together with carbon disulfide (CS_2) it is one of the main constituents of volatile organic compounds (VOCs). As stated in the introduction, a fraction of atmospheric COS comes from natural sources, such as the chemical and biological conversion of soils and sediments, and emissions from volcanos or fumaroles. Besides, it has been estimated that 14 to 32% of the atmospheric COS is ascribable to human activities (Zhao *et al.*, 2019b). The amount of COS released in the atmosphere is progressively increasing, determining growing concerns.

Carbonyl sulfide is geologically present in natural gas and oil, while others sulfur compounds – constituents of coal – can be COS precursors. Considering the massive exploitation of fossil fuels, this aspect is at the basis of the anthropogenic emissions. In natural gas, most of the COS can be hydrolyzed to H_2S through the saturation process with water, making the removal of this compound relatively simple. Nevertheless, its fraction in oil is harder to be separated due to the proximity of boiling points of COS and propane, which leads to a COS recovery in the propene fraction of 90%, with the remaining 10% being into the ethane fraction (Svoronost and Bruno, 2002).

COS has been demonstrated to be inert in the troposphere; indeed, it is transported into the stratosphere where photodissociation and photo-oxidation occur (Inn *et al.*, 1979; Sandalls and Penkett, 1977). Carbonyl sulfide is naturally removed from the atmosphere mainly by oxidation (eq. I-1, leading to SO_2) and hydrolysis (eq. I-2, leading to H_2S), and to a lesser extent by dissolution in atmospheric water and dry deposition on earth (Zhao *et al.*,

2013). In addition, a fraction of the oceanic formation of hydrogen sulfide can be accounted to the presence of COS in the atmosphere: it can reach the ocean water surface and decompose through photolysis or hydrolysis, giving H_2S (Radford-Knęry and Cutter, 1994).

$$COS + O_2 \rightarrow CO + SO_2 \qquad \text{I-1}$$

$$COS + H_2O \rightleftarrows CO_2 + H_2S \qquad \text{I-2}$$

From an industrial point of view, COS presence in the process streams causes several problems. Firstly, it is not possible to convert COS as the other VOCs with a catalytic oxidation process, because sulfur is a poison for most of the catalysts. Furthermore, the oxidation may lead to the formation of SO_3 instead of SO_2 (eq. I-3): SO_3 is an unstable compound, which can form sulfuric acid in presence of water, leading to corrosion of the construction materials (Ojala *et al.*, 2011).

$$COS + 2O_2 \rightarrow CO_2 + SO_3 \qquad \text{I-3}$$

Among the possible pathways for COS conversion, oxidation to SO_2 is particularly harmful, considering that the oxide can react with other pollutants to form sulfate particles, which alter the radiative properties of the Earth's atmosphere (Zhao *et al.*, 2019b) and strongly influences the stratospheric aerosol layer (Crutzen, 1976). Moreover, these sulfate particles are constituents of fine particulate matter ($PM_{2.5}$) (EPA, 2018; Fioletov *et al.*, 2016). For all these reasons, the threshold for SO_2 emissions in Italy has been fixed from D.Lgs. n°183 (15th November 2017) in the range 35-400 mg Nm^{-3} depending on the industrial application. As the emission of all the sulfur compounds is quantified as equivalent SO_2, this limitation applies also to COS emission. These restrictions are getting progressively more stringent worldwide; hence, COS abatement is currently gaining increasing interest, attracting the attention of both the scientific and the industrial world.

I.2 The anthropogenic emissions and the Claus reaction

The presence of sulfur compounds (mainly sulfides and mercaptans) in fossil fuels is well known, and plenty of desulfurization technologies have been developed to efficiently clean the raw materials to be employed in chemical catalytic processes. Among them, hydrodesulfurization is one of the most consolidated technologies to this aim. The main problem related to this strategy is that H_2S, which is toxic and highly corrosive, represents one of the main products. It is further converted into elemental sulfur through a sulfur recovery unit (SRU), which is usually based on the Claus process. Besides the small fraction of COS naturally contained in fuels, most of the anthropogenic carbonyl sulfide comes from the Claus, where it is unintentionally produced in the anoxic region of the thermal stage.

The Claus process involves two steps: hydrogen sulfide is firstly fully oxidized to SO_2 (eq. I-4), which is then partially reduced to elemental sulfur (eq. I-5). This stepwise conversion is achieved through a thermal stage (oxidation) and several catalytic units aimed at the partial reduction of SO_2, generally two or three. The thermal stage employs a furnace reactor, operating in the temperature range of 900-1300 °C (with higher temperatures reached in the proximity of the flame). Due to the presence of the flame, the thermal stage reactor can be further divided into a partially oxidizing flame zone, in the proximity of the burners and with the highest concentration of oxygen, characterized by temperatures around 2500 °C, and an anoxic zone, with temperatures in the range 900-1200 °C (Clark *et al.*, 2001). The catalytic stages further convert SO_2 in S_x at low temperature, approximately 300 °C. The lower the temperature in the catalytic stages of the Claus process, the higher the H_2S conversion. Nevertheless, it is not feasible to work below sulfur dewpoint (around 260 °C), as solid sulfur can accumulate in the catalytic bed. Therefore, more than one catalytic stage is conventionally part of the Claus process, which is then coupled to a TGT (tail gas treatment) unit (Kohl and Nielsen, 1997a). A schematic representation of a generic Claus process is given in Fig. I-1.

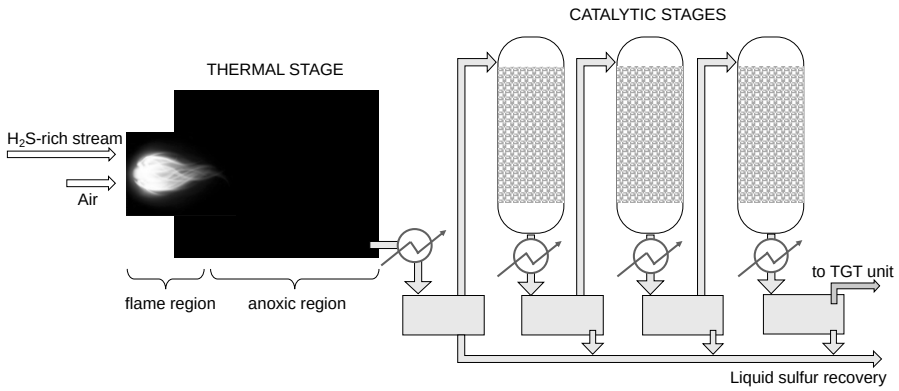

Fig. I-1: Schematic representation of the Claus process

Of course, this is a simplified description of the process. The feed stream is not constituted by pure hydrogen sulfide but it can be considered H_2S-rich. Considering that other compounds, in particular hydrocarbons in traces, are sent to the Claus process, it is characterized by the occurrence of several competitive reactions, leading to the formation of a sensible number of by-products. Particularly, most of the side reactions occur in the thermal stage, since nothing can be used to tune the selectivity. Hence, several combustion products such as SO_2, CO_2 and H_2O are produced. In the anoxic region, these products further react with H_2S. The combination of all the existent species in the system leads to the occurrence of a wide number of side equations (eqs.

I-6 to I-14), which are the main responsible for COS and CS_2 formation (Karan *et al.*, 1998).

$$H_2S + \frac{3}{2}O_2 \rightleftarrows SO_2 + H_2O \quad \text{I-4}$$

$$SO_2 + 2H_2S \rightleftarrows \frac{3}{x}S_x + 2H_2O \quad \text{I-5}$$

$$CO_2 + H_2S \rightleftarrows COS + H_2O \quad \text{I-6}$$

$$CO_2 + 2H_2S \rightleftarrows CS_2 + 2H_2O \quad \text{I-7}$$

$$CH_4 + SO_2 \rightleftarrows COS + H_2O + H_2 \quad \text{I-8}$$

$$CH_4 + 2S_2 \rightleftarrows CS_2 + H_2S \quad \text{I-9}$$

$$CS_2 + H_2O \rightleftarrows COS + H_2S \quad \text{I-10}$$

$$CS_2 + CO_2 \rightleftarrows 2COS \quad \text{I-11}$$

$$CS_2 + SO_2 \rightleftarrows COS + SO + \frac{1}{2}S_2 \quad \text{I-12}$$

$$CS_2 + SO \rightleftarrows COS + S_2 \quad \text{I-13}$$

$$CS_2 + 4H_2 \rightleftarrows CH_4 + 2H_2S \quad \text{I-14}$$

Based on the above, the Claus process can be considered the most relevant anthropogenic COS source, and for this reason the greatest part of the research about carbonyl sulfide abatement deals with the treatment of the Claus tail gas. Furthermore, the process reports an efficiency in hydrogen sulfide conversion of about 90-93%, leading to a tail gas containing residual H_2S together with COS (Rhodes *et al.*, 2000). This is a problem in several COS abatement processes, as it will be better discussed in the following paragraph.

I.3 COS removal technologies

As briefly discussed, the Claus tail gasses are generally sent to further tail gas treatment units. The aim of these processes is mainly to convert the hydrogen sulfide presents in traces in the outlet stream of the Claus. There is a multiplicity of TGT units, since different reactions can be suitable to the aim. Between them, several downstream processes usually perform the catalytic hydrogenation of the residual species, and this also includes COS: two popular options are the Beavon and the SCOT process. Both of them realize a catalytic reduction of all sulfur compounds to hydrogen sulfide, using

hydrogen or reducing gas mixtures (Fenton and Gowdy, 1979). Considering the great variability in composition that a tail gas can have, the selectivity of these processes is not always satisfying with respect to COS. Indeed, oxidized sulfur (mainly SO_2) is the compound that can more easily undergo hydrogenation, while COS and CS_2 are only slightly reactive, and tend to combine with water through the hydrolysis reaction. Selective COS hydrogenation can be performed (following either eq. I-15 or I-16), but it requires expensive Co-Mo catalysts and not-so-mild operating conditions, i.e. 350-400 °C (Tong *et al.*, 1992). For these reasons, the process has not been intensively studied.

$$COS + H_2 \rightleftarrows CO + H_2S \qquad \text{I-15}$$

$$COS + 4H_2 \rightleftarrows CH_4 + H_2S + H_2O \qquad \text{I-16}$$

The same consideration applies to COS oxidation and thermal decomposition processes. Very few and old papers report the study of these reactions, attesting the poor interest towards these topics (Homann *et al.*, 1969; Partington and Neville, 1951).

In conclusion, the problem of COS removal was not faced directly, so far. The processes that are able to partially reconvert COS can be considered a casualty, and they are not particularly effective, while the issue of COS presence into the process streams is becoming progressively more impactant.

The solution would be the insertion, within the process chain of sulfur abatement, of a unit dedicated to the challenging COS conversion, as represented in Fig. I-2.

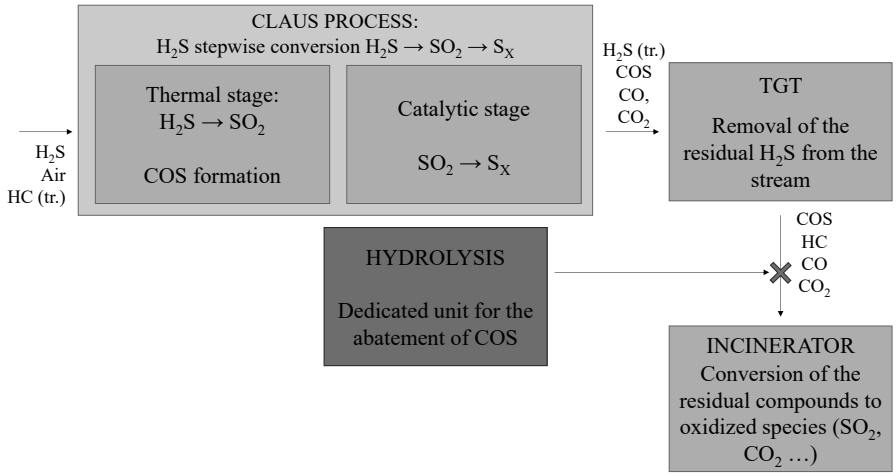

Fig. I-2: How the proposed technology fits into current sulfur recovery process chain: a simplified scheme

The most advantageous and consolidated technology for COS removal from sour gas is the absorption with amines, and the most promising is represented by the hydrolysis reaction.

I.3.1 Absorption with amine solutions

Absorption applied to gas purification processes can occur via three main mechanisms: (i) physical solution, which is achieved when the solubility of the component being absorbed is higher in the amine solution rather than in the gaseous stream in which it is contained; (ii) reversible reaction, which involves a chemical reaction among the component being absorbed and the amine that leads to loosely bonded product and allows the amine regeneration; (iii) irreversible reaction, that cause the formation of products which cannot be decomposed to release the absorbate (Kohl and Nielsen, 1997b). In this view, absorption of COS in an aqueous amine solution can occur following three possible paths: (i) physical absorption, i.e. depending on the solubility of COS in the solution; (ii) liquid-phase hydrolysis, with subsequent physical absorption of the reaction products, H_2S and CO_2; (iii) direct reaction with the amine, forming a relatively stable compound. The latter mechanism, in the case of COS, often leads to an irreversible reaction, with the formation of products that cannot be converted into the amine again. Of course, even though this mechanism is effective in the removal of the undesired compound, this is extremely costly. For this reason, the kind of amine that can be suitable for COS absorption is always chosen to avoid the occurrence of direct reactions. The physical solubility of COS in amines is very low, but of course it contributes, even though to a minor extent, to the carbonyl sulfide removal. In conclusion, liquid-phase hydrolysis is considered the primary mechanism of COS removal from gaseous streams by amine solutions.

Amines can be classified based on the number of substituent groups: a primary amine has structure RNH_2 with the only substituent R-; a secondary amine is R_1R_2NH and a tertiary amine is $R_1R_2R_3N$. Among the possible amine solutions, monoethanolamine (MEA) solutions have been widely used for H_2S and CO_2 removal from synthesis gas but their use cannot be applied to gaseous streams containing COS and CS_2, so their application has been reduced over the years. Indeed, COS reacts with MEA (primary amine) forming irreversible reaction products, mainly protonated amine thiocarbamate salts, determining in an excessive chemical loss of the amine if the gas stream contains significant carbonyl sulfide amounts (Speight, 2018). Secondary amines are much less reactive with COS and CS_2, thus diethanolamine (DEA) represents a valid alternative in COS absorption. The main drawback is that DEA has high reactivity with CO_2, forming corrosive degradation products, thus its application is suitable only in presence of low-CO_2 containing streams.

CO_2-rich streams can, instead, be treated with a tertiary amine, such as methyl diethanolamine (MDEA), which allows the selective absorption of H_2S

in presence of CO_2 even with high H_2S/CO_2 ratios. MDEA is also more stable than primary and secondary amines. It has a lower vapor pressure, resulting in minor losses in the vapor phase, and for this reason, it can be used in concentrations up to 60 wt.%. The expression of COS absorption in aqueous MDEA solutions can be expressed following eq. I-17 (Al-Ghawas *et al.*, 1989).

$$COS + H_2O + R_1R_2R_3N \rightleftarrows R_1R_2R_3NH^+ + HCO_2S^- \qquad \text{I-17}$$

MEA, DEA and MDEA (Fig. I-3) are the most widely employed amines in sour gas treatment. Nevertheless, none of them is suitable for COS absorption. Indeed, MEA reacts too strongly with COS leading to the non-recoverability of the original amine and, to a lesser extent, DEA presents the same issue. On the other hand, MDEA has a very low affinity with COS, particularly when the treated gas also includes other sour compounds, such as H_2S and CO_2. As discussed, MDEA offers the possibility to selectively remove H_2S in a CO_2 containing stream, thus it is clear that the amine affinity with CO_2 is relatively low: an even lower fraction of COS is removed by MDEA when the stream contains the three compounds (R. J. Littel *et al.*, 1992; Magné-Drisch *et al.*, 2016). Despite the discussed issues related to COS absorption with amines, plenty of studies are reported in the literature concerning this topic, considering the perspective of a combination of this treatment with other TGT units, which could offer a satisfactory abatement of the COS concentration.

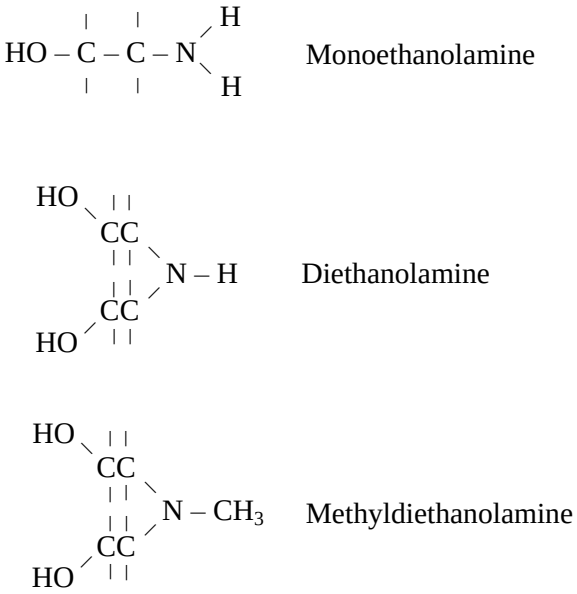

Fig. I-3: Structure of the most common amines

I.3.2 Hydrolysis reaction

The COS catalytic hydrolysis reaction (eq. I-2) is widely considered the most effective solution for COS removal from a gaseous stream. It has several advantages, with the most important being the mild operating conditions, and the possibility of using water instead of hydrogen as a reactant.

The reaction has a slightly exothermic nature ($\Delta H°_{298\ K}$ = -30 kJ mol^{-1}). Therefore, thermodynamic limitations fix the optimal range for operating this reaction at temperatures below 200°C. Considering this, the most relevant issue is constituted by the kinetic limitations due to the low temperature. The employment of metallic species which could enhance the catalytic performances leads to another issue, the catalyst stability. Indeed, metallic particles easily undergo sulfidation, causing deactivation. Furthermore, because of the extremely high COS conversion required from the strict regulations on sulfur emissions, it should be performed below 100 °C, at atmospheric pressure. The studies available in the literature point out other two limitations, when hydrolysis is operated below 100°C: the competitive adsorption of the two reactants limits the COS conversion; diffusion limitations become determining for the observed reaction rate. For these reasons, the research scenario is, at first, focused on the development of new catalytic formulations with extremely high activity, thus being able to overcome the kinetic limitations.

Chapter II.
State of the art

II.1 Context and stats on COS hydrolysis

As discussed in the Introduction, hydrolysis of carbonyl sulfide is an exothermic reaction, thus thermodynamically promoted by low temperatures. To some extent, it occurs spontaneously in the catalytic stage of the Claus process, where the COS formed in the previous thermal stage is hydrolyzed to H_2S again. Indeed, some commercial Claus catalysts – typically titania – already partially provides for COS destruction within the process, even though most of the produced COS is sent to further treatments, where its removal is challenging (Sui *et al.*, 2020). Unfortunately, the temperature in the catalytic stage is still too high for the hydrolysis to take place to the desirable extent: COS conversion within the Claus catalytic stage has been reported being about 75% at ~340°C (Rhodes *et al.*, 2000). Therefore, COS hydrolysis has progressively become a dedicated stage, having its own catalysts and optimized operating conditions.

Evaluating the studies nowadays available in the literature, according to the Scopus database, it is possible to observe the interest towards this process, born in the '40s and increased over the decades, according to Fig. II-1.

Furthermore, the process is acquiring interest if compared to the more credited absorption technology by means of amine aqueous solutions. Indeed, according to Scopus, most of the recently published works dealing with COS removal are related to hydrolysis, as shown in Fig. II-2.

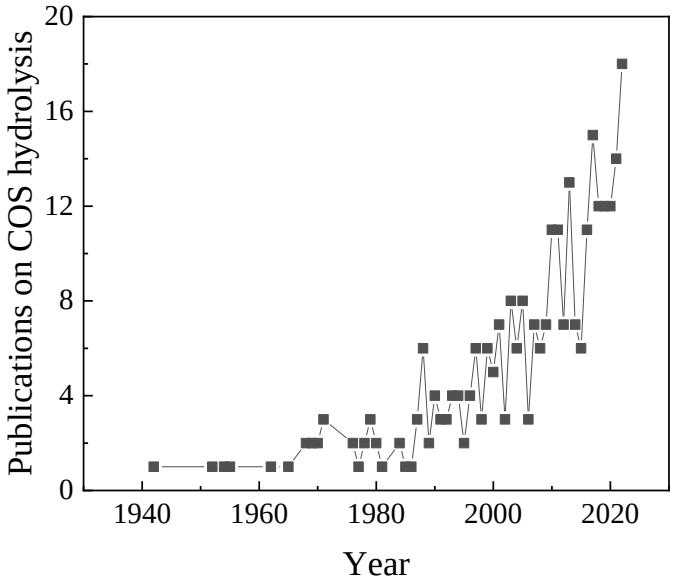

Fig. II-1: Increase of scientific interest toward COS hydrolysis

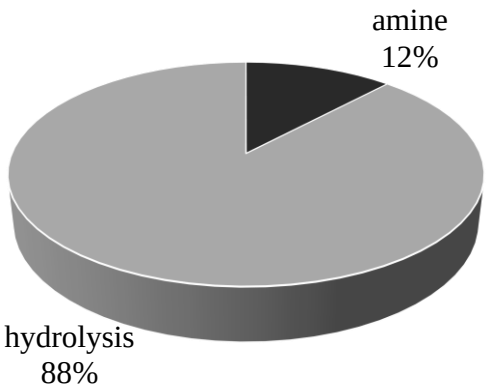

Fig. II-2: Comparison of the scientific interest toward COS hydrolysis and absorption with amine solutions

A deeper evaluation of the research works available in the literature points out that COS hydrolysis can be differentiated into low-temperature and high-temperature process. This is mainly due to the criticisms that this reaction offers: on one hand, low temperatures limit operating costs and promote the reaction with respect to its thermodynamic equilibrium; on the other hand, kinetic constraints and diffusional limitations limit the activity of the low-temperature system, determining better suitability of higher temperatures to conduct the reaction. Nevertheless, high temperatures are costly and determine thermodynamic limitations to COS conversion, resulting in a worse match with the environmental restrictions. The latter topic has determined a

strong increase in interest towards the low-temperature process, leading to a different distribution of studies across the decades, according to Fig. II-3.

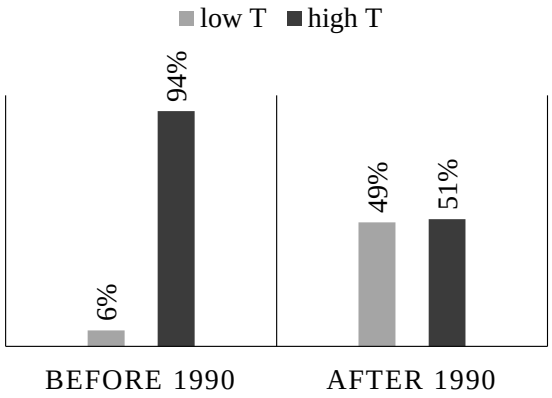

Fig. II-3: Interest (%) in low-temperature and high-temperature hydrolysis

Despite the newborn interest in low-temperature COS hydrolysis, the existent plants still operate at relatively high temperatures, to minimize the issues related to kinetic limitations (Nimthuphariyha *et al.*, 2019; Williams *et al.*, 1999). For this reason, several studies are carried out investigating new catalytic formulations at industrial operating conditions, which can be beneficial in improving the existing processes. Therefore, this dissertation will review COS hydrolysis in two separate sections, highlighting the differences, advantages, and disadvantages of each technology.

II.2 COS hydrolysis in liquid phase: the removal via amine solutions

As discussed, secondary and tertiary amines are the most suitable for COS removal, but in general MEA, DEA, MDEA and piperazine-promoted MDEA aqueous solutions are for sure the most widely employed and investigated (Vaidya and Kenig, 2009). Above all, literature studies mainly report the reaction mechanism and the evaluation of the kinetic parameters for COS absorption with a large variety of amines; furthermore, some comparative studies dealing with absorption efficiency may also be found. Most of these studies do not consider the amine regeneration, either as a possibility or as a regeneration technique, thus there is not any reference to the type of reaction (whether it is irreversible or not) and reaction product that is formed. Nevertheless, before approaching the literature review, is important to mention the effect of the irreversible reaction on a generic amine absorption unit.

In a wide range of applications, the reaction between the compound being removed and the amine does not lead to the formation of non-re-convertible products: it is also the case of H_2S or CO_2 removal. In these circumstances, we can say that the amine has a certain *resistance to breakdown*; nevertheless,

on prolonged use, alkanolamines may however be converted into undesirable products, from which is not possible or not easy to regenerate the amine. The same can occur in presence of compounds that interact with the amine via irreversible reactions, as COS and CS_2 actually do. This phenomenon is commonly referred to as *amine degradation*, and not only leads to amine losses, which of course are an important economic factor, but it also contributes to operational problems such as corrosion or foaming which shorten the life of the equipment (Islam *et al.*, 2011). It is clearly reported that degradation of the amine deals with the protonation, which leads to carbamate (in the case of CO_2) or thiocarbamate salt (in the case of COS and CS_2) formation. The formation of foam in the absorber, which depend of course on the liquid solution's physical properties such as surface tension, density and viscosity, determines the replacement cost of amine and also an increase in the cost of solvent pumping, as its viscosity tends to increase. Corrosive compounds which can be formed in the amine degradation process may act as chelants to remove protective films from metal surfaces, and the prevention of this issue mainly consists in using more expensive construction materials. In addition to all the mentioned expenses, it is worth considering also that the cleaning of piping and process units may be pricey and may impact remarkably on the overall cost of the plant.

The reaction mechanism of COS with primary and secondary amines (from now on respectively PAs and SAs) has been reported for the first time by Sharma in 1965 (Sharma, 1965). The author found that the reaction of COS both with primary and secondary amines is exactly the same as CO_2, as reported in Table II-1, where the instantaneous reactions were denoted with *(inst.)*. He suggested that this could be due to the same linear structure of the two molecules, and that this should result in a strict correlation between the COS and CO_2 kinetic. The experimental results confirmed this hypothesis, and the obtained correlation is reported in eq. II-1.

$$\log_{10} k_{AM-COS} \approx \log_{10} k_{AM-CO_2} - 2 \qquad \text{II-1}$$

Table II-1: Comparison of COS and CO_2 mechanism *(Sharma, 1965)*

COS mechanism	CO_2 mechanism
$COS + RNH_2 \rightarrow RNHCOS^- + H^+$ $RNH_2 + H^+ \rightarrow RNH_3^+$ (inst.)	$CO_2 + RNH_2 \rightarrow RNHCOO^- + H^+$ $RNH_2 + H^+ \rightarrow RNH_3^+$ (inst.)
$COS + R_1R_2NH \rightarrow R_1R_2NCOS^- + H^+$ $R_1R_2NH + H^+ \rightarrow R_1R_2NH_2^+$ (inst.) $COS + 4OH^- \rightarrow CO_3^{2-} + S^{2-} + 2H_2O$	$CO_2 + R_1R_2NH \rightarrow R_1R_2NCOO^- + H^+$ $R_1R_2NH + H^+ \rightarrow R_1R_2NH_2^+$ (inst.) $CO_2 + 2OH^- \rightarrow CO_3^{2-} + H_2O$

Littel et al. proposed a more detailed study of COS reaction with primary and secondary amines in a wider temperature range and for different values of the amine concentration (R. J. Littel *et al.*, 1992). They reported that, for primary amines, a linear dependence of the kinetic constant k_{app} from the amine concentration was observed, and that this dependence is still linear with the temperature increase from 10 to 50°C. The experimental results pointed out also those primary amines had a fractional reaction order, in particular 1.4 for MEA and 1.6 for DGA (diglycolamine). All the secondary amines have been studied in the same concentration range while for what concerns the temperature conditions DEA has been studied in the same MEA temperature range, while DIPA (diisopropanolamine), AMP (2-amino-2-methyl-1-propanol) MMEA (methylmonoethanolamine), and MOR (morpholine) were studied only at 30°C. The experimental evaluations resulted in a kinetic order for all the secondary amines of almost 2. The authors concluded that all kinetic experiments could be described by the zwitterion mechanism proposed at first by Caplow for CO_2 with secondary amines reaction (Caplow, 1968). The mechanism is comprehensive of the formation of the zwitterion compound (eq. II-2) and the deprotonation reaction by means of a base B resulting in a thiocarbamate formation (eq. II-3), where $R_1R_2NH^+COS^-$ is the zwitterion compound; this led to an overall forward reaction rate reported as eq. II-4.

$$COS + R_1R_2NH \rightleftarrows R_1R_2NH^+COS^- \qquad \text{II-2}$$

$$R_1R_2NH^+COS^- + B \rightleftarrows R_1R_2NCOS^- + BH^+ \qquad \text{II-3}$$

$$R_{COS} = \frac{[R_1R_2NH][COS]}{\frac{1}{k_2} + \frac{1}{k_{H_2O}[H_2O] + k_{R_1R_2NH}[R_1R_2NH]}} \qquad \text{II-4}$$

Lee et al. agreed with the mechanism proposed by Littel et al. but reported instead a second order for MEA and a first order for COS, suggesting that the rate-determining step for the overall reaction was the zwitterion deprotonation, thus obtaining the simplified reaction rate expression reported in eq. II-5 (Lee *et al.*, 2001).

$$r = k_3[COS][MEA]^2 \qquad \text{II-5}$$

A similar result has been obtained by Hinderaker et al. with COS in aqueous DEA, leading to eq. II-6, which is the same reaction rate expression (Hinderaker and Sandall, 2000).

$$r = k_3[COS][DEA]^2 \qquad \text{II-6}$$

Rivera-Tinoco et al. adopted the two-step zwitterion mechanism for the estimation of the kinetic parameters in the COS – DEA system for aqueous and methanolic solutions, assuming each of the two steps of the mechanism. The study validates the zwitterion mechanism (always used for aqueous solutions only) also for alcoholic solutions, and a comparison of the obtained results showed that methanol enhanced the pre-exponential factor, improving the reaction rate.

Despite the weak affinity of COS with MDEA, this tertiary amine is actually widely studied because at least it does not imply the problems of irreversible reaction that raise for PAs and SAs. The first expression of the reaction between COS and MDEA was given by Al-Ghawas et al., and it is given by eq. I-17; the authors reported that the experimental evidence through a spectrophotometric analysis of the saturated amine highlighted a difference among the reaction products of H_2S and CO_2 absorption rather than COS absorption (Al-Ghawas *et al.*, 1989). The saturated amine resulted in a different color and absorbed light at different wavelengths (518 nm for COS absorption and 503 nm for CO_2+H_2S). The reaction of COS in MDEA can be presented as eqs. II-7, II-8 and II-9 and eq. II-7 can be considered almost instantaneous; eq. II-9 leads to the same H_2S+CO_2 in MDEA reaction products. Because of the saturated amine characterization results, the authors concluded that eq. II-9 is very slow if not totally negligible. Thus, the overall reaction is given by the sum of eq. II-7 and II-8 and results in eq. I-17, with a first-order kinetic for MDEA and COS and a second-order kinetic for the overall reaction. The kinetic parameters were also estimated in the study.

$$H_2O + R_1R_2R_3N \rightleftarrows R_1R_2R_3NH^+ + OH^- \qquad \text{II-7}$$

$$COS + OH^- \rightleftarrows HCO_2S^- \qquad \text{II-8}$$

$$HCO_2S^- + OH^- \rightleftarrows HCO_3{}^- + HS^- \qquad \text{II-9}$$

A further step in the reaction mechanism of COS with tertiary amines (TAs) was achieved by Littel et al., who analyzed the interaction in presence of TAs aqueous and nonaqueous amine solutions (Rob J. Littel *et al.*, 1992a)(Rob J. Littel *et al.*, 1992b). They proposed a two-step mechanism in which the equilibrium constant for eq. II-11seemed to be very high, as they observed an almost total absorption of COS.

$$COS + H_2O + R_1R_2R_3N \rightleftarrows R_1R_2R_3NH^+ + HCO_2S^-H_2O + \qquad \text{II-10}$$
$$R_1R_2R_3N \rightleftarrows R_1R_2R_3NH^+ + OH^-$$

$$HCO_2S^- + H_2O + R_1R_2R_3N \rightleftarrows R_1R_2R_3NH^+ + HCO_3{}^- + HS^- \qquad \text{II-11}$$

As the presence of water seemed to be essential for the occurrence of the first reaction, the study further evaluated the absorption of COS in solution of MDEA in ethanol and octanol, obtaining that only physical absorption was observed in nonaqueous solutions of TAs, which agreed well with the proposed mechanism. Thus, water presence was found to be actually essential, as it acts as a base promoting the interaction between COS and the amine, and this mechanism is addressed as a "base-catalyzed mechanism".

COS removal was studied in the case of aqueous solutions of DEA and MDEA by Amararene et al. in the temperature range 25 – 80 °C (Amararene and Bouallou, 2004). The authors estimated the kinetic parameters in both cases, adopting for COS in DEA absorption the zwitterion deprotonation mechanism and for COS in MDEA the base-catalyzed mechanism for COS hydrolysis.

A detailed kinetic study of COS – MDEA system was proposed by Rivera-Tinoco et al., who considered for the kinetic parameters estimation both mass transfer and chemical reaction, respectively through Henry's law and the zwitterion mechanism, in the temperature range 40 – 80 °C (Rivera-Tinoco and Bouallou, 2007). The obtained kinetic parameters found a good agreement with the previous literature results and allowed the reaction modeling in a wide range of temperatures and amine concentrations.

A study on the hydrolysis of COS catalyzed by tertiary amine was also proposed by Chen et al. whit an absorbent solution consisting in a non-specified tertiary amine in a mixture of dimethyl ethers of polyethylene glycols containing a variable percentage of water, in the range 1 – 9.7 wt.% (Ernst *et al.*, 1990). The authors found a first-order dependence on the amine, performing batch experiments with different residence times and amine concentrations. They also evaluate the effect of water percentage in the solvent solution on the estimated kinetic constant, obtaining a trend with a maximum reaction rate for an intermediate water amount (2 – 5 vol.%). The obtained results suggested a two-step mechanism involving (i) the complexation of COS with the amine and (ii) the subsequent hydrolysis of the complex.

A comparative study of the removal efficiency and stability of SAs and TAs was proposed by Palma et al. adopting very low amine concentrations (Palma *et al.*, 2019). The study pointed out that DEA and DIPA are the most suitable amines for COS removal, while MDEA showed a minor removal efficiency and the worst stability and MEA actually performed at the best in the first screening but was excluded from further investigations because of its high vapor pressure and because of the irreversible reaction with COS. The authors reported also that a reduction in the overall solution volume caused a decrease in the COS removal, but this phenomenon was more evident for

DIPA, leading to the conclusion that DEA could be selected as the most suitable amine for COS absorption.

Sometimes, the absorption efficiency is enhanced with the employment of activated aqueous amine solutions: these consist in a TA aqueous solution in which a small amount of a SA or PA is added as an activator. In the framework of a research program that focused on acid gas removal with amines, Huttenhuis et al. studied COS absorption in presence of piperazine, a cyclic secondary amine frequently used as an activator (Huttenhuis *et al.*, 2006). The kinetic study resulted in a 1.6 reaction order for piperazine, suggesting the occurrence of the zwitterions mechanism.

Table II-2: Summary of the reviewed COS absorption with amines processes

Selected Amine	Amine concentration (mol/m^3) **	Temp. (°C)	Amine kinetic order*	Ref.
PAs, SAs	200 – 3000	10 – 50°C	MEA 1.4 [a] DGA 1.6 [a] SAs 2 [a]	(R. J. Littel *et al.*, 1992)
PAs, SAs	1000	25°C	1 [a]	(Sharma, 1965)
MEA	10 – 40 wt%	25 – 65°C	2 [b]	(Lee *et al.*, 2001)
DEA	500 – 2500	25°C; 75°C	2 [b]	(Hinderaker and Sandall, 2000)
MDEA	1259 – 2599	20 – 40	2 [b]	(Al-Ghawas *et al.*, 1989)
TEA, DMMEA, DEMEA	300 - 1000	30	1 [b]	(Rob J. Littel *et al.*, 1992a)
DEA, MDEA	5 – 40 wt.% DEA 5 – 50 wt.% MDEA	25 – 80	2 [b]	(Amararene and Bouallou, 2004)
MDEA	415 – 4250	40 – 80	1 [b]	(Rivera-Tinoco and Bouallou, 2007)
TAs	250 – 1000	25	1 [a]	(Ernst *et al.*, 1990)
MEA, DEA, MDEA, DIPA	1 wt.%	20°C	2 [b]	(Palma *et al.*, 2019)
Piperazine	100 – 1500	20 – 40	1.6 [a]	(Huttenhuis *et al.*, 2006)
DEA	380 – 2030	25 – 50	1 [b]	(Rivera-Tinoco and Bouallou, 2008)

* COS kinetic order was always found to be 1

** where not indicated

[a] This refers to a determined value

[b] This refers to an assumed value

II.3 Low-temperature COS hydrolysis

Low-temperature hydrolysis (LTH) is often performed at the operating temperature of 30 °C, and in any case below 80 °C. The research in this field is mainly devoted to the individuation of peculiar structure and textural properties able to minimize diffusion limitation within the system; therefore, plenty of different oxides have been evaluated, but a limited number of studies deal with efficient catalytic active phases.

II.3.1 Alumina and alumina-doped catalysts

Alumina is one of the most utilized metal oxides in catalysis, and it is for sure the most employed species in COS hydrolysis. Despite its role is usually being a support for other metals, which are the active sites for a generical reaction, in case of COS hydrolysis it can be used directly as final catalyst. Indeed, it is well recognized that COS hydrolysis is a base-catalyzed reaction, thus the conversion of carbonyl sulfide is mainly demanded to the presence of basic sites, which can be offered by alumina itself. As a general concept, when the addition of a species to the support produces a modification of the superficial basicity, increasing the density of basic sites which are demanded to the COS absorption, then the final catalyst can be more efficient than bare alumina. If no relevant modifications are generated, or if the density of basic sites is even decreased, the addition of a metal can be detrimental for the catalytic activity. For these reasons, alumina or different metal oxides can also be used without further modification in COS hydrolysis.

The porous structure and the specific surface area of the catalysts employed in COS hydrolysis are generally strongly relevant, as the reaction can be controlled by diffusional phenomena. Al_2O_3 and TiO_2 with complex structures were prepared and tested by He et al. (He *et al.*, 2019) obtaining the so-called 3DOM (three dimensional ordered microporous) structure. The proposed structure demonstrated to enhance the hydrolysis reaction, as it allowed an effective pulling out of H_2S, thus

diminishing the sulfur deposition on the catalyst surface. The study of the exhausted catalysts showed also that the most abundant deposited sulfur specie was elemental sulfur for the TiO_2 catalyst, while sulfate species for Al_2O_3 catalyst: the latter species have a particularly negative effect, as they not only block the pores but also deactivate the catalyst for their marked acidity.

Alkali-free ordered mesoporous alumina prepared via one-pot synthesis was studied for COS hydrolysis by Jin et al (Jin *et al.*, 2021). The authors reported that the catalyst showed improved catalytic activity with the enlargement of the mesopore size. Furthermore, due to sulfur deposits, the samples with smaller pores demonstrated a prompt loss in activity, while the catalysts with larger mesopores maintained longer the COS conversion at high

values. Smelting grade alumina was found to catalyze COS hydrolysis in presence of traces of moisture (Mikhonin *et al.*, 2013), demonstrating an enhancement in the activity corresponding to the increase in temperature. Wang et al. (Wang *et al.*, 2008) studied the COS hydrolysis on alumina catalysts in presence of oxygen through experimental and mathematical evaluations, under atmospheric pressure and at 40 – 70°C. They estimated a deactivation coefficient and found it to be remarkably sensitive with the relative humidity, while it changed less with temperature. An increase in O_2/COS ratio led to a higher COS concentration at the outlet of the reactor, and this value increases overtime because of the progressive deactivation.

In case of low-temperature hydrolysis, the overcoming of kinetic limitations can be handled through doping with transition metals or alkali and alkaline-earth metals. West et al. (West *et al.*, 2001) studied the effect of γ-Al_2O_3 promotion with Na and transition metals, namely Fe, Co, Ni, Cu and Zn, on the COS hydrolysis performances at 30°C, COS and H_2O concentration respectively equal to 150 and 1200 ppm and 122000 h^{-1}. The study showed that all the selected metals are able to enhance the catalytic performances of bare Al_2O_3, in terms of specific activity (mol COS hydrolyzed/g/h). Nevertheless, in the greatest part of the formulation this improving effect only lasted for a short time: then, a rapid decrease in the activity was observed for all the catalysts but Ni and Zn doped alumina. Ni and Zn modifiers enhanced the specific activity while keeping the same stability overtime of the original Al_2O_3. The retention of sulfur during the initial time of the test suggested the formation of sulfided catalyst surfaces, which is consistent with the deactivated samples results: the exception of Ni and Zn modified γ-Al_2O_3 may be ascribed to stabilized sulfided surfaces, which still allowed the presence of hydroxyl groups on the surface. Alkali doping of γ-Al_2O_3 with Li, Na, K, Cs, Mg, Ca and Ba was studied by Thomas et al. (Thomas *et al.*, 2003) in low-temperature hydrolysis conditions (at 20°C) and for different metal loadings. In their 5 h experiments, the authors observed that the majority of alkali additives acted as a poison: K and Cs showed a slight enhancement in COS conversion but only at the highest loading (5 wt.%) while Na and Mg showed a significant improvement in the activity at all concentrations, but this effect only lasted for the first 3 hours of testing.

II.3.2 Mixed oxides

In the past 10 years, the academia has moved its interest toward the study of different metal oxides as support or catalyst for several reactions. Among these, transition metals oxides and hydrotalcite-like compounds have aroused remarkable interest for the application in COS hydrolysis.

Song et al. (Song *et al.*, 2020) performed an experimental and theoretical study on the simultaneous removal of COS and CS_2 over Fe_2O_3 and CuO. The synergistic effect of the Fe_2O_3+CuO improved the removal of both sulfur

compounds. For what concerns the COS removal, the reaction was carried out at 70°C, in presence of 400 ppm of COS and relative humidity of 49 vol.%, setting a space velocity of 10000 and 80000 h^{-1} over Fe_2O_3, CuO and with both the oxides. The higher COS removal efficiency was obtained on the Fe_2O_3+CuO catalysts at a space velocity of 10000 h^{-1}, for which the COS conversion was stable at 100% for the first 5 h. From the experimental data it was observed that CS_2 is firstly adsorbed on Fe_2O_3, achieving the CS_2 hydrolysis and leading to the formation of COS, which then migrates from Fe_2O_3 to CuO where the COS hydrolysis occurs.

Hydrotalcite-like compounds (HTLCs) are a particular natural class of the anionic clays. The generic formula of these compounds can be given as $[M^{(II)}_{1-x}M^{(III)}_x(OH)_2]_x\cdot (A^{n-}_{x/n})\cdot mH_2O$ where $M^{(II)}$ and $M^{(III)}$ are respectively divalent and trivalent cations which occupy octahedral positions within the hydroxide layer. A^{n-} are anions which counter balance the positive charges in the hydroxide sheets, which result when trivalent cations are substituted with divalent cations; the $M^{(III)}/(M^{(II)} + M^{(III)})$ ratio is equal to x and represents the layer charge density (Wang *et al.*, 2011; Zhao *et al.*, 2012). In general, the employment of HTCLs could offer good performances: at 25°C, a COS conversion of about 100% was reported, but for all the catalysts it decreases overtime, showing the highest values for the above-mentioned preparation conditions (Wang *et al.*, 2011). The $M^{(II)}/M^{(III)}$ ratio is a fundamental parameter that is able to influence the textural properties of HTLCs, because of the different dimension of the cations, which alter the structure. Zhao et al. (Zhao *et al.*, 2012) investigated a series of Zn-Ni-Fe containing HTLCs prepared with different $M^{(II)}/M^{(III)}$ ratios. They observed that this parameter could strongly affect the surface area and the basic properties of the resulting oxide, thus influencing the catalytic performances. The textural properties always have a noteworthy influence on the activity, in particular at such low temperatures. Hydrotalcites prepared with the ultrasonic technique were found to have a higher particle dispersion and a smaller crystallite size with respect to the sample prepared by the co-precipitation method without ultrasonic assistance (Zhao *et al.*, 2016). The improved pore structure enhances the diffusion and the physical/chemical adsorption of the gaseous pollutant. The effect of the ultrasonic treatment was very significant on the efficiency of COS removal because promoted the interaction between Ni and Al, also involving the increase of the number of weak basic sites (OH^-) and moderate basic sites (M-O) and the diminution of the strong basic sites (O^{2-}) that are responsible of the catalyst deactivation. In fact, the strong basic sites promote the H_2S oxidation with consequent sulfur formation leading to the occlusion of the pores of the support. The desulfurization performance was investigated at temperature of 60°C for the both the catalysts prepared; the COS removal was complete in the first 90 min over the catalysts treated with the ultrasonic irradiation (NiAl-UHTO), while for the NiAl-HTO the total COS conversion was only observed for 30 min. Zhao et al. (Zhao *et al.*, 2019b) studied Zn-Ni-

Al HTLCs adjusting the pH value from 7 to 12. They observed the highest COS conversion in the pH range 9.5 – 10.5 and these samples also reported the highest stability; the study of the catalysts surface pointed out that the density of the basic sites decreased in the order HTO-10 > HTO-9 > HTO-11 (where HTO denotes the HTLC derived oxide), thus explaining the best catalytic performances for the samples prepared with a pH around 10. In a subsequent study, Zhao et al. (Zhao *et al.*, 2019a) investigated also the effect of Al atomic-scale doping in NiAl-HTO. The authors varied the Ni/Al ratio from 1 to 5 obtaining samples which activity decreased in the order Ni3Al-HTO > Ni5Al-HTO > Ni1Al-HTO; nevertheless, all samples deactivated in the 3 hours test. The characterization analyses demonstrated that Al doping of the HTO determined the presence of abundant surface basic sites; moreover, in Ni3Al-HTO was evident a striking reduction of Ni^{2+} by Al doping in NiO, which suggested a large amount of oxygen vacancies. Promotion with potassium determined a dramatic improvement in activity (Zhao *et al.*, 2018). Modification of the catalyst with the appropriate amount of KOH and K_2CO_3 allowed to obtain outstanding performances when compared to the un-doped samples, while KCl and KNO_3 were found not suitable for this application, as they decrease the desulfurization efficiency. In particular, they suggested that K_2CO_3 is decomposed on the catalyst surface in K_2O: it enhances the catalytic activity because of its electron donation, which can improve the Lewis basicity of Ni atoms.

Further studies on HTLCs report the doping of hydrotalcites with alkali and/or rare earth metals. Zhao et al. studied the effect of Ce-doping on a series of Zn-Ni-Al-HTLCs at 50°C (Zhao *et al.*, 2010). The activity tests performed highlighted that Ce doping remarkably enhanced the catalytic performances, with a maximum reached at the Al/Ce ratio equal to 50, but excessive Ce-loading led to a negative effect on COS hydrolysis. SEM results reported that Ce-doping strongly influenced the surface morphology of the catalyst, and in particular from EDS results the authors found that Ce addition increased the degree of dispersion. Wang et al. (Wang *et al.*, 2012) evaluated the catalytic performances over CoNiAl-HTLCs modified by cerium with several Al/Ce ratio, namely 60, 50, 20, 10, 5. The CoNiAl-50 catalyst was found to be the most active and stable in COS hydrolysis conducted at 50°C and 2000 h^{-1} with a 2.67 vol.% relative humidity. Guo et al. (Guo *et al.*, 2015) prepared MgAlCe hydrotalcite-based compounds with different ratio of Al/Ce by co-precipitation methods. The authors investigated the effect of the operating conditions, e.g. ratios of Al/Ce, pH during the preparation, hydrothermal and calcination temperature on the COS removal efficiency at 50°C. The optimal operating conditions were found to be a ratio of 16/1, pH=8, a hydrothermal temperature of 140°C and a calcination temperature of 600°C. The catalyst synthesized under these conditions was tested at 50°C, by feeding 470 ppm COS with a relative humidity of 2.7 vol.% H_2O. A total COS conversion was observed for 80 min. A strong decrease of the catalytic activity was observed

at calcination temperatures higher than 600°C. This was ascribable to the destruction of the pore structure of the hydrotalcite, which led to the reduction of the number of active sites.

Together with the above-discussed materials, principally alumina, HTLCs and transition metals mixed oxides, used both as support and as catalyst, several other substances have been studied for the COS removal. Mi et al. (Mi *et al.*, 2019) investigated a particular support, MgAl layered double hydroxide nanosheets, for simultaneous removal of COS and H_2S. The layered double hydroxides (LDHs) are a complex 2D structure, and because of their well-defined geometry they represent an interesting material as well as HTLCs. LDHs are composed of positively charged metallic layers, interlayer anions and water, and they can be designed by the formula $[M^{2+}_{1-x}M^{3+}_{x}(OH)_2]^{x+}\cdot(A^{n-}_{x/n})^{x+}\cdot mH_2O$. The authors developed a solid-state mechanochemical method to prepare these structures and compared the synthesized MgAl-LDH to commercial MgAl-LDH (c-MgAl-LDH) and co-precipitated MgAl-LDH (MgAl-LDH-cp). The work pointed out that the synthesized MgAl-LDH resulted in a higher SSA and higher exposed OH^- active sites. Wei et al. (Wei *et al.*, 2021a) prepared N-doped MgAl-LDO for the COS hydrolysis at low temperature. N-doped MgAl-LDO catalysts were calcined at a temperature of 650°C in NH_3 for 4 h. N-doping method was used to modify the basic sites preserving the surface area and the pore structure. The basicity and the H_2O adsorption-desorption properties resulted particularly enhanced by the presence of the N-species formed in surface and bulk. A complete COS conversion was obtained at 70°C for 24 h without any deactivation phenomena. Sulfur species were observed by increasing the reaction temperature at 90°C due to the H_2S oxidation reaction.

II.3.3 Carbon-based materials

The interest toward carbon-based materials has progressively increased in the past 10 years, mostly because of the relatively low environmental impact, resulting in their employment in a wide number of applications, for example hydrocarbon conversion (Di Stasi *et al.*, 2021a, 2019) and synthesis (Di Stasi *et al.*, 2021b; Renda *et al.*, 2021). Besides, in the scenario of environmental catalysis, activated carbons (AC) and biochar have been extensively studied and applied for removal treatments. Activated carbons are well-known coal-derived materials, with a widespread application in waste-water treatment and H_2S adsorption (Feng *et al.*, 2005; Roddaeng *et al.*, 2018; Thompson *et al.*, 2016; Yan *et al.*, 2002). They are actually expensive materials, as they require high energy-intensive thermal activation in order to achieve the desirable adsorption properties (Thompson *et al.*, 2016). On the other hand, biochar is less costly and, more important, it is a biomass-derived material, so even more environmentally friendly. Biochar is a bio-sorbent with a carbon content varying from 50 to 93 wt.% which is obtained through biomass pyrolysis: raw

materials for biochar production may be any natural resource with a high carbon content, such as agricultural residues, woody plants or animal wastes (Alhashimi and Aktas, 2017). Both biochar and AC find a solid application in COS hydrolysis, because of their well-developed pore structure and high specific area (Song *et al.*, 2017; Yi *et al.*, 2013).

Li et al. (Li *et al.*, 2010) reported the evaluation of the low temperature hydrolysis performances on promoted AC, in particular Al-Na-AC. The authors reported that the realized formulation acted as bi-functional catalysts, with two different active sites: (i) the hydrolysis site, where COS is converted to H_2S and (ii) the oxidation sites, where H_2S is subsequently oxidized to elemental S or sulfuric acid, thus not appearing in the outlet gas stream. Of course, the deposition of a solid product onto the surface lead to a certain deactivation of the catalyst, due to the textural changes and active sites losing. The authors evaluated the reaction performances in different condition of temperature, relative humidity (RH) and space velocity. In the low temperature conditions evaluated, COS hydrolysis is by far more sensitive to temperature than oxidation, thus it was considered as the rate determining step (RDS) of the reaction: as the hydrolysis performances increased with temperature, it was observed an increase in the breakthrough time at higher temperatures. The stability properties were quantified by means of a deactivation coefficient, α, and a sulfide deposition coefficient, β: the authors found that β was not affected by temperature while a slight variation in α was observed, obtaining a minimum at 50 °C. The influence of the relative humidity on these parameters was instead remarkably higher, with a marked decrease both in α and β with the increase in RH, which then determined an enhanced increase in removal efficiency. Nevertheless, this also couples to the negative impact which water has on COS hydrolysis rate, due to the competitive adsorption of the reactants on the catalyst surface.

The effect of the operating conditions on simultaneous COS and CS_2 hydrolysis in presence of Al_2O_3-K/CAC (where CAC is a coal-based activated carbon) was also studied by Sun et al. (Sun *et al.*, 2014) in the temperature range 30 – 70°C. The authors observed that calcination temperature has a non-monotonic effect on the catalyst stability, in fact a remarkable advantageous condition was found to be at 300 °C, in the investigated range of 200-600 °C. The change in temperature found a good agreement with the literature studies: COS hydrolysis was always promoted by a temperature increase, even if reporting the same trend overtime and slightly different conversions when raising from 50 to 70 °C, while CS_2 hydrolysis showed its better performances at lower temperatures and in particular at 50 °C. Moreover, the sulfur capacity (mg_S/g_{AC}) reached its maximum at 50 °C. This was why the hydrolysis product (H_2S) can be converted in elemental sulfur (S) or sulfuric acid, and the yield rate to the latter increases faster than that to S, thus leading to poisoning of the catalyst.

Yi et al. studied microwave activated carbons for LTH of COS using two different AC types, in particular microwave coal-based activated carbon (MCAC) and microwave coconut shell activated carbon (MCSAC), doping both the blank samples with Fe-Cu-Ni mixed metal oxides (Yi *et al.*, 2013). The study pointed out that pore volume and specific surface area (SSA) are important parameters for the hydrolysis performance, as Fe-Cu-Ni/MCSAC, which gave the best activity and stability, showed more pores and higher SSA. Furthermore, the stability of the sample was related, by XPS analysis, to the presence of a smaller amount of S and SO_4^{2-} species on the catalyst surface.

In general, AC were found to present very high COS conversions, but their stability only lasts few hours. Guo et al. compared the stability of K^+/AC with K^+/PCN and X-MPCN (where X could be Li^+, Na^+, K^+, Rb^+, Cs^+) (Guo *et al.*, 2019). Polymer carbon nitride (PCN) is a N-and-C compound that presents a unique structure and intrinsic abundant basic sites, thus it actually is promising in acid compounds-related processes, while metalated PCN (MPCN) is a metal promoted compound, where the doping agents frequently are alkali metals. The study pointed out that MPCN catalysts always have a lower initial COS conversion but, with they have an incredible stability overtime. Thus, the more active formulations, namely K^+-MPCN and Rb^+-MPCN, overcome the K^+/AC conversion value after 3 hours of reaction.

Song et al. (Song *et al.*, 2017) evaluated the performances of low temperature COS hydrolysis in presence of a series of walnut shell biochar (WSB), studying the effect of type and amount of metal oxides and alkali in the formulation and of the calcination temperature. The proposed work reports an interesting evaluation on the effect of several transition metals on the hydrolysis performances. In particular, the catalysts were prepared by loading 13% KOH on WSB and the activity and stability of the WSB supported catalysts can be listed in decreasing order as follows: Fe-KOH/WSB > 13%KOH/WSB > pure biochar > Ni-KOH/WSB > Cu-KOH/WSB > Zn-KOH/WSB > Cr-KOH/WSB > Co-KOH/WSB. The sample Fe-KOH/WSB was found to perform as its best when Fe was impregnated by $Fe(NO)_3$, with an optimal loading of 5 wt.% and at the calcination temperature of 400 °C. Bimetallic formulations were also evaluated, obtaining a decreasing activity and stability in the order Fe-Cu > Fe-Zn > Fe-Ni > Fe-Co > Fe > Fe-Cr.

II.4 High-temperature COS hydrolysis

II.4.1 Al_2O_3 and other metal oxides

As already discussed for low-temperature COS hydrolysis, a relevant parameter, together with the density of hydroxyls on the surface, is the specific surface area (SSA) of the catalyst. In the case of alumina, the work of Williams et al. (Williams *et al.*, 1999) demonstrated that the higher the SSA, the higher was the reaction rate observed. Further significant information comes from

the work of Huang et al. (Huang *et al.*, 2006a) performed on a 300 m^2/g γ-Al_2O_3. The authors observed that when COS hydrolysis is performed al 220°C with a simplified stream, only containing COS and water (with dilution in N_2), a mixture of solid and liquid elemental sulfur is produced with a selectivity of ca. 18%. Therefore, if this was the industrial conditions, alumina would not be suitable for large-scale applications. Nevertheless, the experiments performed with an industrial simulated stream containing CO, CO_2 and H_2 showed the absence of elemental sulfur deposited in 20 h of time-on-stream reaction, leading to the conclusion that these compounds hinder the sulfur formation, making alumina perfectly suitable for industrial applications.

Even though alumina is the most widely studied oxide for COS hydrolysis, both as catalyst itself and as support for active metals, other oxides have been evaluated, such as titania or rare earth metal oxides. Bachelier et al. reported a comparative study on the activity of different metal oxides, namely Al_2O_3, ZrO_2 and TiO_2, towards COS hydrolysis (Bachelier *et al.*, 1993). The study pointed out that hydrolysis proceeded with higher extent on ZrO_2 and the author attributed this result to the high density of OH groups, which presence on the catalyst surface was higher on zirconium oxide. The remarkable activity of ZrO_2 was reduced by both SO_2 addition and sulfidation, even though the order of activity was not varied, and zirconia was still the best performing catalyst compared to alumina and anatase.

Yang et al. investigated pure SnO_2 and rare earth metal-doped SnO_2 for the high temperature simultaneous COS and H_2S removal (Yang *et al.*, 2016). SnO_2 was doped with Y and La, and the comparison of the pure and doped oxide showed that the latter had a remarkably higher breakthrough sulfur capacity. The authors ascribed this evidence to the higher pore volume and smaller pores of the doped SnO_2, which led to a better dispersion of Y and La and consequently to higher COS conversion and a lesser extent in SnS formation during desulfurization. The 40 wt.% La-SnO_2 sample resulted in a breakthrough sulfur capacity (BSC) of 148.4 mg/g with a nearly 100% COS conversion.

The introduction of the oxygen vacancies in metal oxides could represent an interesting approach to enhance the catalytic activity by promoting the water dissociation and the formation of the hydroxyls. The formation of asymmetric oxygen vacancies in transition-metal doped CeO_2 catalysts was studied for the COS hydrolysis reaction (Zhao *et al.*, 2020a). The transition metals (Fe, Ni, Co) were inserted in the lattice of CeO_2 and formed a solid solution structure. The catalytic performances were evaluated in the range of temperature of 100-200°C. The Co/CeO_2 exhibited the highest COS removal efficiency (87%) any showing deactivation phenomena within 50 h of testing. The COS hydrolysis reaction was studied over this catalyst in presence of the 20 vol.% CO under humid conditions (2.5 vol.% H_2O). The authors observed that when water and CO were fed to the reactor, the COS removal was complete, while when they were cut off the COS conversion decreased

suddenly to zero. When water was resupplied, the removal efficiency of COS and the selectivity of H_2S returned to the initial values (100%) due to the replacement of the hydroxyl groups. The presence of oxygen could also be detrimental for COS hydrolysis catalysts, as H_2S oxidation leads to elemental sulfur deposition on the surface, which can cause continuous changes in the textural properties and a decrease in the number of the active sites because of the physical covering.

II.4.2 Active species for high-T COS hydrolysis

The comparative studies present in literature which compare alumina catalysts with other metal oxides highlight that alumina is by far the most suitable species for the catalysis of COS hydrolysis. Nevertheless, modification of bare alumina with other components often allows to enhance the catalytic performances and the sulfur-poisoning resistance, impacting on the life time of the catalyst. In general, two types of doping can be distinguished: transition-metals doping or alkali and alkaline-earth metal doping. The formers are often employed because the presence of a metal offers a different kind of active site which can be more suitable for the adsorption of reactants; on the other hand, the latter are employed thanks to their basic behavior, which not only promotes the activity of the catalyst but also hinders sulfur deposition or sulfidation of the active sites.

The promotion effect of Zn on alumina at 150 °C was investigated by Huang et al. (Huang *et al.*, 2005), through a series of catalysts with a variable Zn loading and obtained with different preparation method (incipient wet impregnation and co-precipitation). Untreated bare alumina rapidly deactivates, reaching in 4 h a stable value of COS conversion; the same value was achieved with a previous sulfurization of the catalyst with H_2S or with H_2S in presence of water. In the Zn-doped sample, instead, a continuous decrease in the activity was observed both for the untreated and the sulfided catalyst, while the fully sulfided catalyst showed a remarkably low activity. Zn addition to γ-Al_2O_3 decreases the rate of deactivation, which is very pronounced for the undoped alumina catalyst, but the ZnO acts like sink for sulfur species, thus the enhancement in intrinsic activity is intended to be short lived. These catalysts were further tested at higher temperature (220 °C) and in presence of more complex feedstocks (Huang *et al.*, 2006a). The work pointed out that in this condition the ZnO-doped catalyst was the most long-living, allowing a running time of 591 h, further highlighting the promotional effect of zinc addition.

Shangguan et al. studied the performances of a synthesized magnesium-aluminum spinel in the range 150-250 °C and compared the performances with a bare alumina (Shangguan *et al.*, 2019). They observed that, in general, $MgAl_2O_4$ catalyst resulted in better performances in any experimental condition, changing the temperature and the space velocity in the range 2000

– 12000 h^{-1}. The greatest difference between the un-doped alumina and the magnesium-aluminum spinel was observed in the stability, which was evaluated at 250 °C and 9000 h^{-1} for almost 30 h. The $MgAl_2O_4$ catalyst showed a reduction in conversion from 99% to 97%, while γ-Al_2O_3 was 100% active at the beginning of the test, but the COS conversion dropped to 87% at the end of the experiment. The authors ascribed these results to the higher pore volume and pore size showed by the $MgAl_2O_4$ spinel catalyst, which led to an improved diffusion rate of COS hydrolysis.

Nimthuphariyha et al. reported a study on COS hydrolysis at 7000 h^{-1} and T = 150 – 250°C on a series of Pt/Al_2O_3 catalysts doped with barium, in which both the metals loadings were optimized (Nimthuphariyha *et al.*, 2019). They found that the Al_2O_3 gradually deactivates in an atmosphere containing 500 ppm of COS, but the activity showed a sudden decrease when the COS concentration was risen to 750 ppm. The addition of Pt allowed to hinder this phenomenon, and the positive effect was as marked as Pt loading was higher. Nevertheless, the trend in deactivation observed for alumina with 500 ppm of COS was the same for $0.5\%Pt/Al_2O_3$ with 1000 ppm of COS. Further stabilization was achieved with Ba addition to alumina: in particular, the best performances were achieved by the $0.5\%Pt/5\%Ba/Al_2O_3$ formulation, which allowed to obtain a complete COS conversion at 200°C for the whole 10-hours test at different COS concentrations. The authors evaluating also the effect of the effect of temperature, reporting that a decrease in temperature leads to a decrease in activity in any condition.

Pt addition, together with K_2O, was reported also by Shangguan et al., who highlighted that these components addition allowed to enhance the hydrolysis performances. The CO_2-TPD evaluation pointed out that Pt and K increased the number of basic centers, and in particular that the weak basic centers are the active sites for COS hydrolysis.

Not always the addition of other component has a positive effect on the reaction performances of the hydrolysis catalyst. Xu et al. reported a study on the promotion of Al_2O_3 with Mo and K, with the aim of improving the deoxidization ability of the catalyst (Xu *et al.*, 2018). In fact, the authors observed that the presence of oxygenated compounds in the reacting system may lead to sulfidation of the catalyst. Even though the study was effective in finding a formulation which could improve the deoxidation ability of the catalyst, in particular with K addition, at the same time it was observed that the addition of Mo to alumina decreases the surface basicity, thus leading to a worsening in the hydrolysis performances. The COS conversion was further decreased by pre-sulfidation of the catalyst, when MoS_2 became the species present on the surface.

II.4.3 Oxysulfides

Oxysulfides are also studied as catalysts for COS hydrolysis, as they demonstrated to have a higher resistance to O_2 and SO_2 presence than a more conventional oxide such as alumina or titania. Zhang et al. investigated several oxysulfide catalysts, in particular sulfidized oxides of rare earth metals (Zhang *et al.*, 2004). The order of activity was found to be La ≈ Pr ≈ Nd ≈ Sm > Eu > Ce > Gd ≈ Ho > Dy > Er with an almost complete COS conversion found for the most active formulations at 200°C and 5000 h^{-1}. La_2O_2S was tested in presence of O_2 and SO_2 and the results showed that the catalyst had an excellent resistance in presence of the former, while the activity resulted depressed by SO_2 introduction. Nevertheless, the poisoning effect could be suppressed by increasing the reaction temperature and the catalyst was found to be able to recover its initial activity once SO_2 was removed from the gas stream.

Sulfides are widely present in sour gas abatement process because the former part of an oxide-catalytic bed of a desulfurization reactor is often sulfurized; if the formed sulfide is active towards COS hydrolysis, there is the concrete possibility of COS conversion before the contact with the oxide. In this view, as ZnO was widely studied as a good sorbent for sulfur compounds, Taniguchi et al. studied COS hydrolysis over ZnS formed from ZnO sulfurization (Taniguchi *et al.*, 1995). The authors found that ZnS is active towards COS hydrolysis and, to a lesser extent, also towards COS hydrogenation. From the results of the experimental activity, the study suggests that if the contact time between COS and ZnS is sufficient, the equilibrium of COS conversion in H_2S is expressible with eq. II-12.

$$2COS + H_2 + H_2O \rightleftarrows 2H_2S + CO + CO_2 \qquad \text{II-12}$$

II.5 Comparison between low-T and high-T process

As widely discussed in the previous sections, the low-temperature process particularly suffers of the limitation to diffusion. Therefore, a strong focus on the textural properties is evident in literature works. On the other hand, the high-temperature process can easily work under kinetic-controlled conditions, and consequently more conventional metal oxides are involved in the literature studies, as reported in Fig. II-4. Furthermore, a consistent fraction of the research involves alkaline and alkaline-earth metals, which exhibit basic properties, resulting the most suitable species to be employed for a base-catalyzed reaction as COS hydrolysis.

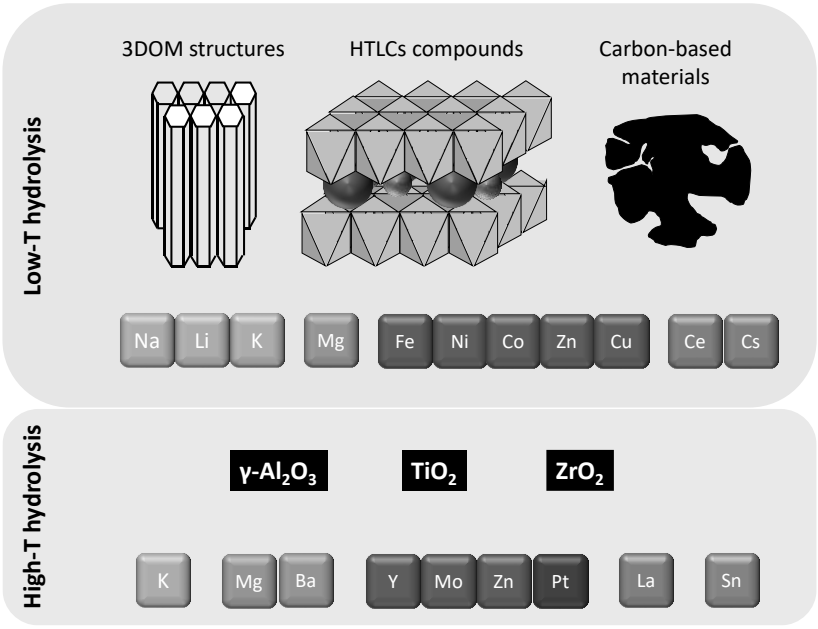

Fig. II-4: Catalytic systems available in literature for performing low-T and high-T hydrolysis

A summary of the discussed studies is reported in Table II-3.

Table II-3: Summary of the literature review on catalysts for COS hydrolysis at Low/High Temperature

LOW-TEMPERATURE HYDROLYSIS (LTH)			
Catalyst	**Highlights of the study**	**Year**	**Ref.**
Fe_2O_3	Fe_2O_3 catalyzes COS hydrolysis and stabilizes H_2S as iron sulfide: simultaneous removal	1992	(Miura *et al.*, 1992)
Na, Fe, Co, Ni, Cu and Zn doped γ-Al_2O_3	Ni and Zn enhance the specific activity without losing in stability	2001	(West *et al.*, 2001)
Li, Na, K, Cs, Mg, Ca and Ba doped γ-Al_2O_3	Na and Mg enhance the performance but are short living; K and Cs slightly improve the conversion at high loadings	2003	(Thomas *et al.*, 2003)
Commercial Al_2O_3	O_2 presence is detrimental for COS hydrolysis; the deactivation coefficient is a function of relative humidity	2008	(Wang *et al.*, 2008)
Zn-Ni-Al-Ce HTLCs	Ce doping remarkably enhance the catalytic performances, with a maximum reached at the Al/Ce ratio equal to 50	2010	(Zhao *et al.*, 2010)
Al-Na-AC	RH is the driving factor, as it decreases the hydrolysis rate but enhances the removal efficiency by shrinking the deactivation	2010	(Li *et al.*, 2010)
HTLCs	Non-stable samples; best activity overtime observed with the preparation condition of 25°C and pH = 7 – 9.5	2011	(Wang *et al.*, 2011)
Zn–Ni–Fe containing HTLCs	Very high conversion and stability with $M^{(II)}/M^{(III)} = 3$	2012	(Zhao *et al.*, 2012)
CoNiAl-HTLCs modified by cerium	Al/Ce ratio equal to 50 gave the best active and stable catalyst	2012	(Wang *et al.*, 2012)
Fe-Cu-Ni promoted MCAC and MCSAC	Fe-Cu-Ni/MCSAC: highest pore volume and SSA and smallest amount of S/SO_4^{2-}, thus was the most active and stable catalyst	2013	(Yi *et al.*, 2013)

State of the art

Al_2O_3-K/CAC	Simultaneous COS and CS_2 hydrolysis finds its maximum sulfur capacity at 50°C	2014	(Sun *et al.*, 2014)
MgAlCe hydrotalcite-based compounds with different ratio of Al/Ce	The effect of the ratios of Al/Ce, pH during the preparation, hydrothermal and calcination temperature on the COS removal efficiency was investigated	2015	(Guo *et al.*, 2015)
Preparation of NiAl-HTLCs with ultrasonic treatment	The hydrotalcite treated with ultrasonic presents a higher particle dispersion and a smaller crystallite size with respect to the sample prepared by the co-precipitation method	2016	(Zhao *et al.*, 2016)
Transition metals on KOH-activated biochar	Fe>KOH>biochar>Cu>Zn>Cr>Co $Fe(NO)_3$, Fe = 5%wt, T_{calc} = 400°C Fe-Cu>Fe-Zn>Fe-Ni>Fe-Co>Fe>Fe-Cr	2017	(Song *et al.*, 2017)
K doping of NiAl-HTO	KCl and KNO_3 decrease the desulfurization efficiency; KOH and K_2CO_3 enhance the activity by modifying the Lewis basicity of Ni	2018	(Zhao *et al.*, 2018)
K_2CO_3 doped 3DOM structures of Al_2O_3 and TiO_2	The structure allows an effective pulling out of H_2S, thus enhanced COS hydrolysis activity	2019	(He *et al.*, 2019)
ZnNiAl-HTO	HTO-10 achieved an almost total stable conversion; the basic sites decreased in the order HTO-10 > HTO-9 > HTO-11	2019	(Zhao *et al.*, 2019b)
NiO_xAl-HTO where x = 1, 3, 5	activity decreased in the order Ni3Al-HTO > Ni5Al-HTO > Ni1Al-HTO	2019	(Zhao *et al.*, 2019a)
X-MPCN and K^+-AC (X = Li^+, Na^+, K^+, Rb^+, Cs^+)	K^+-MPCN and Rb^+-MPCN: highest COS conversion and no loss of activity in 10 h	2019	(Guo *et al.*, 2019)
MgAl-LDHs nanosheets	New solid-state mechanochemical synthesis method	2019	(Mi *et al.*, 2019)

Transition metals (Fe, Ni, Co)- on CeO_2	CeO_2, Fe/CeO_2, Co/CeO_2, Ni/CeO_2 showed high stability for the COS hydrolysis reaction	2020	(Zhao *et al.*, 2020b)
Fe_2O_3 and CuO Fe_2O_3+CuO catalysts	The higher COS removal efficiency (100%) was obtained on the Fe_2O_3+CuO catalysts for the first 5h	2020	(Song *et al.*, 2020)
N-doped MgAl-LDO	A complete COS conversion was obtained at 70°C for 24 h without any deactivation phenomena	2021	(Wei *et al.*, 2021b)

HIGH-TEMPERATURE HYDROLYSIS (HTH)

Catalyst	Highlights of the study	Year	Ref.
ZrO_2, TiO_2, Al_2O_3	ZrO_2 has higher OH groups presence on the surface and results in better activity	1993	(Bachelier *et al.*, 1993)
ZnS	ZnS is active towards COS hydrolysis and, to a lesser extent, COS hydrogenation	1995	(Taniguchi *et al.*, 1995)
Oxysulfides	Activity order: La ≈ Pr ≈ Nd ≈ Sm > Eu > Ce > Gd ≈ Ho > Dy > Er La_2O_2S underwent deactivation only in presence of SO_2 (good O_2 resistance)	2004	(Zhang *et al.*, 2004)
ZnO/γ-Al2O3	Zn addition to γ-Al_2O_3 decreases the rate of deactivation	2005	(Huang *et al.*, 2005)
Al_2O_3	The simulated industrial stream contributes to enhance the selectivity to H_2S	2006	(Huang *et al.*, 2006b)
SnO2 + Y + La	La and Y promote COS hydrolysis; 40%La-SnO_2 resulted in BSC of 148.4 mg/g	2016	(Yang *et al.*, 2016)
Mo and K doped Al_2O_3	Mo and K increase the deoxidation ability but decrease the hydrolysis performances	2018	(Xu *et al.*, 2018)
$MgAl_2O_4$, Al_2O_3	$MgAl_2O_4$ offers higher pore volume, thus higher removal efficiency	2019	(Shangguan *et al.*, 2019)
Pt-Ba/Al_2O_3	0.5%Pt/5%Ba/Al_2O_3 achieved a total COS conversion for 10 h	2019	(Nimthuphariyha *et al.*, 2019)

**LTH has T < 80°C; HTH has T > 100°C*

II.6 The industrial interest

COS removal from natural gas, synthesis gas or process and fuel gasses has acquired a huge importance, as widely discussed in the Introduction. The interest of industry toward this application is demonstrated by the large number of patents concerning the hydrolysis reaction in gas/liquid phase that were registered over the last 50 years. Patents give a solid representation of the point reached by the research, at least in terms of applicable solutions, and provide for a strong indication on the main achievements, on what is still missing and what can be further done in this field.

In this paragraph, the most recent solutions proposed over the past 20 years were listed and summarized. The patents refer to the formulation and synthesis of novel catalysts for COS hydrolysis in gas phase, and the design of plants for the purification of the gaseous stream containing sulfur compounds such as COS, H_2S, SO_2 or other contaminants as NH_3, HCN. The claims for each patent and the most relevant information, in terms of species and operating temperature, are reported in Table II-4.

Table II-4: Summary of the patents pending on COS removal since 2010

Patent no.	Speci	Claims	T (°C)	Year	Ref.
US 7846325	COS, H_2S	-COS-hydrolizing catalyst comprising TiO_2 supported on carrier, silica or metal ions of Group VB, VIB, VIIB -H_2S Removal on adsorbents including ZnO and inorganic support material	COS removal: 140-200°C H_2S removal 70-260 °C	2010	(Martijn *et al.*, 2010)
US 9278312	CO, CO_2, COS, H_2S	CO shift reaction COS hydrolysis H_2S and CO_2 absorption Generating power by using the fuel gas without CO_2	COS hydrolysis 150-350 °C H_2S absorption 40-60 °C	2016	(Sato *et al.*, 2016)
US 9394490	COS	COS removal by adsorption in two packed bed columns Adsorbent comprises alkali impregnated Al_2O_3, zeolites	Adsorption T=15-100 °C Regeneration T=149-316 °C	2016	(Trucko *et al.*, 2016)
US 9604206	COS	Method for regenerating a COS hydrolysis Ba/TiO_2 honeycomb catalyst washing with acid or alkali	Regeneration T = 25-60 °C Heat Drying T = 80-200 °C	2017	(Yonemura *et al.*, 2017)
US 9845438	COS, H_2O, CO_2, H_2S	Apparatus and method for the purification of a gaseous stream A TiO_2, Al_2O_3, chromium-based catalyst is used for the COS hydrolysis	200-400 °C	2017	(Kato and Nakamura, 2017)
US 20200398256A1	COS	-Ba with $K_2O/Na_2O/Cs_2O$ b supported on TiO_2	T=150-300°C	2020	(Nochi *et al.*, 2020)

A solution of high interest and remarkable potential in terms of industrial application is the one commercialized by IFP Energies Nouvelle (France). The company focused on the objective of reaching the highest possible removal efficiency, by performing the hydrolysis reaction in presence of a suitable heterogeneous catalyst and properly coupling this unit with other cleaning technologies. To date, the removal of sulfur compounds from gaseous streams is performed via absorption in aqueous amines solutions, in the so-called sweetening technology. The existing sweetening processes do not have the capability to remove all the COS while maintaining high H_2S/CO_2 selectivity (typically achieved with the employment of MDEA solutions), therefore the coupling of this technology with the hydrolysis of carbonyl sulfide is highly attractive. The COSWEET^{TM} process, developed by IFP Energies Nouvelles (IFPEN), is the technology for a deep COS removal closest to the industrial application. Through the evaluation of several plant configurations, the company ended up with the proposal of a catalytic reactor integrated within the selective removal of H_2S by a MDEA amine unit, following the scheme given in Fig. II-5.

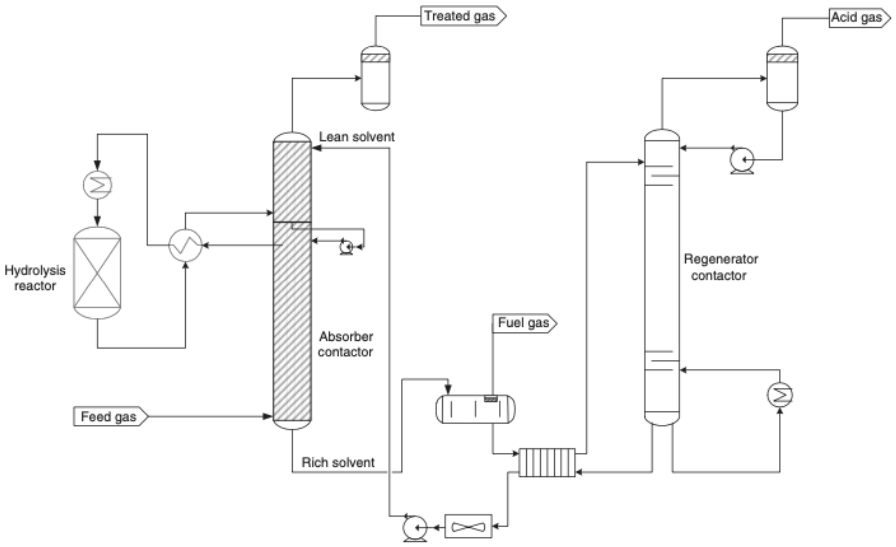

Fig. II-5: COSWEET^{TM} process developed by IFPEN

The solution proposes a sort of integration of the hydrolysis with the absorption, by connecting the inlet (COS reach) and the outlet (H_2S reach) of the hydrolysis reactor with two different section of the absorber contactor. In this way, the H_2S produced with the hydrolysis reaction still has a portion of the absorber available to be removed. This solution is highly attractive, even though it is as far as possible to the idea of low expenses. The proposed configuration, if compared to the absorber alone, implies the addition of a reaction unit, two heat exchangers and a compression stage. Indeed, the COS

hydrolysis is currently performed at higher temperature than the sweetening process because of the kinetic limitations of the reaction, and the conventional pellets catalysts determine a remarkable pressure drop in the hydrolysis unit, requiring the pressurization of the feed stream.

As discerned in this chapter, the state of the art of COS hydrolysis has proposed several catalysts with the potential of being applied at room temperature; nevertheless, the investigations limited to the lab scale applications and the simulated streams keep these results still too far from the industrial perspective.

Chapter III.
Aims of this thesis

As examined in the previous sections, the removal of carbonyl sulfide is a key issue in the modern era, and its relevance could potentially grow. This Ph.D. project was proposed and funded by the company KT-Kinetic Technology of Rome (Italy). The company is an international EPC contractor in crude oil refining industry, specialized in sulfur recovery and gas treatment. The interest of the company - and of the industrial sector in general - toward the process intensification of COS hydrolysis is related to the necessity of an efficient, inexpensive and reliable removal technology. At the present time, different solutions are applied, but none of them allows to reach a competitive removal efficiency.

Therefore, this project has been structured to the aim of putting a step forward in the industrialization and commercialization of the COS hydrolysis technology, keeping as main objective the process intensification, in its founding principles of compactness and optimization.

To pursue this aim, the research has been conducted to address different types of targets:

- Investigation to reach the optimal **catalytic formulation**, to match the industrial need of inexpensiveness and easy supply with the specific requirement of high low-temperature activity
- Experimental evaluation of the possibility to couple the hydrolysis stage to the sweetening process in an **open-architecture plant configuration**
- **Process intensification**, from a catalytic and technological point of view, with the investigation respectively on structured catalysts and integrated closed-architecture configuration.

Chapter IV.
Materials and Methods

IV.1 Characterizations

For the characterization of the samples in this work, several analytic techniques have been employed: specific surface area (SSA) determination, X-ray diffraction (XRD), scanning electron microscopy (SEM) with EDS elemental mapping of the species, thermogravimetric analysis (TGA) and Raman analysis.

The SSA determination was conducted in a NOVAtouch Sorptometer (Anton Paar, Malmö, Sweden). The samples have been degassed at 150 °C for 12 hours and than N_2 at 77 K was adsorbed and desorbed for the determination of the full adsorption/desorption isotherm.

X-ray diffraction patterns were recorded under a CuKα radiation (λ=1.5406 Å) using a Bruker D2 instrument (Billerica, MA, United States); the samples were scanned over a 2θ range of 10-80° with a step of 0.05°.

The optical analysis was performed by means of a Scanning Electron Microscope (SEM) Philips Mod.XL30 (Amsterdam, the Netherlands), coupled to an Energy Dispersive X-ray Spectrometer (EDS) Oxford (Oxford Instruments, Abingdon, UK).

TGA was performed in the TA Instrument Q600 (New Castle, DE, United States), coupled with a Pfeiffer Quadrupole Mass Spectrometer (Pfeiffer Vacuum GmbH, Asslar, Germany) in order to analyse the gaseous phase produced during the analysis.

The Raman spectra were produced in a dispersive MicroRaman inVia, Renishaw (Renishaw, Wotton-under-Edge, UK), equipped with 514 nm Ar ion laser, in the range 200-2000 cm^{-1} Raman shift. Once selected, the optimized laser power of 25 mW was applied to all the samples.

IV.2 Experimental setup

The experimental setup used for this activity has been entirely designed and realized in the framework of this Ph.D. project; to the aim of following the different activities, it has been adjusted over the years, obtaining several dedicated configurations. Recalling the objectives of this work, the hydrolysis of carbonyl sulfide has been studied in "gas-phase" (with heterogeneous catalysts), in "liquid-phase" (non-catalytic) and in a three-phase trickle bed reactor. Therefore, different reactors and plant layout are described in this section.

For safety reason, each configuration of the experimental setup has been confined under a fume hood, to avoid possible toxic gasses leakages.

IV.2.1 Gas-phase COS hydrolysis

The experimental study on gas-phase COS hydrolysis comprehended both the screening of the catalytic formulation and operating conditions conducted over pellet catalysts and the process intensification with the study of structured catalysts.

The laboratory tests were carried out in a tubular stainless-steel reactor, reported in Fig. IV-1(a), heated with a 120 Ω heating element controlled by a PID device connected to a K-type thermocouple positioned on the external wall of the reactor. Since the dependency of the operating temperature was observed to be particularly strong, three K-type thermocouples were inserted within the catalytic bed through a 1/8'' sheath, and distributed axially to monitor the temperature for ensuring a perfect isothermal condition.

The reactor was vertically located in the plant layout proposed in Fig. IV-1(b). The gas feed was regulated by thermal mass flow controllers, connected to pure N_2 and pure CO_2 cylinders, and precision mixtures of COS in Ar (1 vol.% of COS) and H_2S in N_2 (0.2 vol.% of H_2S).

To ensure a precise control over water concentration, the typical literature configuration with a water saturator was avoided. Instead, the exact amount of water was fed in liquid phase and vaporized in a specifically designed boiler (Fig. IV-1(c)). This is constituted of a coil (Ø 3 mm) wrapped around a cartridge resistance (700 W) in which an exact amount of water is fed by a thermic-type mass flow controller (MFC). The outlet of the coil is connected to a shell (Ø 70 mm), in which N_2 is fed and a perfect mixing of vapor and inert is achieved; this is enhanced by the presence of steel wool within the shell.

Due to the presence of water in the reactant mixture, a vessel for water condensation and separation was always present before vent. Furthermore, each vent line was connected to an activated carbon vessel, to avoid COS and H_2S dispersion in the atmosphere.

The product stream was evaluated continuously by means of a Hiden Analytical mass spectrometer, following masses 18, 28, 34, 40, 44, 60, 64, 76 (respectively water, nitrogen, hydrogen sulfide - H_2S, argon, carbon dioxide, COS, sulfur dioxide - SO_2 and carbon disulfide - CS_2). The interference matrix and the electric parameters, i.e. the emission current and electron energy, were optimized in order to minimize the fragmentation within the chamber and to simultaneously intensify the signals for "small components", namely H_2S, COS, SO_2 and CS_2, which are present in ppm concentrations.

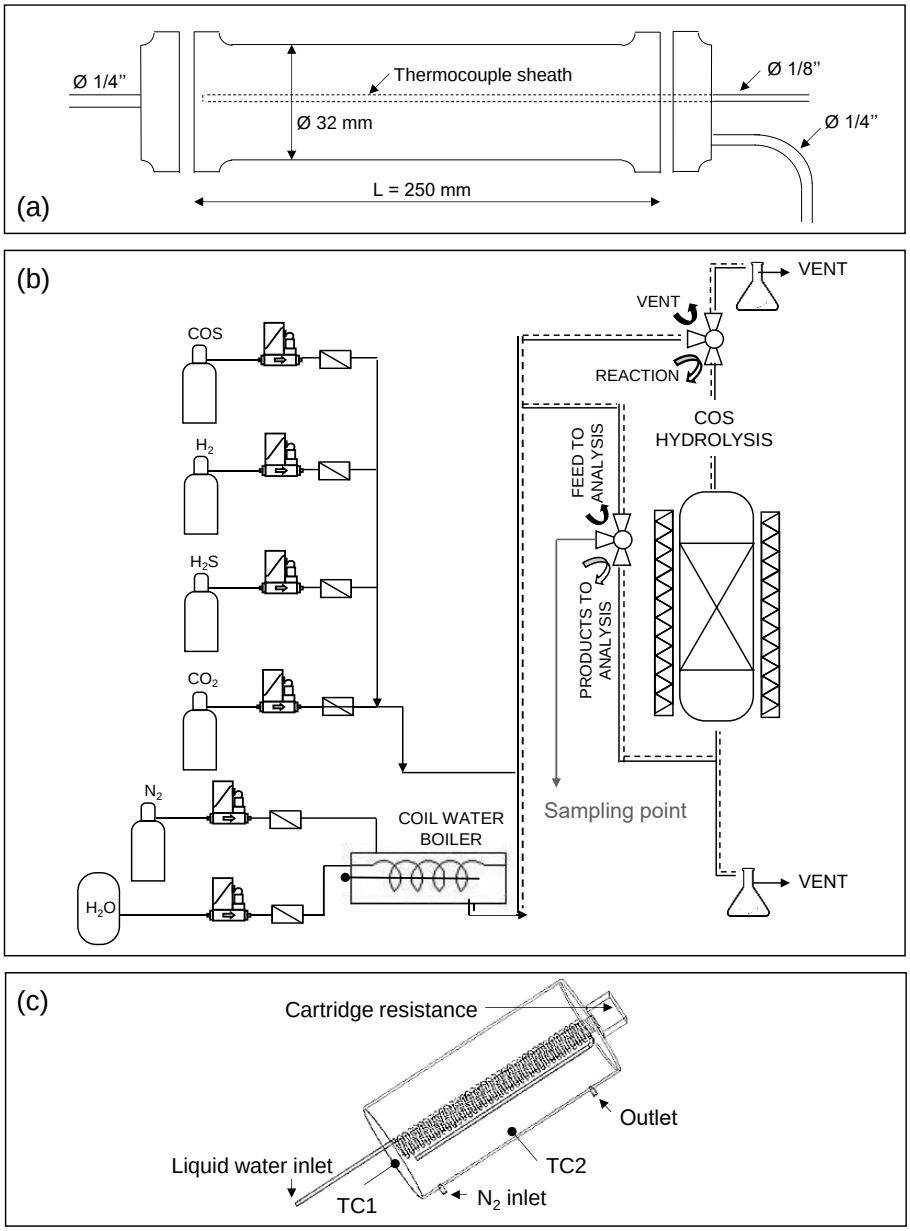

Fig. IV-1: Laboratory setup and units for COS gas phase hydrolysis: a) reactor; b) plant layout; c) water boiler design

IV.2.2 Liquid-phase hydrolysis and open-architecture configuration

The study of COS hydrolysis in liquid phase, using aqueous solutions of amines, was performed in a plant layout identical to the one illustrated in Fig. IV-1(b), but with the adequate change of the reactor. To avoid the motion of the liquid phase, a glass vessel (Ø30 mm) designed as a saturator was employed, as Fig. IV-2(a). The gas flows through a 6 mm ID tube concentric to the vessel from top to bottom, and rise through the amine solution in small bubbles, developing a high contact gas/liquid surface. The outlet gas is collected in another 6 mm ID tube in the upper part of the saturator.

The open-architecture configuration designed for the coupling of the hydrolysis section to the absorber is shown in Fig. IV-2(b). The absorption unit is downstream to the hydrolysis reactor, in order to work with a stream containing both H_2S and COS, and three different sampling points have been included, to the aim of analyzing the reactants stream (#1), the hydrolysis products (#2) and the products of the overall process (#3).

The analysis of the gaseous stream was performed as previously described with the mass spectrometer. The analyzer is able to process only one of the three sampling streams at time, so the choice of the time for switch between them is a relevant parameter.

IV.2.3 Integrated plant units and layout

The optimization of the absorber and the integration of the hydrolysis and sweetening steps in a single three-phase reactor led to the obtainment of a completely different reactoristic solution. The three-phase reactor, reported in Fig. IV-3(a), was designed as a Ø½" tube 130 mm long, with a cone in the upper part to discourage the entrainment of small droplets of liquids.

The reactor was properly located in the plant, obtaining the final layout reported in Fig. IV-3(b).

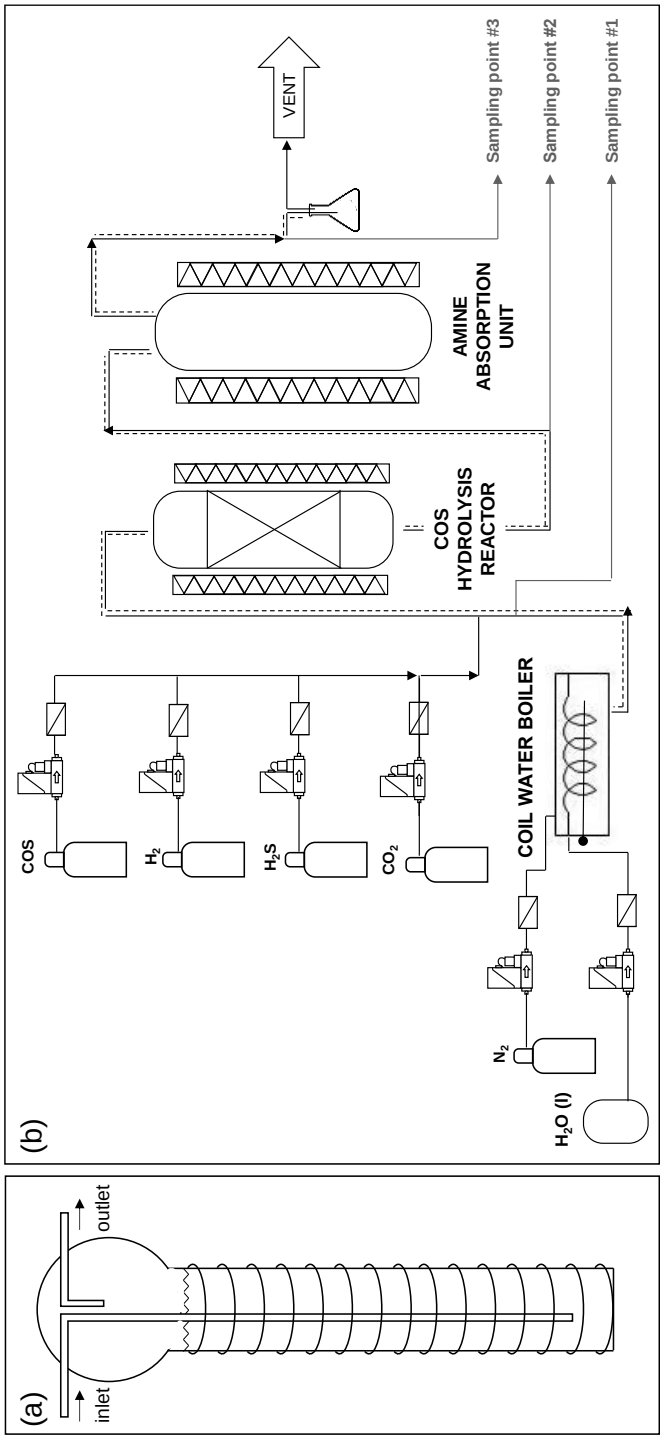

Fig. IV-2: Layout configuration for conducing the coupled system, COS gas phase hydrolysis + COS absorption in amine solutions

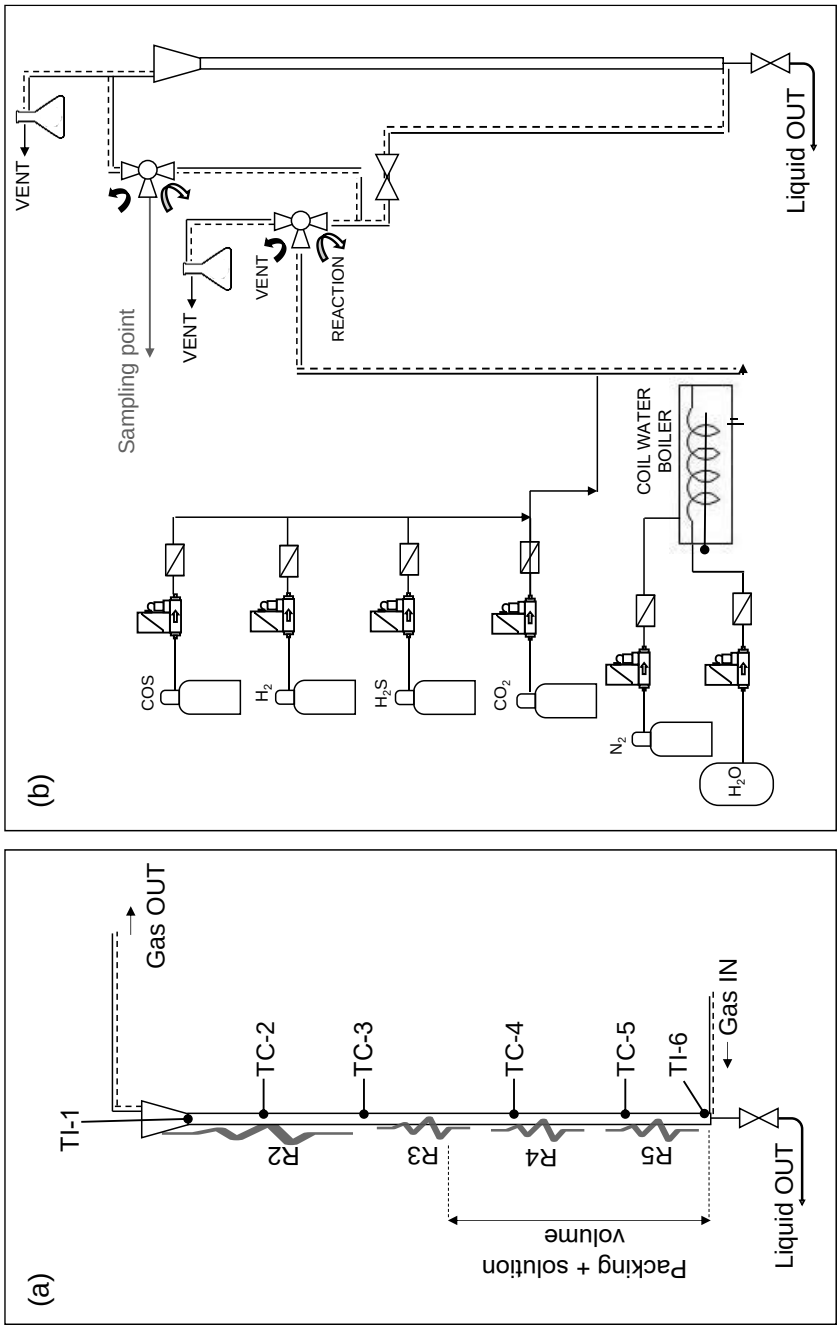

Fig. IV-3: (a) reactor for the three-phase process; (b) final layout configuration

IV.3 Pellets catalysts preparation

For the study of COS hydrolysis in gas phase, pellets catalysts in sphere shape were tested at first. Commercial γ-Al_2O_3 was calcined at 200°C and then employed as catalyst. 3 mm and 5 mm pellets (respectively provided by Fluka and Sigma-Aldrich) were employed in this phase. To enhance the catalytic activity, a modified-alumina was prepared on both supports. Following the wet impregnation procedure, calcined alumina spheres were immersed in a basic solution (KOH, provided by Sigma-Aldrich) for 1 h; the solution was prepared to obtain a 10 wt.% loading of K_2O after calcination. Then, the solution was filtered, and the recovered catalyst was dried overnight at 120°C and calcined at 200°C to obtain the complete conversion of KOH into K_2O.

Activation of the K-modified samples has been carried out with a 20% CO_2 in N_2 stream at 60°C, until complete transition of K_2O in K_2CO_3.

IV.4 Structured catalysts preparation

Structured catalysts are conventionally obtained using a carrier and a washcoat. The carrier is a complex 3D structure which can have different shapes and can be made of different materials; the characteristic is that a single piece or a modular configuration of several pieces constitutes the whole catalytic bed. On such structures, the adhesion of a catalytic material is usually obtained through the washcoating procedure: a slurry of the support or the active species themselves, called washcoat, is deposited on the carrier through a several steps procedure and, after drying and calcination, the structured catalyst is obtained.

In this work, the selection of the most adequate carrier was carried out, considering the following structures: (i) cordierite flow-through monoliths, (ii) steel wire mesh, (iii) OB-SiC foams with ppi = 10, (iv) Al foams with ppi = 40, (v) Ni-Fe alloy foams with ppi = 20.

IV.4.1 Washcoat preparation

The washcoat prepared in this work is a suspension of γ-Al_2O_3 in an aqueous solution containing pseudobohemite and methylcellulose. Considering that γ-Al_2O_3 is a catalyst for the hydrolysis of carbonyl sulfide, the washcoat itself is the active phase. For the modified-alumina formulation, potassium addition can be achieved through impregnation directly on the structured catalyst, following the same procedure adopted for the pellet-shaped samples. The washcoat was prepared as follows.

- A suspension of methylcellulose in water was prepared through stirring for 24 h (500 rpm) to achieve the polymer swelling.

- Once the suspension was completely transparent, pseudobohemite (γ-$Al_2O_3 \cdot xH_2O$, PS) was added and the suspension was kept stirring at 400 rpm for 12 h.
- In order to avoid the possible jellification of the slurry, the pH was adjusted at 4 by adding nitric acid (HNO_3).
- γ-Al_2O_3 was finally added at the suspension. The slurry was constantly stirred at 500 rpm for 24 h.

The amount of solids in the slurry was set at 20 wt.%, while the PS: γ-Al_2O_3 ratio was set at 3:10 and the methylcellulose content was fixed at 1 wt.%, based on previous works (Palma *et al.*, 2018).

For the described procedure, the following reactants were employed: pseudobohemite Pural SB (Sasol), γ-Al_2O_3 Puralox SCCa 150/200 (Sasol), nitric acid (Sigma-Aldrich), methylcellulose (Sigma-Aldrich). Before addition to the suspension, γ-Al_2O_3 is grounded in a mill Retsch RM100 until an average dimension inferior to 10 µm was achieved (the procedure takes approximately 1 h or milling). Average dimension was evaluated through optical microscopy.

IV.4.2 Washcoat deposition

Washcoat can be deposited on a structured carrier through several methods. Considering the shape of the carriers selected for this study, the dip-coating procedure was adopted as deposition system. The standard dip-coating procedure (Visconti, 2012) was at first followed, in order to discriminate the best carrier among the selected possibilities. This consists in a cycling procedure of: 1) dipping the carrier within the washcoat (20 min to 1 h); 2) remove the washcoat excess; 3) drying; 4) calcination. Usually, 5 to 10 cycles are necessary in order to deposit the desired washcoat amount on the carrier. Subsequently, the washcoat adherence is often verified with a mechanical solicitation, which can be compressed air blowing or ultrasound stress test. The achievable washcoat loading, the number of required steps and the mass of whashcoat lost after the solicitation are the parameters to be taken in consideration for the carrier choice.

Then, such procedure was optimized for the selected carrier as reported in Fig. IV-4. Drying was performed at 120°C for 1 h, while calcination was conducted at 450°C for 3 h, to achieve the transition from pseudobohemite to γ-Al_2O_3.

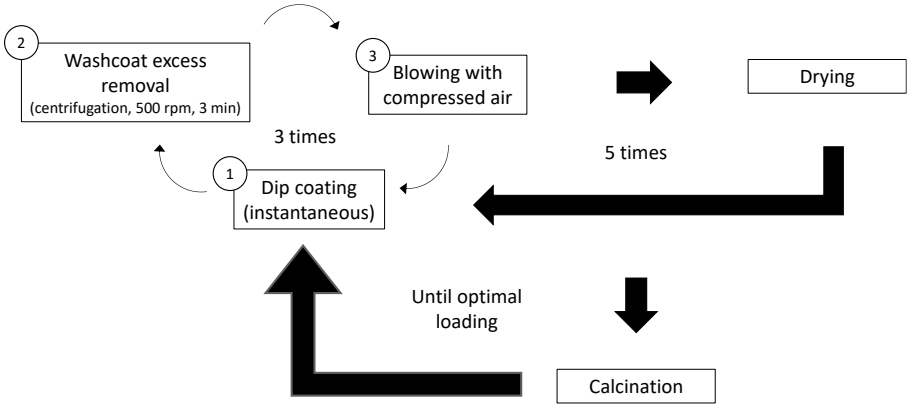

Fig. IV-4: Scheme of the dip coating optimized procedure

Washcoat excess removal was performed either by suction with a rotative pump or with a benchtop centrifuge, optimizing the rpm value: the latter method was found to be the most suitable for all the evaluated carriers, and the optimal velocity was set to 500 rpm.

Once reached the desired washcoat loading, the structured catalyst was doped with K, following the same impregnation procedure described for pellets catalysts; it was activated in a 20 vol.% CO_2 stream as well.

IV.5 Experimental evaluations

Operating conditions for all the experimental evaluations are briefly reported in this paragraph. A wide number of tests has been carried out, with a variety of operating conditions: for this reason, here are reported the ranges of investigation of each process; further information will be given alongside the results, for better clarity.

The COS hydrolysis in gas phase was conducted in the experimental setup reported in Fig. IV-1(b). Catalytic activity was evaluated at room temperature or slightly higher (30-80 °C), contact time was varied in the range 0.75 to 6 s and the concentration of the feed gas was constituted as follows: 500 ppm COS, water in the range 5-10 vol.%, eventual CO_2 presence, N_2 balance.

The absorption in amines solution was evaluated in presence of DEA and a customized tertiary amine solution provided by KT in the experimental setup showed in Fig. IV-1(b) using a saturator-like reactor showed in Fig. IV-2(a). Amines were diluted in aqueous solution with a mass concentration in the range 20-60%, and the absorption capacity was tested varying the temperature between 30 and 60°C. COS concentration was varied between 200 and 1000 ppm and then set to 500 ppm (simulating a condition without the hydrolysis step) and H_2S abatement was evaluated with concentration in the range 100-500 ppm in N_2 stream. The contact time realized in the absorber was varied between 30 and 60 s.

The efficiency in coupling COS hydrolysis and absorption unit was evaluated in the configuration of in Fig. IV-2(b). Both the units were operated at 60°C with a COS concentration in the feed stream of 500 ppm (10% H_2O, N_2 bal.); the contact time ensured was 3 s for the hydrolysis reactor and 18 s for the absorber.

The process intensification performing an integrated step of COS hydrolysis + gas sweetening was investigated in the designed reactor and plant layout respectively reported in Fig. IV-3(a) and (b). For these tests, the contact time was varied in the range 5-17 s.

Reaction performances were evaluated in terms of COS conversion in the hydrolysis unit (X_{COS}, eq. IV-1), COS and H_2S removal efficiency in the absorber (R_{COS}, R_{H2S}, eqs. IV-2 and IV-3 respectively) and the concentration of the sulfur compounds in ppm.

$$X_{COS} = \frac{COS(mol)_{IN} - COS(mol)_{OUT}}{COS(mol)_{IN}} \qquad \text{IV-1}$$

$$R_{COS} = \frac{COS(mol)_{IN} - COS(mol)_{OUT}}{COS(mol)_{IN}} \qquad \text{IV-2}$$

$$R_{H_2S} = \frac{H_2S(mol)_{IN} - H_2S(mol)_{OUT}}{H_2S(mol)_{IN}} \qquad \text{IV-3}$$

IV.6 Kinetic evaluations

IV.6.1 Power-law kinetic expression

A series of concentration-versus-contact time data can be processed using the differential or the integral method in order to analyze the kinetic data. Through the integral method, the rate equation is guessed and, after an appropriate integration and mathematical manipulation, the trend of the integrated concentration function versus time is observed. If it yields a straight line, the guessed expression describes adequately the rate of the studied reaction, and the kinetic constant is given by the slope of the obtained line. In the differential method, the fit of the rate expression to the data is verified directly and without any integration (Levenspiel, 2001). Bearing in mind such characteristics, the differential method of analysis requires a large number of experimental evaluations. Moreover, when a simple reaction rate expression is guessed, the integral method is always preferred.

In the preliminary hypothesis of no variation in temperature or water concentration, only the dependence from the COS concentration should be considered in the kinetic analysis. For this reason, the integral analysis method was adopted, guessing a rate expression as eq. IV-4, with n = 0, 1 or 2.

$$-r_{COS} = -\frac{dC_{COS}}{dt} = k_{app} {C_{COS}}^{n} = k_{app} {C^0_{COS}}^{n} (1 - X_{COS})^n \quad \text{IV-4}$$

The rate expression can be integrated for the variable X_{COS} instead of C_{COS} considering that no change in volume occur during the reaction. Hence, the integrated expressions are reported in eqs. IV-5, IV-6 and IV-7 respectively when $n = 0$, $n = 1$ or $n = 2$.

$$C^0_{COS} X_{COS} = k\tau \quad \text{IV-5}$$

$$-\ln(1 - X_{COS}) = k\tau \quad \text{IV-6}$$

$$\frac{1}{C_{cos}} \frac{X_{cos}}{1 - X_{cos}} = k\tau \quad \text{IV-7}$$

Considering then the effect of water concentration on the reaction rate, the power-law can be expressed as eq. IV-8.

$$-r_{COS} = -\frac{dC_{COS}}{dt} = (-r_{COS}) = k_{app} (C_{COS})^m (C_{H_2O})^n \quad \text{IV-8}$$

IV.6.2 Langmuir-Hinshelwood kinetic expression

For the Langmuir-Hinshelwood kinetic model, the COS hydrolysis reaction as expressed in eq. IV-9 was considered the only reaction to occur.

$$COS + H_2O \rightleftarrows CO_2 + H_2S \quad \text{IV-9}$$

Since the amount of reacting species is particularly low, the whole reacting domain was assumed to be isotherm despite the exothermicity of the system. The validity of this hypothesis was ensured by monitoring the temperature alongside the catalytic bed. As a first approximation, the power law expression for the reaction rate was considered (eq. IV-10). Nevertheless, according to the literature, the low-temperature reaction follows the Langmuir-Hinshelwood behavior, with the adsorption of both the reactants. Therefore, the reaction rate can be expressed as eq. IV-11, where θ_i is the number of active sites occupied by the i-species. In this expression, the effect of the reverse reaction was considered neglectable, taking into account the thermodynamic equilibrium of the system and the operating conditions adopted in this study (T < 100 °C).

$$r_{COS} = k_c \cdot {p^n}_{COS} \cdot {p^n}_{H_2O} \quad \text{IV-10}$$

$$r_{COS} = k_c \cdot \theta_{COS} \cdot \theta_{H_2O} \quad \text{IV-11}$$

The Euler method was used for the discretization of the system, applying the hypothesis of differential reactor, and the optimization of the parameters was based on the minimization of an objective function defined as eq. IV-12, where *c* represents the test, $X_{exp,c}$ represents the experimental value of test *c* and $X_{mod,c}$ represents the model results for the *c* condition.

$$f = \min\left(\sum_{c=1}^{n}(X_{exp_c} - X_{mod_c})^2\right) \qquad \text{IV-12}$$

To apply the hypothesis of differential reactor and to minimize the errors related to a less precise analysis of the products composition, the conditions with too high (> 90%) or too low (< 10%) COS conversion were excluded by the objective function.

Chapter V.
Characterizations

V.1 Characterizations results

V.1.1 Pellets catalysts

The pellet catalysts have been at first analyzed through SSA determination. Considered that the support employed was commercial γ-alumina, it was expected to have a high SSA value. Nevertheless, the support was calcined in order to produce the final catalyst, hence the specific surface area of the final catalyst K/Al3 was determined through BET method, and additional information on the porous structure have been obtained through the observation of the complete adsorption/desorption isotherm.

The sample showed a specific surface area of 204 m^2/g, and as can be observed from Fig. V-1 its porous structure is mainly characterized by the presence of mesoporosity. A non-neglectable amount of micropores was also present, and it can be deduced by the height of the knee of the curve, at low relative pressure values.

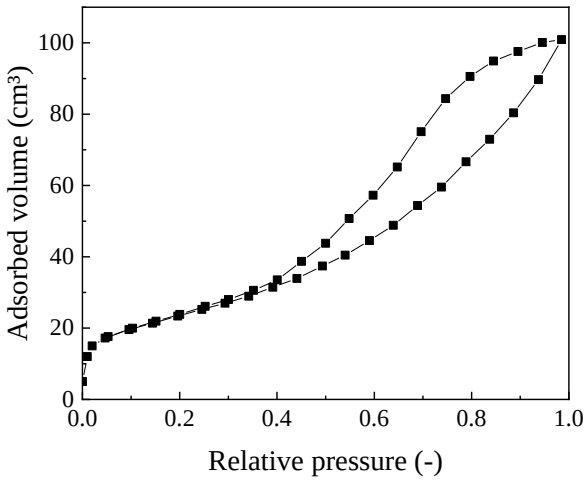

Fig. V-1: Adsorption isotherm of the pellet catalyst

The XRD spectrum of the catalyst showed only the characteristic peaks of the γ-alumina, in particular 28°, 38°, 49° and 67°, as displayed in Fig. V-2.

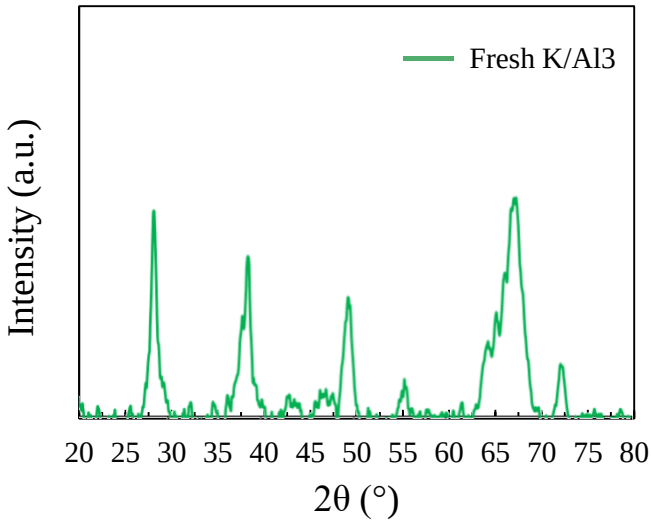

Fig. V-2: XRD spectrum of the fresh K/Al3 sample

Then, the dispersion of potassium was evaluated through SEM-EDX characterization, obtaining the elemental maps reported in Fig. V-3. From the images it is possible to appreciate the homogeneous dispersion of the deposited K onto the Al_2O_3 spheres, which is particularly important for the availability of the active sites and confirmed the suitability of the selected catalyst preparation method and of the potassium precursor employed.

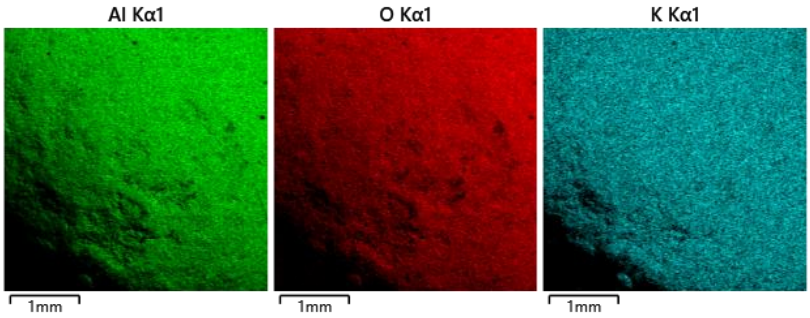

Fig. V-3: SEM-EDX images of the fresh sample K/Al3

Finally, the sample was tested via Raman analysis. As anticipated in section IV.5, the catalyst is activated in presence of a CO_2-rich stream to stabilize the formulation. Hence, the Raman spectrum of the final catalyst was directly compared to the one of potassium carbonate, as given in Fig. V-4. The main peak characteristic of K_2CO_3 is t 1063 cm^{-1}, and this Raman response

can be observed also in sample K/Al3, despite the peak is broader and less intense. Therefore, through this particular analysis it was possible to conclude that the activation procedure converts the K_2O formed during the calcination procedure into the more stable form of potassium carbonate.

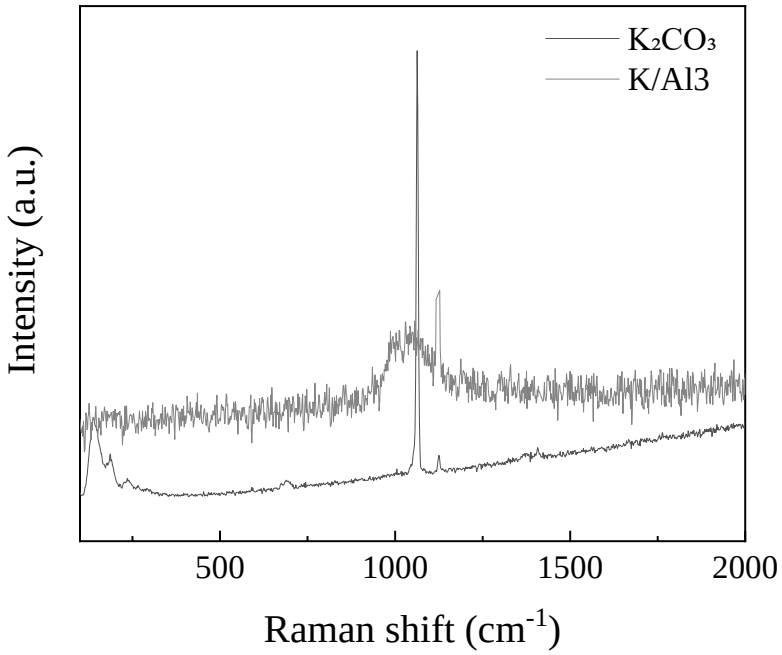

Fig. V-4: Raman spectrum of fresh K/Al3 compared to K_2CO_3

V.1.2 Structured catalysts

The most suitable carrier to prepare structured catalysts for COS hydrolysis was optimized in this work. Among five different kind of structures and materials, the selected one was a Ni-Fe foam, with a pores density of 20 ppi. The carrier, and the washcoat deposited according to section IV.4.2, have been observed with an optical microscope. The foam carriers widely used in catalysis are distinguished by several geometric parameters, but in particular the are described as "constituted by filament, and each crossing point between filament is called a node". From Fig. V-5 (a) it is possible to observe that the carrier is constituted by flat filaments, which is uncommon, since mostly they have a tubular shape. In addition, the randomic arrangement of the pores is particularly appreciable from the image, and it is possible to observe that the cells of the structure have remarkably different dimensions.

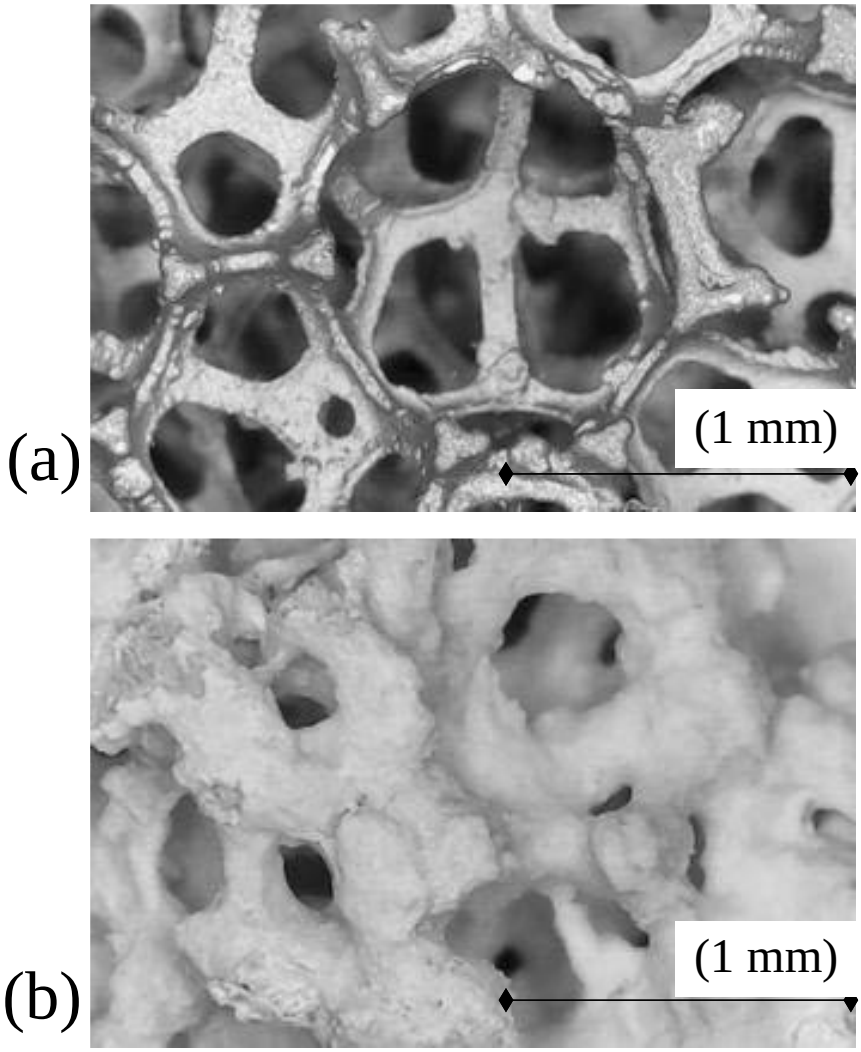

Fig. V-5: Optical microscope observation of: (a) NiFe foam carrier; (b) washcoated structure

From Fig. V-5 (b) it is possible to observe that the high loading of washcoat deposited onto the structure creates a layer of non-neglectable thickness. Indeed, also the cell size is remarkably reduced by the presence of the washcoat layer.

As discussed, a previously studied procedure was adopted for the washcoat preparation. Before the deposition of the washcoat onto any of the structured carriers, the liquid slurry was characterized in order to verify the content of solids in the slurry and in order to set the optimal calcination temperature. The former is particularly important for the viscosity of the washcoat: too low viscosity does not ensure the optimal adhesion on the carrier and too high

viscosity increases the risk of plugging the carrier structure. The latter impacts on the crystalline structure of the layer but also on the specific surface area: the choice of a too low calcination temperature could not ensure the complete transition of PS into γ-Al_2O_3; on the other hand, a too high calcination temperature would damage the exposed surface, negatively impacting on the mass transfer phenomena.

The content of solid was evaluated through thermo-gravimetric analysis (TGA). As displayed in Fig. V-6 (a), the sample undergoes a remarkable weight loss below 200 °C. This is to be ascribed to the water loss, and the remaining mass, which corresponds to the solids content in washcoat, was exactly 20 wt.% of the initial slurry. Further evaluation of the mass produced by calcination in air – given in Fig. V-6 (b) – highlighted the water removal from the sample; CO_2 can be addressed to decomposition of methylcellulose.

The crystalline structure was observed via x-ray diffraction (XRD) analysis on washcoat samples calcined at 200 and 450°C (W200 and W450 respectively). The diffraction spectra obtained for both samples are reported in Fig. V-7; standard diffraction peaks for pseudobohemite and γ-Al_2O_3 were added as reference. The comparison among the samples clearly showed that W200 presented the diffraction peaks characteristic of PS, while W450 has the crystalline structure of γ-Al_2O_3. Hence, despite calcination at 200°C allows to obtain the complete water removal and the decomposition of the polymer, it is not sufficient to ensure the transition of PS into γ-Al_2O_3. For this reason, the calcination temperature of all the samples was set at 450°C.

Finally, the activated structured catalyst has been characterized as well via Raman analysis, in order to be sure that the K_2CO_3 species obtained on the pellets was still available on the structured sample. As reported in Fig. V-8, the foam catalyst showed a sharp peak at 1063 cm^{-1} corresponding to K_2CO_3, perfectly in agreement with the observations made on the pellet sample.

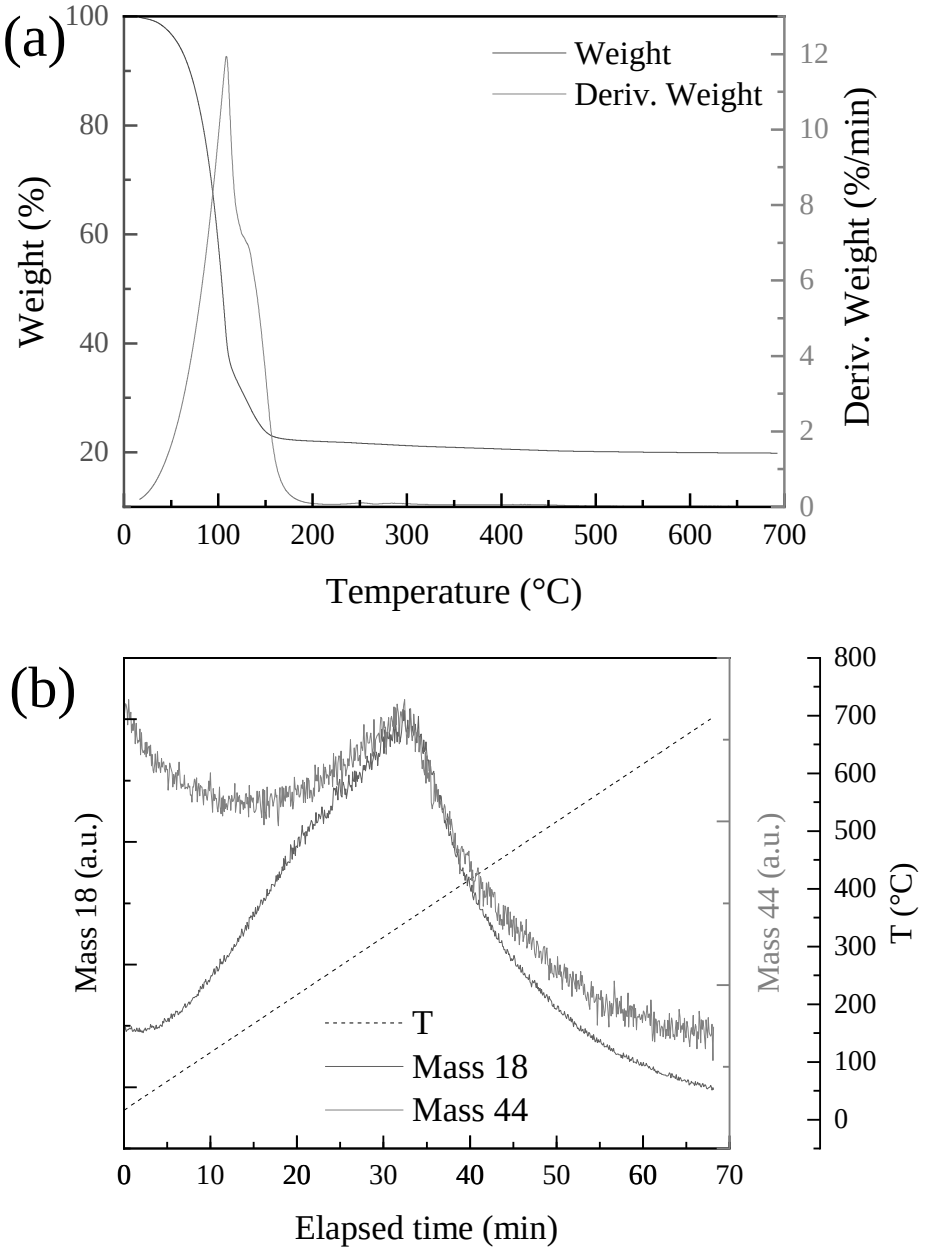

Fig. V-6: TGA of the prepared washcoat: (a) weight and derivative weight trend with temperature; (b) mass analysis performed through the mass spectrometer

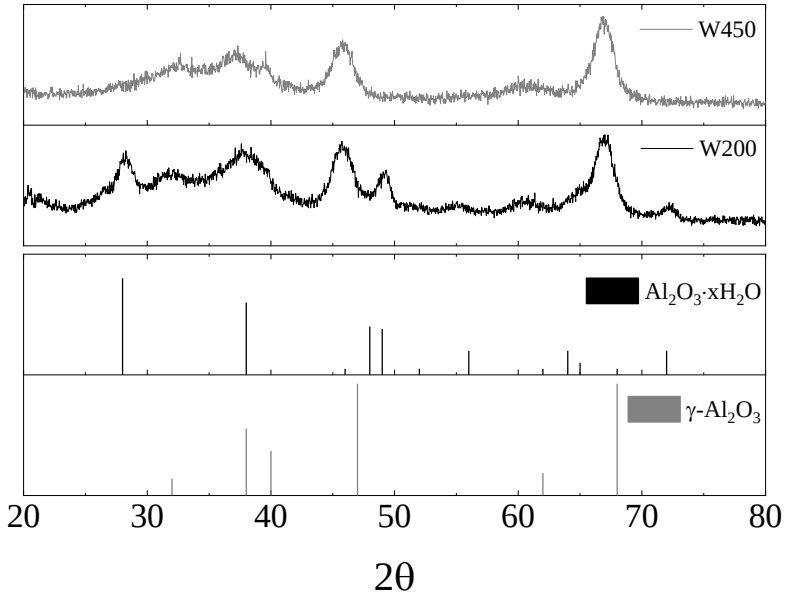

Fig. V-7: XRD analysis of W200 and W450 compared with the standard diffraction peaks of pseudobohemite and γ-Al_2O_3

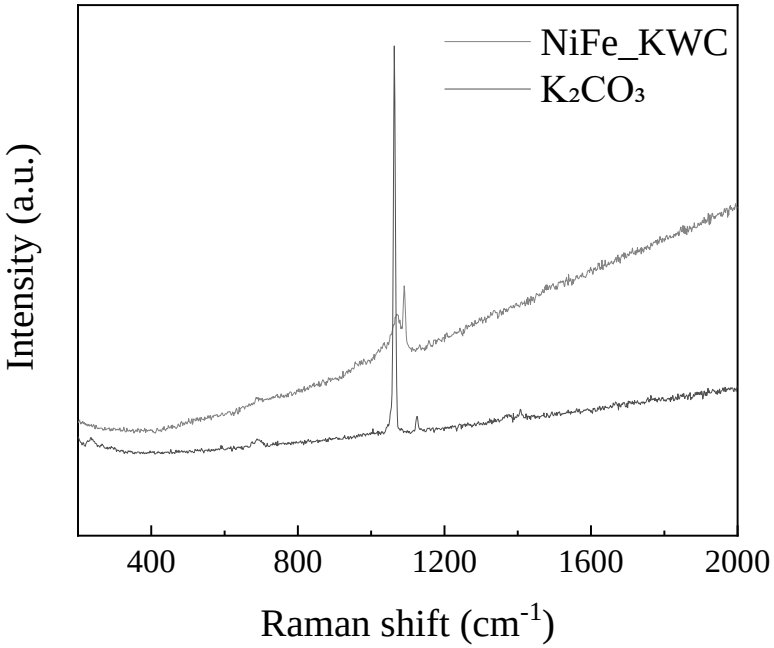

Fig. V-8: Raman spectrum of NiFe_KWC compared to K_2CO_3

Chapter VI.
Catalyst optimization

VI.1 Catalysts screening and influence of operating parameters

As widely discussed through the introduction and literature review sections, COS hydrolysis is a process that receives a deep interest from the industrial sector. In particular, low-temperature hydrolysis acquired the greatest relevance, as it represents the less expensive treatment. Indeed, the economic aspect cannot be neglected in the development of tools for the industry. Therefore, the most suitable catalyst to be employed in this process should be: i) as simple as possible; ii) with an inexpensive choice of support/active phase; iii) active at low temperature and high contact times; iv) reliable, thus stable over time in presence of sulfur compounds. Considering this, the first approach to the study of the reaction was focused on the research of a formulation and operating conditions which could be suitable to conduct the reaction.

The study of the recent literature pointed out that some Claus catalysts could provide, to some extent, COS conversion via hydrolysis (Sui *et al.*, 2020). Therefore, the former evaluations on the process were conducted on a commercial TGT alumina-based catalyst in pellets shape (3 mm) "Promoted alumina Claus catalyst" (Eurosupport, The Netherlands). For this commercial sample, the activity was evaluated in the temperature range 40-60 °C, which was selected as the most interesting gap, and varying the GHSV (Gas Hourly Space Velocity) in the range 600-3000 h^{-1}. COS hydrolysis was performed with a feed mixture composed of: COS 500 ppm, H_2O 5 vol.% and N_2 bal.

The results of this preliminary screening are displayed in Fig. VI-1. As can be observed, both the operating parameters have a strong influence on the reaction performances of the catalyst, leading to the conclusion that such commercial catalyst requires at least 60 °C and a remarkably high contact time (6 s, corresponding to the GHSV of 600 h^{-1}) to reach a COS conversion close to 100%, which is the thermodynamic equilibrium (Th.Eq.) value in every condition.

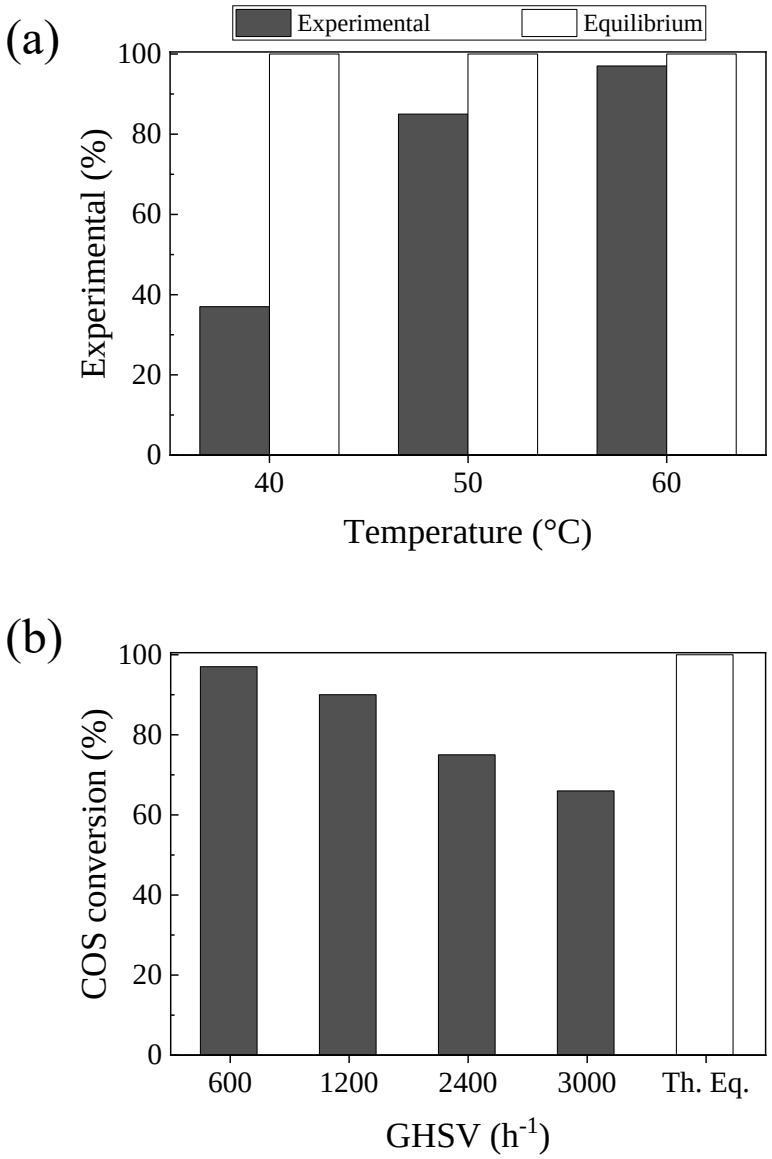

Fig. VI-1: Promoted alumina Claus catalyst activity. COS conversion over a) temperature; b) space velocity. Operating conditions: COS 500 ppm, H_2O 5 vol.%, N_2 bal., a) GHSV=600 h^{-1}; b) T=60°C.

This preliminary screening on a commercial catalyst allowed to understand the operating range in which the COS hydrolysis can be performed to achieve a considerable COS conversion. Nevertheless, these outcomes state how much the research is far away from commercialization. Indeed, despite the total conversion was achieved in some conditions, these require either one between

high temperature or elevated contact time. In particular, the latter implies large reaction volumes, which are not likely to be employed on an industrial scale.

In addition, the experimental evaluations reported so far were conducted in presence of a stream only containing COS and water. The industrial treatment of Claus tail gasses involves a stream that includes several other species that could influence the hydrolysis extent. Among all of them, the presence of CO_2 rises the major concern, for two reasons: on one hand, it is a reaction product, thus the chemical equilibrium of the reaction is strongly altered by its presence; on the other hand, CO_2 is a molecule which has several physical characteristics in common with COS, thus it potentially results in competitive absorption phenomena on the catalyst surface.

For this reason, a dedicated analysis was performed to evaluate the influence of CO_2 presence in the feed stream, choosing a concentration value corresponding to a conventional content of a TGT stream, 20 vol.%. The outcomes are reported in Fig. VI-2. As expected, such a large amount of CO_2 in the feed stream has a detrimental effect on COS conversion, and this effect is progressively more pronounced with the increase of the space velocity, suggesting the hypothesis that CO_2 negatively influences the conversion, not because of a chemical equilibrium limitation but mostly because of mass transfer and competitive adsorption issues.

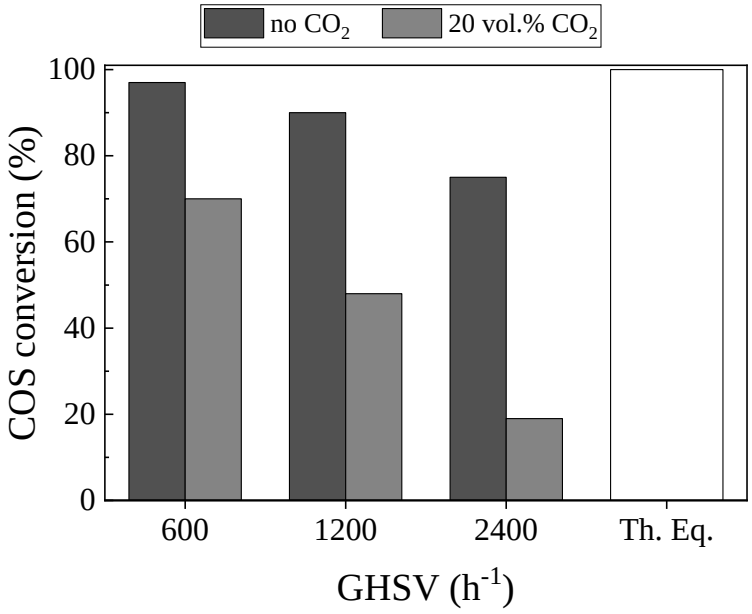

Fig. VI-2: Influence of CO_2 presence in the feed stream on COS conversion. Operating conditions: COS 500 ppm, H_2O 5 vol.%, N_2 bal., GHSV=600 h^{-1}, T=60 °C

Based on these evaluations on the selected commercial sample, the optimization of the catalyst was mandatory.

COS hydrolysis is widely recognized as a base-catalyzed reaction, and it is well-known that diffusion phenomena may easily influence the reaction performances, especially at low temperatures. Therefore, a γ-Al_2O_3 with a high specific surface area was selected and tested (Sigma-Aldrich, Germany); for conformity, the catalyst was chosen in spherical-shaped pellets (3 mm). A further step was to modify the catalyst with the addition of potassium, which gives basic properties to the surface. The catalysts were tested in the same operating condition of the commercial promoted Claus alumina catalyst and in presence of CO_2, with the aim of discriminating their potential in an unfavorable condition. The samples were labeled as PROMOTED (promoted Claus alumina catalyst), Al3 (γ-Al_2O_3 with 3mm pellets diameter) and K/Al3 (potassium-promoted γ-Al_2O_3 with 3mm pellets diameter). The results are shown in Fig. VI-3 (black columns). Even though the commercial catalyst PROMOTED has a non-declared formulation, one could speculate that it is alumina, and probably doped with a small content of active species. Despite that, its activity in presence of CO_2 strongly decreased. On the other hand, the bare gamma alumina showed remarkably higher activity. This could be easily addressed to the textural properties of the selected material, which enhanced the transport phenomena within the particles. The addition of potassium to the formulation further increased the COS conversion, even though the effect was slightly appreciable due to the close-to-the-equilibrium conditions. The remarkable difference in activity among the considered catalysts was observed instead in presence of different feed streams. Indeed, to the aim of simulating a refinery stream, other compounds were gradually added to the reaction mixture, to evaluate the effect of each. In particular, since the hydrolysis unit is expected to process the Claus tail gas stream, the species considered in this study had been H_2S, H_2 and CO_2. The feed conditions have been summarized in Table VI-1.

Table VI-1: Feed composition in each experiment

	Feed 1	Feed 2	Feed 3	Feed 4
COS	500 ppm	500 ppm	500 ppm	500 ppm
H_2O	5 vol.%	5 vol.%	5 vol.%	5 vol.%
CO_2	0	20 vol.%	20 vol.%	20 vol.%
H_2S	0	0	100 ppm	100 ppm
H_2	0	0	0	36 vol.%
N_2	bal.	bal.	bal.	bal.

The results were added to Fig. VI-3. Two main conclusions can be driven from the observation of the COS conversion in each system configuration. At first, that CO_2 addition confirms to have a detrimental effect on COS conversion, as already observed from Fig. VI-2, while the presence of other compounds, especially hydrogen, seems to mitigate this negative influence. In addition, it was observed that each catalyst suffered differently the presence of CO_2, with the K-doped alumina having the highest resistance to CO_2 addition.

Hence, besides the enhancement in COS conversion due to the change in catalysts could not be observed in presence of the simple hydrolysis stream, it was then clearly visible when the catalyst was tested in more stressful operating conditions. The same conclusion has been driven by reducing the contact time from 6 s to 1 s in presence of Feed 1. Based on these outcomes, a formulation constituted by potassium-modified γ-Al_2O_3 was selected as the best alternative for this process.

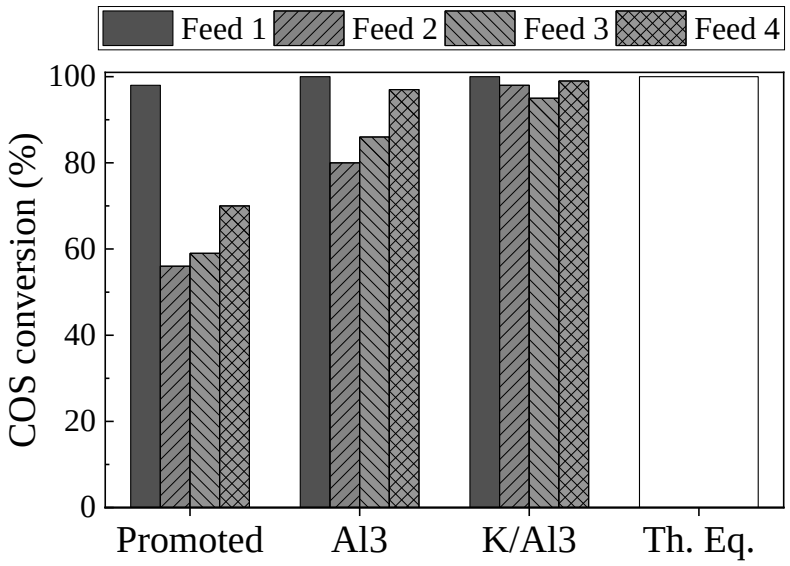

Fig. VI-3: Screening of the catalysts for COS hydrolysis. Operating conditions: COS 500 ppm, H_2O 5 vol.%, GHSV=600 h^{-1}, T=60 °C

Another important aspect in COS hydrolysis is the concentration of water in the feed mixture. Indeed, especially at low temperatures, water frequently shows a competitive adsorption on the catalyst surface, which hinders the COS adsorption and, consequently, its conversion. For this reason, the water concentration effect was studied over the optimized formulation, K/Al3. To this aim, the operating conditions were determined to be more critical for the COS conversion, to better observe the differences and have a more precise evaluation of the experimental concentrations. Low water contents were

evaluated at 43 °C and 2400 h^{-1}, while higher water contents were studied at 60 °C and 2400 h^{-1}, and the results are respectively reported in Fig. VI-4 (a) and (b). Clearly, water concentration strongly influences the reaction performances. Indeed, by keeping unvaried all the operating parameters but the water concentration, the COS conversion decreases strongly with a hyperbolic trend. Nevertheless, from an industrial point of view, it is convenient to decrease the water content up to the saturation concentration corresponding to the hydrolysis operating temperature, to avoid excessive refrigeration costs. Therefore, depending on the temperature, the water concentration in the feed stream is expected to be above 5 vol.%.

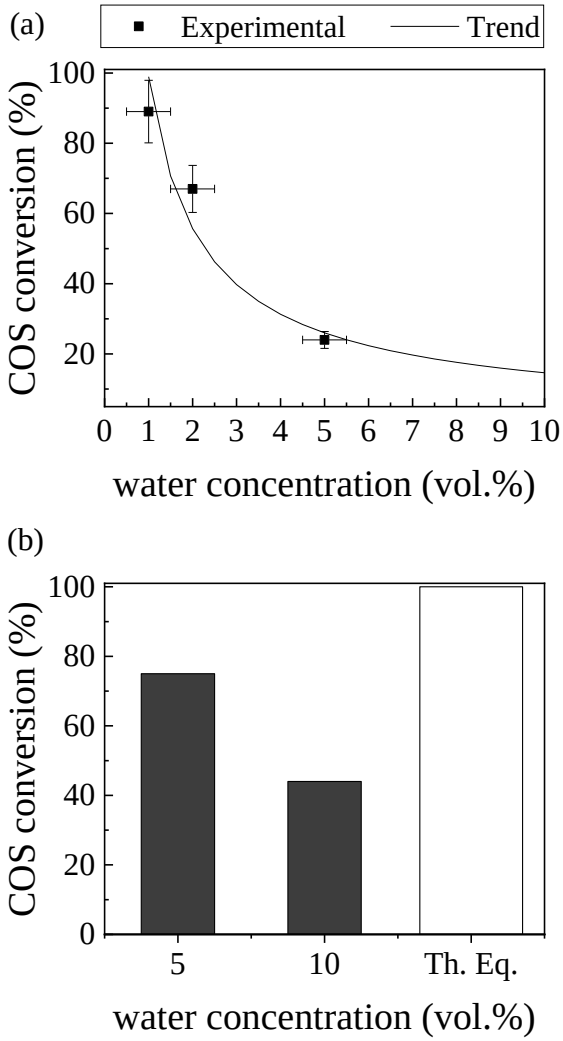

Fig. VI-4: Effect of water concentration on COS hydrolysis over K/Al3. Operating conditions: COS 500 ppm, N_2 bal., GHSV=2400 h^{-1}, a) T=43 °C b) T=60°C

In the most severe operating conditions (i.e. 2400 h^{-1} and H_2O 10 vol.%), the catalyst requires an operating temperature of 80 °C to reach a total COS conversion (Fig. VI-5).

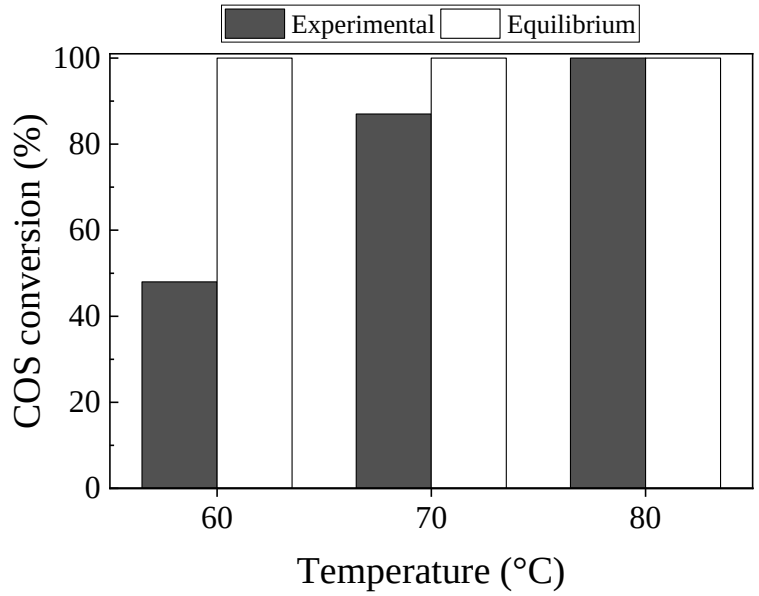

Fig. VI-5: COS conversion over K/Al3. Operating conditions: COS 500 ppm, H_2O 10 vol.%, GHSV=2400 h^{-1}.

VI.2 Evaluation of the transport phenomena

The knowledge of the dependency on the operating parameters does not provide sufficient information for a process like COS hydrolysis. Indeed, due to the low operating temperature, the transport phenomena play a key role. The extents of internal and external diffusion resistance were both evaluated, by varying respectively the pellets dimension and the gas linear velocity. The results of the study are represented in Fig. VI-6, where the limitations to the mass transfer are easily proved. The COS conversion is seen to decrease sensibly when the pellet dimension is increased to 5 mm, for both the bare alumina and the potassium-modified sample (Fig. VI-6a), therefore ensuring that the system suffers of strong internal diffusion resistance. On the other hand, the increase in gas linear velocity (Fig. VI-6b) – keeping the GHSV constant – does not provide for an enhancement of COS conversion, thus leading to the conclusion that there is no external diffusion resistance within the system, at least above 1.25 cm/s.

Nevertheless, it is necessary to bear in mind that the considered phenomena are investigated on a laboratory scale. For what concerns the measure of the

internal diffusion phenomena, the results can be considered reliable, since the phenomenon takes place on the microscale. Instead, the verification of external diffusion phenomena can be limited by the small scale of the investigation, since that there is an operative limit in the gas velocities that can be ensured. Eventually, this will result in higher gas phase velocity on the industrial scale, which would produce a higher mass transfer coefficient, enhancing the COS conversion. For this reason, it is possible to state that, for what concerns the laboratory scale investigations, there are no limitations due to the external diffusion of the reactants. Furthermore, the results can be considered obtained in conservative conditions, since the eventual increase of the gas linear velocity would enhance the mass transfer and thus the availability of COS on the catalyst surface.

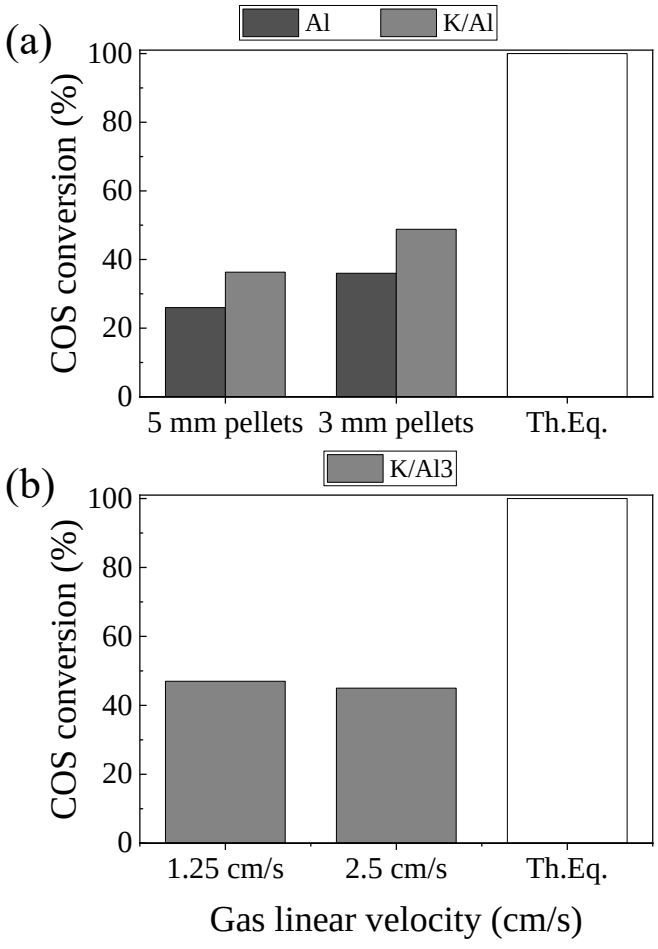

Fig. VI-6: Study of the a) internal and b) external mass transfer resistances. Operating conditions: COS 500 ppm, H_2O 10 vol.%, N_2 bal., GHSV=1200 h^{-1}, T=60°C

VI.3 Evaluation of the stability

The stability of a catalyst is a key issue in an industrial process, since the higher the lifetime the lower the operating costs. Hence, the stability of the optimized catalyst has been evaluated.

A first, short-term stability test was performed in mild and conservative operating conditions: 60 °C and a contact time of 4.4 s allowed the catalyst to convert all the COS present in the feed stream. In this condition, it is possible to evaluate if – at its higher activity – the catalyst deactivates due to a sulfidation of the active sites, which is a phenomenon widely reported in literature. The result is displayed in Fig. VI-7, where a comparison with other literature stability studies is also provided. The literature studies reported as a comparison are listed in Table VI-2.

As it can be noticed, the stability achieved is particularly promising if compared to other formulations available in literature, especially considering the alumina-based ones, which have major similarities with the formulation provided in this work.

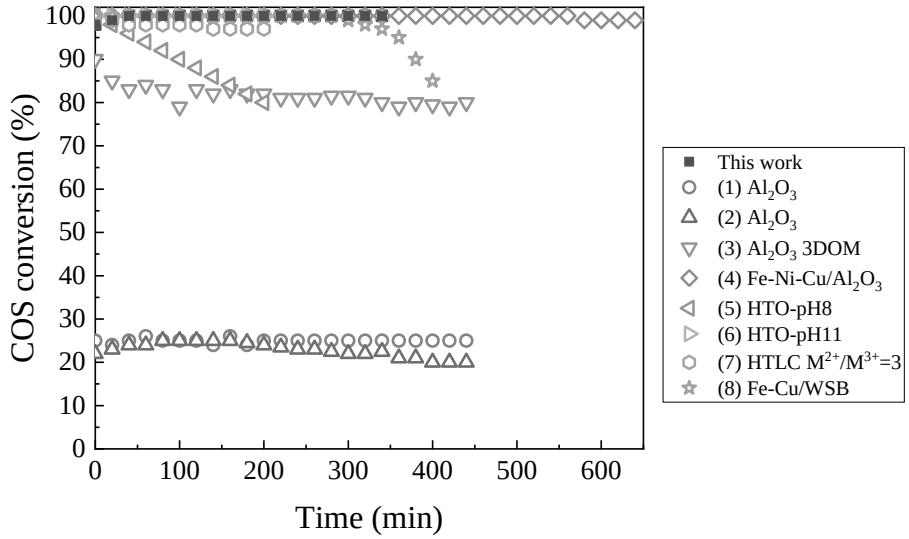

Fig. VI-7: Short-term stability and comparison with literature. Operating conditions: COS 500 ppm, H_2O 5 vol.%, T = 60 °C, tc = 4.4 s.

Table VI-2: Table of references for Fig. VI-7

Ref.	Full citation
1	West, J. et al. Ni- and Zn-promotion of γ-Al2O3 for the hydrolysis of COS under mild conditions. *Catal. Commun.* **2001**, *2*, 135–138.
2	Thomas, B. et al. Ambient temperature hydrolysis of carbonyl sulfide using γ-alumina catalysts: Effect of calcination temperature and alkali doping. *Catal. Letters* **2003**, *86*, 201–205.
3	He, E.et al, **2019**. Macroporous alumina- and titania-based catalyst for carbonyl sulfide hydrolysis at ambient temperature. Fuel 246, 277–284.
4	Sun, X. et al. Simultaneous catalytic hydrolysis of carbonyl sulfide and carbon disulfide over Al2O3-K/CAC catalyst at low temperature. J. Energy Chem. **2014**, 23, 221–226.
5	Zhao, S. et al. **2019**. Calcined ZnNiAl hydrotalcite-like compounds as bifunctional catalysts for carbonyl sulfide removal. Catal. Today 327, 161–167.
6	Wang, H. et al. Calcined hydrotalcite-like compounds as catalysts for hydrolysis carbonyl sulfide at low temperature. Chem. Eng. J. **2011**, 166, 99–104.
7	Zhao, S. et al. Characterization of Zn-Ni-Fe hydrotalcite-derived oxides and their application in the hydrolysis of carbonyl sulfide. Appl. Clay Sci. **2012**, 56, 84–89
8	Song, X. et al. Research on the low temperature catalytic hydrolysis of COS and CS_2 over walnut shell biochar modified by Fe–Cu mixed metal oxides and basic functional groups. Chem. Eng. J. **2017**, 314, 418–433.

In order to evaluate the possible deactivation due to carbon dioxide presence in the feed stream, a long-term stability test was conducted by applying stressful operating conditions. Indeed, it was already observed the detrimental effect of this species on COS conversion, but it could also harm the lifetime of the catalyst.

The stability was investigated with a simulated refinery stream, using the same concentration of species in Feed 4 from Table VI-1. As can be observed from Fig. VI-8, the catalyst demonstrated to ensure the same COS conversion during the whole stability test.

The stability achieved is particularly promising for the scale-up of the process, since the time of the test chosen (50 h) is significant on the lab scale, and it is the average duration of most of the stability tests reported in the open literature.

Furthermore, in this particular system, the deactivation might be due to sulfides formation because of H_2S or sulfates formation because of the simultaneous presence of H_2S and an oxidant agent, as CO_2 could be. Both processes are remarkably fast, occurring in the first 2-3 hours of reaction, as

can be observed from the stability studies from literature reported in Fig. VI-7. Hence, it is reasonable to presume that if no reduction in COS conversion was detected during the first 50 hours of evaluation, it is unlikely that the catalyst will undergo deactivation for longer time-on-stream tests.

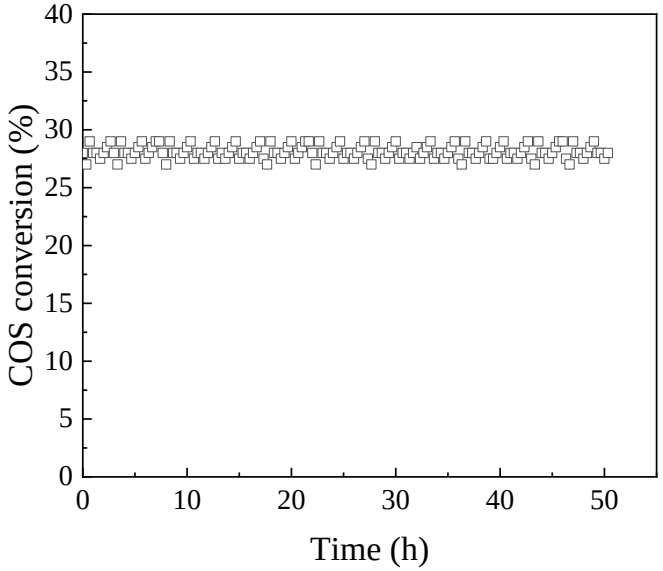

Fig. VI-8: Stability test over pellet catalyst. Operating conditions: COS 500 ppm, H_2O 5 vol.%, CO_2 20 vol.%, H_2 36 vol.%, H_2S 100 ppm, N_2 bal. T = 60 °C, tc = 1.5 s.

At the end of the long-term stability test, the catalyst was characterized with N_2 adsorption isotherms, XRD and Raman spectroscopy, and compared to the results obtained in section V.1.1.

As result, the spent sample SSA was equal to 200 m^2/g, thus no significant changes in the porous structure were provoked by the prolonged activity.

From the XRD analysis reported in Fig. VI-9 it is possible to observe that apparently also the chemical composition of the sample was kept unvaried. Nevertheless, the XRD allowed only the observation of Al_2O_3 characteristic peak, and therefore no conclusion can be drawn so far.

Hence, an additional characterization has been performed through Raman analysis, to observe possible sulfur compounds formation. Since it is well known that sulfides and sulfates have a Raman response at low Raman shift, the analysis was conducted in the range 200-700 cm^{-1}.

Indeed, two peaks arose in the spent spectrum which were not observed in the fresh catalyst, at approximately 220 and 470 cm^{-1}. These can be addressed to the deposition of elemental sulfur in the form α-S_8 (Remazeilles *et al.*, 2011). Despite the sulfur deposition, this result is not discouraging. Indeed, it means that the potassium carbonate seems to be not attacked by the sulfur compounds present in the reacting atmosphere, and that the elemental sulfur

which is deposited on the sample does not cover the active sites (the activity is unvaried) nor has a deleterious effect on the catalyst porosity.

The presence of elemental sulfur onto the catalyst was also demonstrated via SEM-EDX analysis of spent K/Al3. The mapping is given in Fig. VI-11.

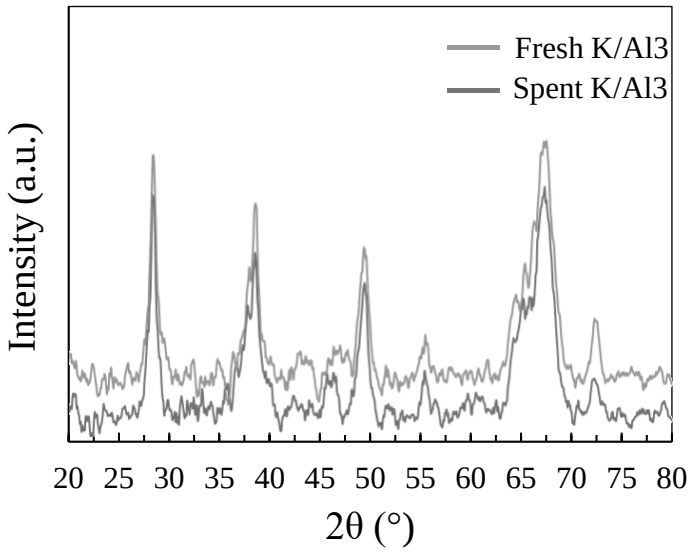

Fig. VI-9: XRD spectra of the fresh and spent K/Al3

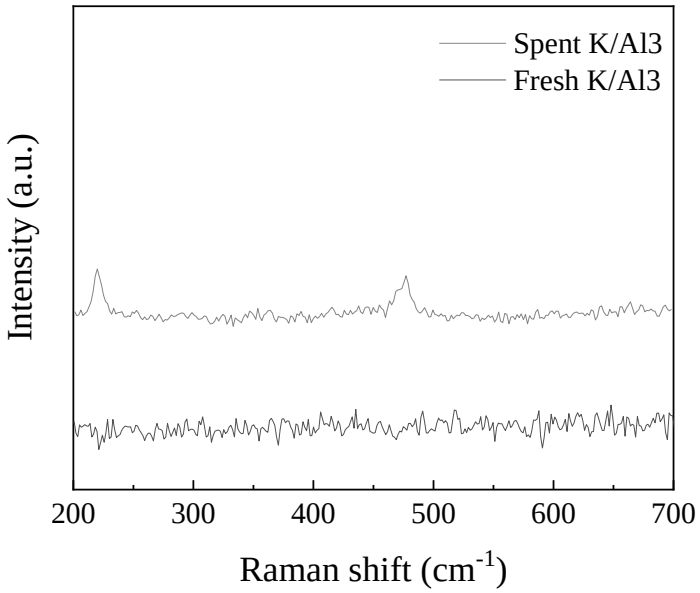

Fig. VI-10: Raman spectra of the fresh and spent K/Al3 in the range 200-700 cm^{-1}

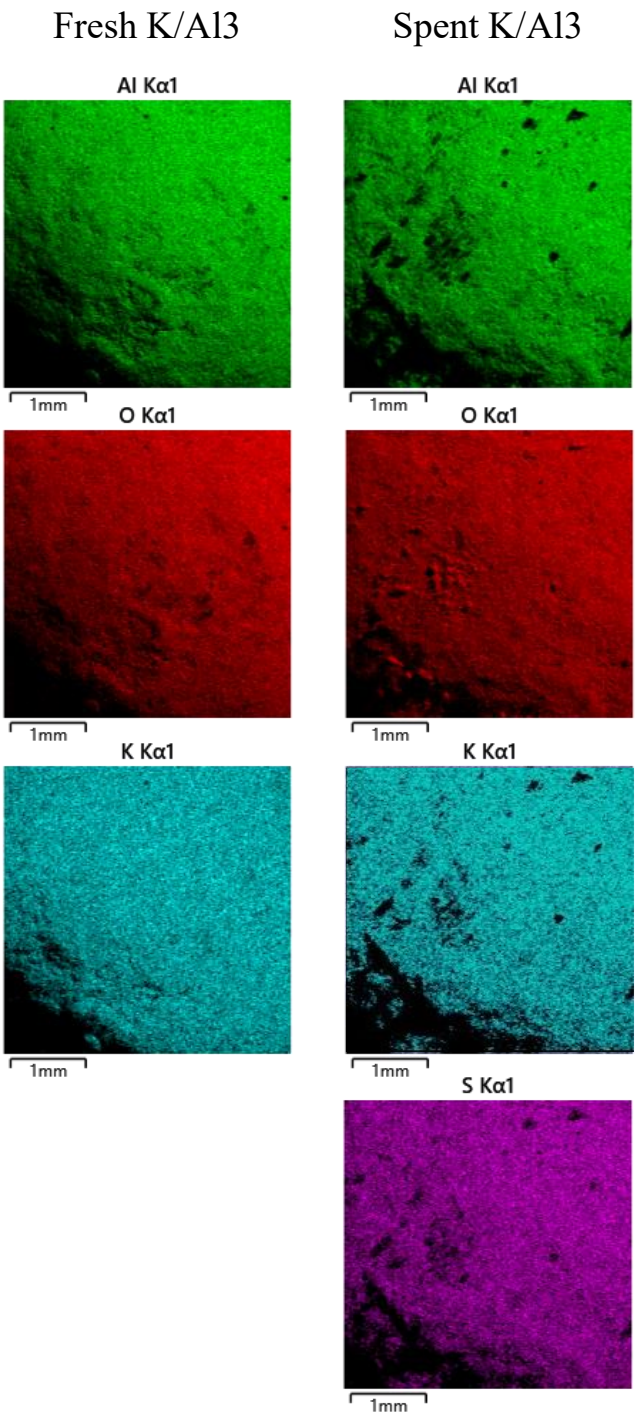

Fig. VI-11: SEM-EDX analysis on fresh and spent K/Al3

Chapter VII.
Liquid-phase hydrolysis and open-architecture system

VII.1 The concept

In the first part of this PhD project, it was selected a catalyst able to satisfy the requirements of the thesis objectives: it is characterized by an affordable and easily providable formulation, demonstrating a remarkable low-temperature activation. Indeed, it was tested in different operating conditions, and in any of them, it was possible to find a noteworthy catalytic activity below 80 °C.

Therefore, this achievement highlighted the potential of coupling the hydrolysis unit with the absorber in a "closed box" configuration in which both reactors operate at the same temperature. It is worth reminding that, to the best of our knowledge, at this stage of research there are no feasibility studies available on this topic.

The aimed configuration is given in Fig. VII-1.

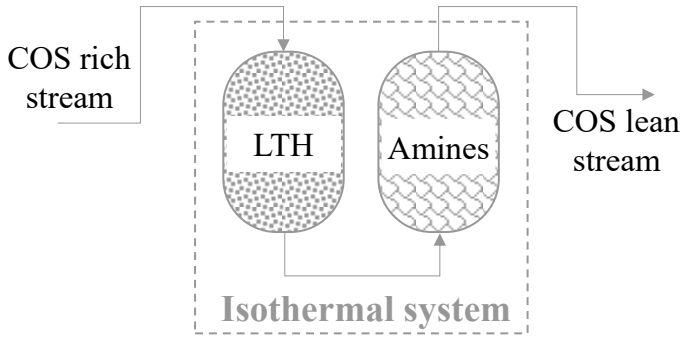

Fig. VII-1: Aimed open architecture configuration scheme

VII.2 Liquid phase hydrolysis: absorption in amine solutions

The liquid-phase hydrolysis tests were conducted following the methodology explained in section IV.2.2.

Because of the poor suitability of primary amines in this kind of process, secondary and tertiary amines only were considered for performing COS absorption. In particular, DEA was chosen at first, for its remarkable COS absorption ability reported in literature.

The dependency of the removal efficiency on the operating parameters was investigated by varying the temperature, the contact time and the concentrations of COS and DEA. The influence of temperature and contact time was investigated with a feed stream of 500 ppm of COS in N_2 and an aqueous solution with 40 wt.% of DEA. The outcomes are reported in Fig. VII-2. As awaited, an increment in temperature or contact time allowed to enhance the COS removal, as both are beneficial to the reaction kinetics. Nevertheless, there is a limit in temperature concerning the vaporization of the solution, depending on the employed amine; furthermore, also too high contact time would not have a satisfactory match with the industrial needs. For this reason, the temperature was not increased above 60 °C and the contact time was kept below 36 s. Furthermore, it is possible to observe that, when the absorption temperature is kept at 30 °C, the COS removal efficiency is constant during the whole test. This could be addressed to a faster deactivation of the absorbing solution at high temperatures, since the condition promotes a higher removal efficiency. The COS removal reached a plateau after almost 2 h test, and the removal efficiency is only slightly higher than the one reported for the test at 30 °C.

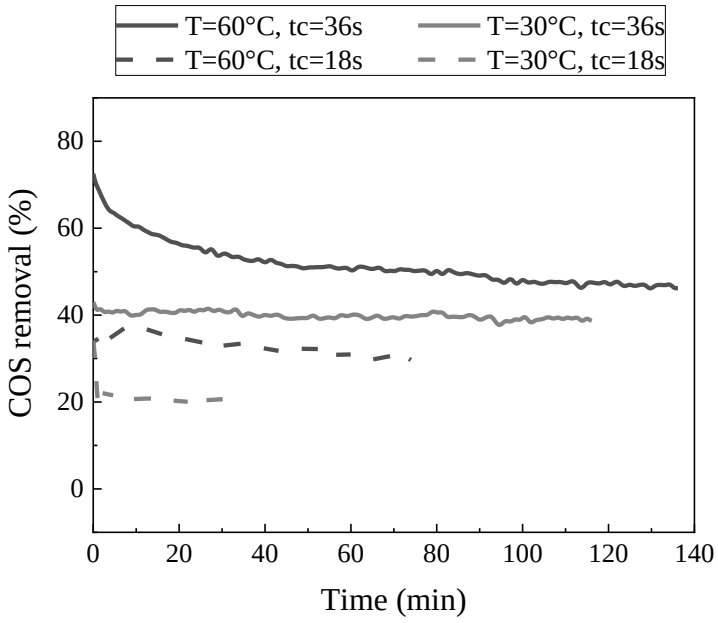

Fig. VII-2: COS removal efficiency in different conditions of contact time and temperature. Feed: 500 ppm of COS in N_2; solution: 40 wt.% DEA in H_2O.

The influence of DEA concentration was evaluated by setting the temperature at 60 °C and the contact time at 18 s. It was observed that an increase in DEA concentration slightly improved the COS removal (Fig. VII-3). This is according to kinetic studies reported in literature, which individuated a fractional reaction order n ($1 < n < 2$) in DEA. In particular, considering the works of Littel et al., at low DEA concentration the reaction kinetic was reported to be first order in DEA while, at increasing DEA concentration, the system showed a change in the reaction order, and the best representation of the experimental data was obtained with a second order in DEA (R. J. Littel *et al.*, 1992). This is according to several other literature works (Amararene and Bouallou, 2004; Hinderaker and Sandall, 2000).

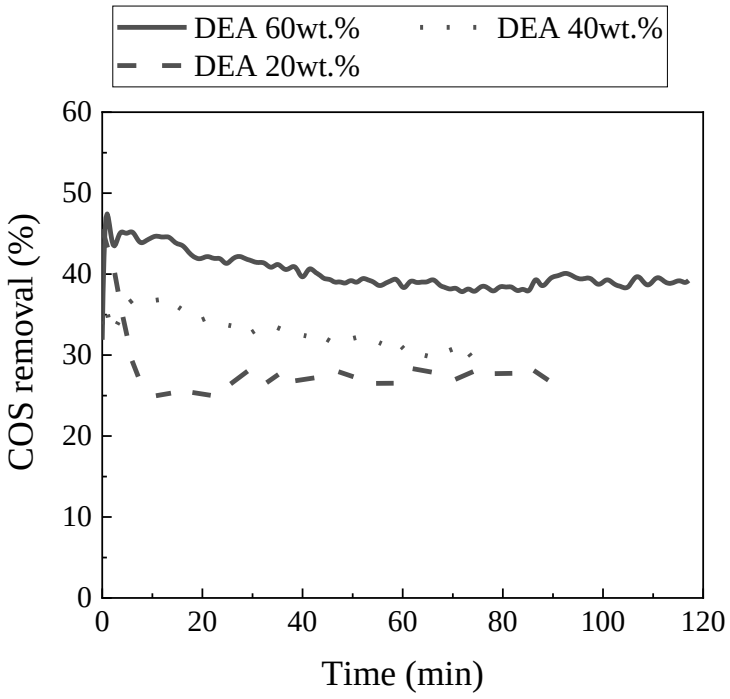

Fig. VII-3: COS removal efficiency in aqueous solution with different DEA concentrations. Feed stream: 500 ppm of COS in N_2; T = 60°C; tc = 18 s.

The influence of COS concentration was investigated at 30 °C and with a contact time of 36 s; the outcomes are reported in Fig. VII-4. As it can be seen, no significant differences can be detected in removal efficiency at three different COS concentrations. This finds a perfect agreement with literature, where the reaction order in COS was always reported to be 1 (Hinderaker and Sandall, 2000; Lee *et al.*, 2001; R. J. Littel *et al.*, 1992; Sharma, 1965; Vaidya and Kenig, 2009). This result is particularly relevant. Indeed, in the perspective of having the absorption unit downstream to the hydrolysis section, COS concentration may vary significantly depending on the catalyst employed for the hydrolysis and on the operating conditions. These results ensure that the amine solution should provide a considerable COS abatement even when a very low concentration is present in the feed stream, thus always providing a further removal compared to the stand-alone hydrolysis unit.

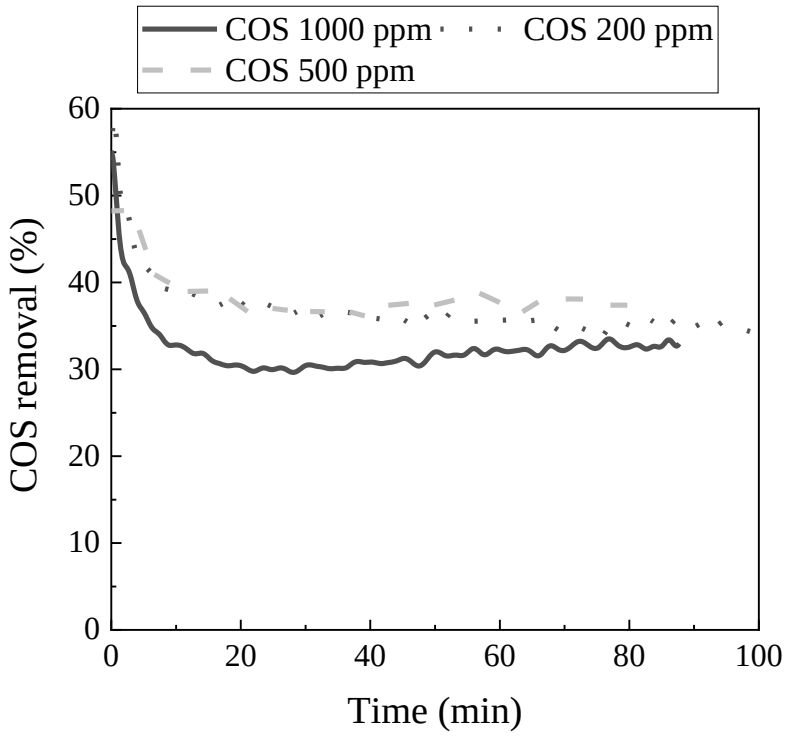

Fig. VII-4: COS removal efficiency in aqueous solution with different COS concentrations. Aqueous solution with DEA 40 wt.%; T = 30°C; tc = 36 s.

VII.3 Hydrolysis + absorption: open-architecture layout

Through the screening of the catalysts, the formulation K/Al was found to be the best-performing catalyst. In addition, it was also observed that, because of the internal diffusion phenomena which take place in this system, the smallest the pellets the highest the COS conversion. To keep open different possibilities regarding the pellets dimension and shape, both the catalysts K/Al5 and K/Al3 were selected for this investigation.

The operating conditions for the experimental evaluation of the open-architecture layout were chosen as the best compromise between the single units. Therefore, they were set to have both the units working at the same temperature, thus without implementing a further heating/cooling step, and with the same gas flowrate. COS hydrolysis was then operated at 60 °C and 3 s, with a feed stream having composition: COS 500 ppm, H_2O 10 vol.%, N_2 bal. COS absorption was performed at 60 °C and 18 s.

The results of the complete system were evaluated through COS conversion in the hydrolysis reactor and the removal efficiency of COS and

H_2S in the absorption unit. From Fig. VII-5 it is possible to observe that the overall COS removal from the feed stream is clearly enhanced in the two-step system with respect to the stand-alone hydrolysis unit, due to the previously discussed ability of the DEA aqueous solution in sequestrating COS. Furthermore, the presence of the amine absorption step allowed to seize a fraction of about 50% of the produced H_2S. It has to be considered that COS hydrolysis accounts for the sulfide conversion, and however another sulfur compound is produced, which has to be separate from the product stream in any case. Coupling the hydrolysis with the absorption step allows achieving a theoretical 100% removal of any sulfide. In our system, around 37% of total sulfur removal from the feed stream was realized for both catalysts, which is a remarkable achievement. Hence, the feasibility of coupling COS hydrolysis unit with an absorber in an open-architecture configuration has been demonstrated by this study, with particularly promising results in terms of sulfur compounds removal.

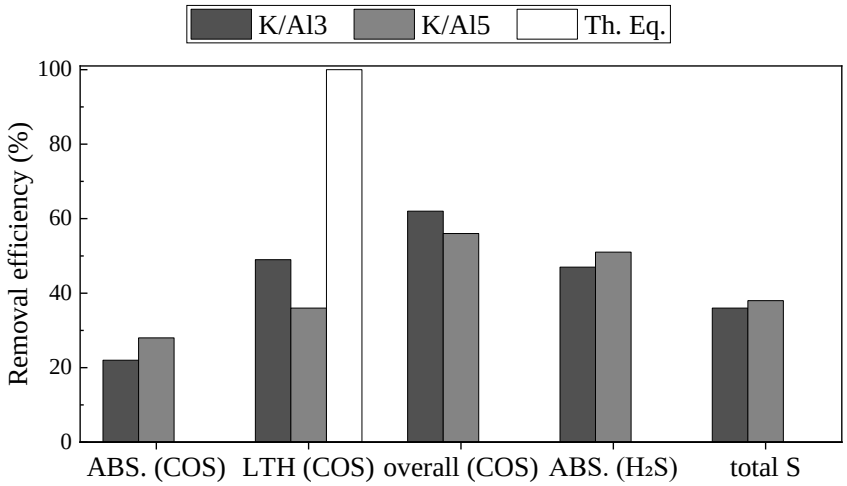

Fig. VII-5: Performances of the *in-series* system of COS catalytic hydrolysis and absorption with amine solutions.

Analyzing the present results in terms of equivalent SO_2, the system allowed to convert a feed stream containing 500 ppm of COS in a product stream containing around 200 ppm of COS and 130 ppm of H_2S, with an overall reduction of equivalent SO_2 at the end of the process chain. This result is particularly promising, considering the target limits in sulfur emissions. Indeed, D.Lgs. n. 183 (15th November 2017) fixed a threshold of 35-400 mg/Nm^3 of equivalent SO_2 that are allowed to be emitted into the atmosphere, depending on the application. This system allowed to reduce the equivalent SO_2 from over 700 mg/Nm^3 in the feed stream to 450 mg/Nm^3, thus our result is approaching the upper limit of the government ordinance and can go beyond, by optimizing operating conditions and plant configuration.

VII.4 Absorption with a customized amine solution

Once stated the functionality of the open-architecture process, several other considerations have been made. The principal aim of this project was to evaluate the possibility of including the hydrolysis step in a pre-existing sweetening process. At this point of the activity, the feasibility and the potential advantages of this application have been corroborated.

Nevertheless, the actual industrial configuration has not been taken into account yet. The existing technology should be altered as less as possible; furthermore, the H_2S removal efficiency of the process must be kept unvaried. As observed through the results of simultaneous absorption of COS and H_2S in DEA solution, this kind of absorber is not able to completely remove hydrogen sulfide from the gaseous stream; instead, the removal efficiency is approximately 50%. Therefore, absorption of COS with DEA solutions cannot be performed in existing sweetening systems, as the H_2S removal efficiency is insufficient.

To solve this limitation, the KT proprietary sweetening technology utilizes a customized product constituted of a mixture of MDEA and additives which enhance the selectivity of the tertiary amine toward H_2S. This absorbent, from now on addressed as cMDEA, was directly supplied by the company KT, and employed for further experimental evaluations.

Despite several changes in the operating conditions in terms of absorbent solution temperature, contact time and gas linear velocity, it was not possible to find a set of operating conditions able to ensure a significant COS removal. The maximum value achieved was 4.7% of COS removed in a condition of high temperature and contact time (60 °C and 36 s).

This result, anyway, is justified by the operating conditions of the laboratory scale process, which result remarkably different from the ones adopted on the large scale. In the experimental setup employed for these tests, the contact time ensured for the absorption (18-36 s) was considerable, if compared to the industrial condition of ~25 s. Nevertheless, this time is a combination of the gas flow rate and the available solution volume, which are both a function of the geometry of the system. The saturator-like reactor allowed to use a solution volume of maximum 80 cm^3, and this forced the gas flow rate to be in the range 100-200 $Ncm^3\ min^{-1}$. Therefore, the average gas linear velocity reached in the annulus section of the reactor is between 0.25-0.5 cm/s. This velocity value is outstandingly lower than the one realized in an industrial absorber. Thanks to the high flow rates due to the large volume of gas processed and to the presence of packing within the column, the gas linear velocity reached is around 15 cm/s.

The absorption is a physical event that is strictly dependent on the transport phenomena within a system. The transferring of a species (here, COS) from

one phase to another is not only related to the difference in concentration, but it is also driven by the phase equilibrium and by the availability of the species at the physical interphase. In particular, the COS concentration at the gas-side interphase is determined by the ability of COS to diffuse within the gas bulk, and it is quantified by the coefficient K_G (diffusion coefficient in the gas side). In turn, K_G is related to the fluid dynamic of the system and, in particular, it is a function of the gas linear velocity. Therefore, a low gas velocity determines a low K_G, and a low K_G value implies an insufficient amount of COS at the interphase: despite the concentration gradient is maximum, no COS is able to change phase.

This is likely what happened in the saturator-like reactor, which gave no COS absorption. Hence, to keep the possibility of system integration and to employ in the system the selective H_2S absorber cMDEA, a modification of the reaction geometry and thus fluid dynamic is mandatory.

VII.5 Preliminary evaluation with packed column

Considering the scarce results obtained with this configuration and the cMDEA solution employed, it was necessary to prove the hypothesis of high resistance to mass transport, before any optimization of the reactor geometry. To this aim, the saturator-like reactor was filled with glass spheres in order to enhance the turbulence within the system, increasing the local gas velocity and therefore the gas-side diffusion of COS into the bulk. As reported in Fig. VII-6, an increase in COS removal efficiency up to 17% was observed, highlighting the importance of optimal fluid dynamic conditions and the presence of packing material.

Then, the glass spheres were substituted with the alumina spheres Al3, to evaluate the possibility of a minimum simultaneous catalytic effect offered by the packing. The spheres were observed to soak within the solution, reducing the apparent volume. The performances were found to be worse than the ones obtained with glass spheres, probably because of the observed phenomenon. Indeed, the volume of amine solution that fills the pores of alumina spheres is not easily available from the gas bubbles, hence the system behaves like it had a lower sorbent volume. To confirm the hypothesis, an additional test was performed using the same Al3 packing but performing a calcination step at 940 °C to reduce the pore volume of the alumina (the sample was labeled as C940). As it can be observed, in this case the COS removal efficiency was as high as the one obtained with glass spheres. Therefore, no catalytic activity offered by alumina was registered in this condition in aqueous solution.

It can be concluded that:

- The coupling of hydrolysis and absorption with amine solutions is promising, as it allows to enhance sulfur removal in terms of equivalent SO_2

- To work with sorbents which can ensure an almost total H_2S removal, the fluid dynamic conditions need to be optimized
- The packing can be substituted with a catalyst, even though the alumina spheres were found to be not suitable to this aim. Further investigations are needed, to evaluate the possibility of finding a catalyst which can ensure a noteworthy activity in COS removal, enhancing the process.

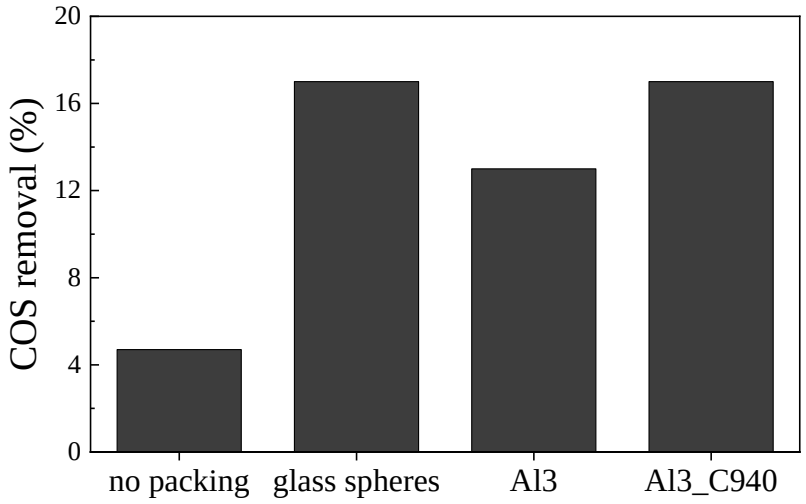

Fig. VII-6: COS absorption in cMDEA in a packed column

Chapter VIII.
Process Intensification

Methods for the process intensification of COS hydrolysis have been investigated in the last part of this Ph.D. project, and they are the core of this research.

As reported, process intensification is "a strategy to reduce dramatically (>100X) the size of a chemical plant, while keeping a target production objective by either shrinking the size or reducing the number of unit operations." (Boffito and Van Gerven, 2019). Following this definition, and considering the COSWEET™ technology as a starting point, to further simplify the chemical plant it is possible to act following three pathways:

1. Reducing the activation temperature of the catalyst up to the operating temperature of the absorber, to avoid the use of heat exchanger
2. Find a catalyst able to ensure a neglectable pressure drop, to avoid the compression stage
3. Integrate the hydrolysis step within the absorber, to eliminate the presence of a dedicated unit for the reaction.

The step 1 of the process intensification can be considered halfway. Indeed, the catalyst optimized during the study of the gas phase hydrolysis was the better formulation matching all the requirements for industrial applicability and ensuring noteworthily high COS conversion values at a relatively low temperature. This also allowed the coupling of this stage to the absorption unit without any heat exchanger in between, which is already a step further the present technology. Nevertheless, as demonstrated by the analysis of the mass transport limitations, the COS catalytic conversion is limited by the internal diffusion; on the other hand, the reduction in the size of the pellets is not a feasible solution, since it would further increase the pressure drop and therefore the operating pressure required.

The reduction of the pressure drop can be performed by substituting the conventional pellets catalysts with structured catalysts. In addition, the conventional functionalization of 3D structures for their application in

catalysis is realized through the deposition of a micrometric layer of a washcoat, which act as catalytic support for a proper active species, if any. This micrometric layer is particularly promising: it would be like reducing the pellet dimension to microns, thus enormously enhancing the mass transport velocity of COS from the gas bulk to the catalyst surface. Nevertheless, structured catalysts have never been applied to the COS hydrolysis process. Hence, this study would allow the accomplishment of pathways 1 and 2, completing the catalytic aspect of this process intensification, but it is a leap of faith.

For what concerns the integration of the hydrolysis and absorption units, it is possible to address this study as the technological part of the process intensification. It also is the most interesting and promising outcome of this work.

VIII.1 Structured catalysts

Prior to any catalytic investigation, it was necessary to identify the most suitable carrier to be applied in COS hydrolysis. To this aim, several carriers, different in constructing material and shape, have been evaluated and the most appropriate was selected based on the amount of washcoat that could be deposited, its adherence, and the easiness of the preparation. Once selected the carrier, the performance of the final catalyst in COS hydrolysis were investigated in different operating conditions.

VIII.1.1 Screening of the carriers

For the individuation of the most suitable carrier to be employed for the preparation of the structured catalyst, the following samples were investigated:

- Cordierite flow-through monolith
- Steel wire mesh
- OB-SiC open cells foam (10 ppi)
- Aluminum open cells foam (40 ppi)
- Ni-Fe open cells foam (20 ppi)

These samples were selected among the most employed structured catalysts. Nevertheless, it is worth highlighting that, prior to each investigation, the foam structures are the most promising to be applied to this catalytic system. Indeed, as was demonstrated in the previous section, COS hydrolysis is a process that suffers of high internal diffusion resistance. On the other hand, no external diffusion resistance was observed experimentally in this work, but it might be due to the limitations in sensibly modifying the operating parameters. The phenomenon is likely to occur when remarkably different fluid dynamic conditions are applied. Hence, the presence of a

catalyst whose structure is able to enhance the mass transport phenomena due to the random geometry which increase the turbulence is particularly encouraging.

All the selected structured carriers were treated before washcoat deposition. The conventional procedure for the ceramic material (i.e. Cordierite monolith and OB-SiC foam) and for the Al foam involves a calcination step prior to the first deposition step. Such pre-treatment was applied also to the steel mesh and to the Ni-Fe foam. Nevertheless, as the latter were new materials and no literature studies were available regarding their use as carrier in catalysis, other pre-treatments were evaluated.

Steel wire mesh were treated in five different ways, as listed. After washing with acid/basic solution the samples were dried overnight at room temperature, prior to the washcoat deposition.

A) Thermal treatment: calcination at 450°C
B) Acid treatment: HCl (20%) + H_3PO_4 (1%) solution, 2 h
C) Acid treatment: HF (60%) solution, 2 h
D) Basic treatment: KOH (20%) solution, 2 h at 130°C
E) Acid treatment followed by basic treatment:
    - HCl (20%) + H_3PO_4 (1%) solution, 30 min
    - KOH (20%) solution, 2 h at 130°C

Such treatments were chosen to partially erode the surface, leading to two possible effects: on a hand, the increase in roughness of the surface could offer a higher grip of the washcoat; on the other hand, the exposure of a more reactive internal layer could offer the possibility of a more stable chemical bond between the wire mesh and the washcoat itself. Each performed treatment determined the modification of the surface of the wire mesh, as verified through the SEM images reported in Fig. VIII-1. Briefly, one can conclude that acid treatment with HF and basic treatment with KOH determined the stronger corrosion of the surface, while intermediate erosion was achieved through mild acid treatment and the two-step treatment. Only a slight modification of the surface was determined by the calcination of the wire mesh.

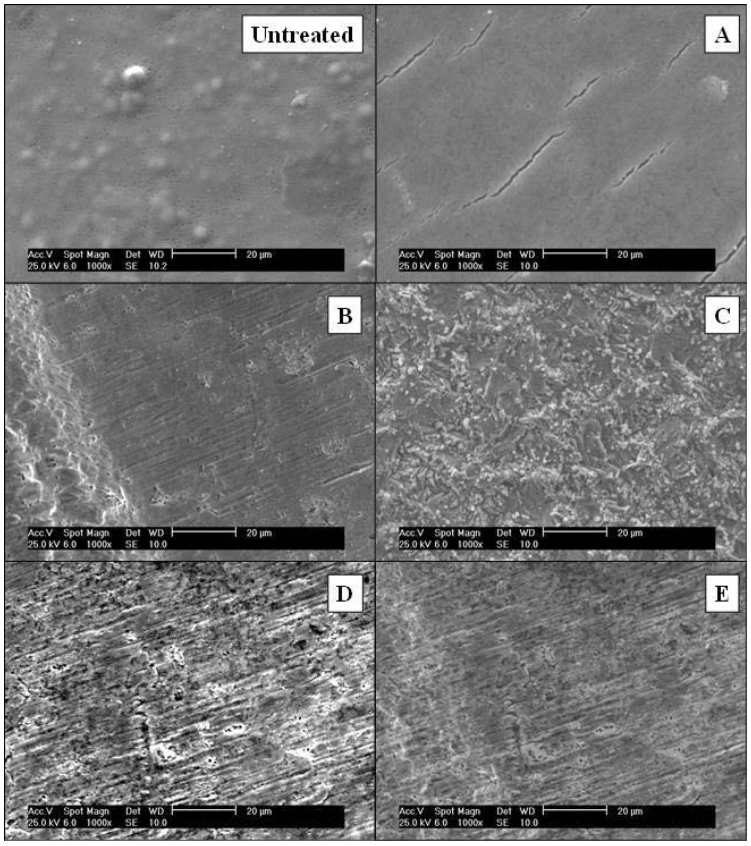

Fig. VIII-1: SEM images of the treated steel wire mesh

The effectiveness of this pre-treatment on the adhesion was evaluated directly by considering the washcoat loading obtained with a single-step deposition. To this aim, the conventional sequence of washcoat deposition (as described in section 2.3.2) was employed for all the selected structures. The results of this analysis are reported in Fig. VIII-2. As outcome, in general acid treatments worked better than basic treatments, with the mild acid washing ($HCl + H_3PO_4$ solution) offering the highest washcoat loading and, indeed, the highest adhesion. The untreated wire mesh (not shown) performed similarly to the thermally treated sample, showing a poor washcoat adhesion.

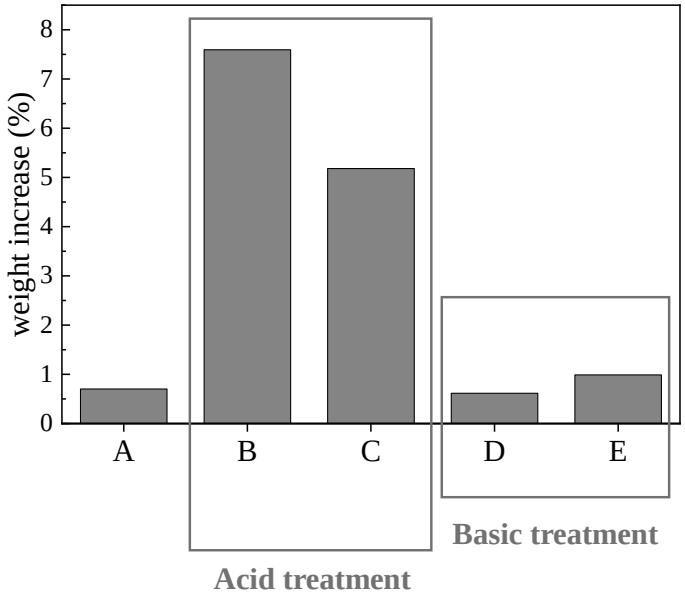

Fig. VIII-2: Washcoat loading obtained through a single impregnation step of pre-treated steel wire mesh

For what concerns the Ni-Fe foams, as suggested by the provider, only the thermal treatment was evaluated, in order to avoid possible damage to the alloy. The calcination of the foam led to the formation of metallic oxides onto the surface, clearly distinguishable through the color of the foam (Fig. VIII-3). Despite that, the single-step washcoat deposition gave almost the same result in terms of loading (around 7 wt.%), leading to the conclusion that either the untreated or the calcined foam can be used for the catalyst preparation.

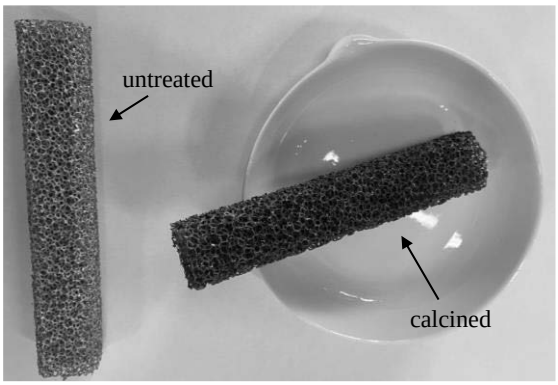

Fig. VIII-3: Untreated and calcined Ni-Fe foam

Therefore, an acid-washed steel wire mesh (treatment B) together with calcined samples of cordierite monolith, OB-SiC foam, Al foam and Ni-Fe foam were employed for washcoat deposition. The suitability of such carriers

was evaluated by considering the maximum washcoat loading achieved and the number of impregnation steps required. The impregnation step is considered complete after the calcination of the sample. To understand the purposes of this analysis, it has to be taken in consideration that the target washcoat loading is higher than the commonly reported in literature, in which loads of 15-25 wt.% were applied (Frey *et al.*, 2015; Montebelli *et al.*, 2014; Palma *et al.*, 2020, 2016).

The outcomes are displayed in Fig. VIII-4.

As it can be easily observed, the foam structures allowed depositing the higher washcoat mass, and among them, the Ni-Fe foam reached the 28 wt.% loading. This result might be ascribed to both the material and the porosity of the foam. Indeed, the dimension of the cells can help in holding the washcoat anchored to the structure, and this finds agreement with the fact that the OB-SiC foam, which has the bigger pores, required the highest number of impregnation cycles to reach the same washcoat amount deposited on Al and Ni-Fe foams. On the other hand, too small pores could make more complex the introduction of the washcoat within the foam. Therefore, it is reasonable that the Ni-Fe foam, which has an intermediate pore average diameter, displayed the best results in terms of washcoat loading and number of deposition cycles.

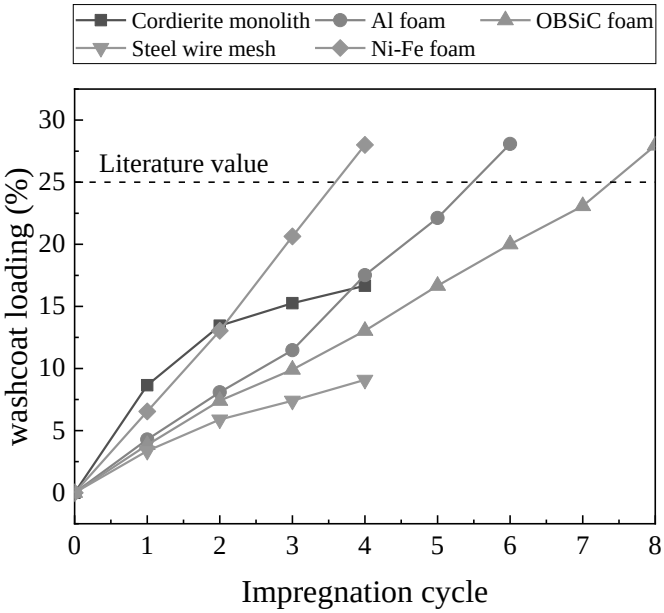

Fig. VIII-4: Washcoat loading of different structured carriers. Loading is intended as percentage of the ratio washcoat-to-carrier mass

Nevertheless, the achieved results were still to be improved. The mass of washcoat per unit of volume reached through this impregnation sequence was too low compared to the pellets density, suggesting that the use of structured

catalysts would remarkably increase the catalytic volume needed for the reaction. To the aim of increasing the washcoat loading and, at the same time, performing the deposition through the lowest number of impregnation cycles, a new procedure has been optimized according to Fig. IV-4. Following the customized procedure, the results in terms of washcoat loading and number of cycles were outstanding: the weight of the washcoated structure was increased from 40 up to 105 wt.%, leading to a maximum washcoat loading of 54 wt.%, and the impregnation steps number was decreased to 3, according to Fig. VIII-5.

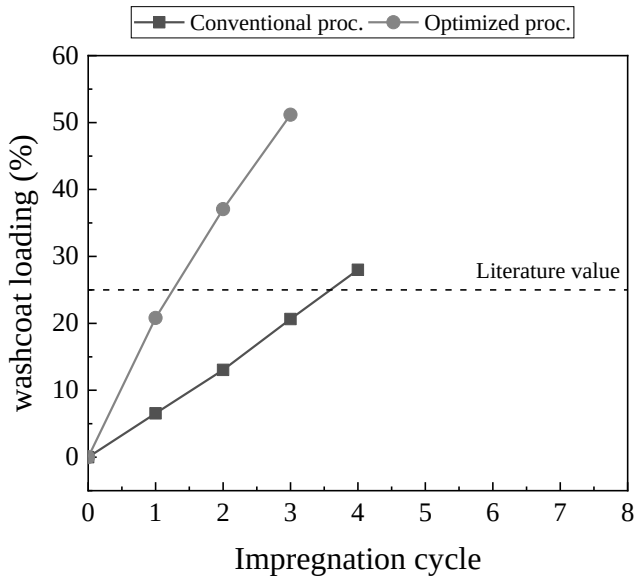

Fig. VIII-5: Washcoat loading as function of cycle number in Ni-Fe foams in case of conventional (black) and optimized (red) procedure

Based on the above, the screening of five different possible carriers pointed out that the Ni-Fe foams are the most suitable to be applied in the preparation of structured catalysts with a 54 wt.% of washcoat loading, therefore they have been employed for the catalytic tests.

VIII.1.2 Activity tests

A preliminary investigation on the employment of a structured catalyst for COS hydrolysis has been carried out on the catalyst NiFe_W450 prepared following the developed procedure. The results, evaluated in terms of COS conversion, were compared to the ones obtained with the sample Al3. To set an adequate operating condition for the first test of structured catalyst in COS hydrolysis, it was considered the different geometry of this sample compared to pellets. Indeed, the foam structure has more than 90% of the apparent

volume constituted by voids; therefore, the actual catalytic volume is far from the apparent one.

To ensure a correct comparability of the performances obtained on NiFe_450 with the sample Al3, a weight-basis evaluation of the space velocity was considered. The structured sample was loaded with 4 g of alumina washcoat. Hence, the same weight of Al3 was employed in the catalytic activity tests. For both samples, the total flowrate fed to the system was 400 Ncc min^{-1}, ensuring a weight-basis gas hourly space velocity (wGHSV) of 6 $NL(hg)^{-1}$. The tests were performed at 60°C and 1 atm, with a feed mixture composed of COS 500 ppm, H_2O 10 vol.%, N_2 bal.

The first, outstanding result is that the sample NiFe_W450 demonstrated to be able of converting COS, confirming the possibility of employing structured catalysts in this process. Furthermore, comparing the observed activity to the COS conversion of the sample Al3 as reported in Fig. VIII-6, NiFe_W450 showed a remarkably higher COS conversion, compared to the pellets.

This result upholds one of the initial hypotheses of lower internal diffusion resistance in structured catalysts: the development of a thin layer of alumina on the foam structure allowed the minimization of such resistance, increasing the reaction rate and thus allowing obtaining higher conversions.

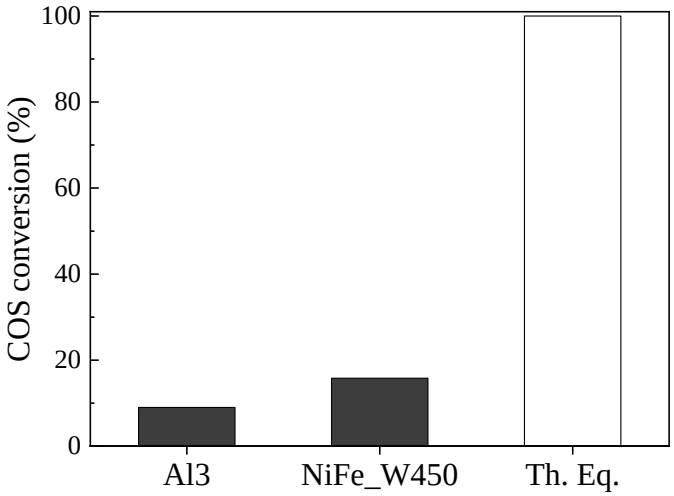

Fig. VIII-6: Comparison of activity for pellets and foam. Operating conditions: COS 500 ppm, H_2O 10 vol.%, N_2 bal. 60°C, 1 atm, cat. mass = 4 g

This preliminary evaluation paved the way to further investigation on structured catalyst application to COS hydrolysis.

To the aim of performing a comprehensive study of the activity of these catalysts, new structured samples were prepared based on NiFe_W450. In particular, new samples were shaped with a central hole to locate the

thermocouple sheat in order to monitor the temperature alongside the whole catalytic bed, and the foams were loaded with washcoat up to the loading of 50 wt.%, as it was for the sample NiFe_W450. Then, the calcined foams were impregnated with a KOH solution, calcined and activated in CO_2 as described in section IV.4.2.The final samples are structured catalyst with an alumina washcoat doped with K_2CO_3, displayed in Fig. VIII-7 (a) and (b), and labeled from now on as NiFe_KWC.

Two foams, each 50 mm long, were wrapped into a quartz wool mat to avoid bypass phenomena between the foams and the reactor wall, and then located into the reactor up to the final loading of about 10 g (washcoat + K_2CO_3), as displayed in Fig. VIII-7 (c).

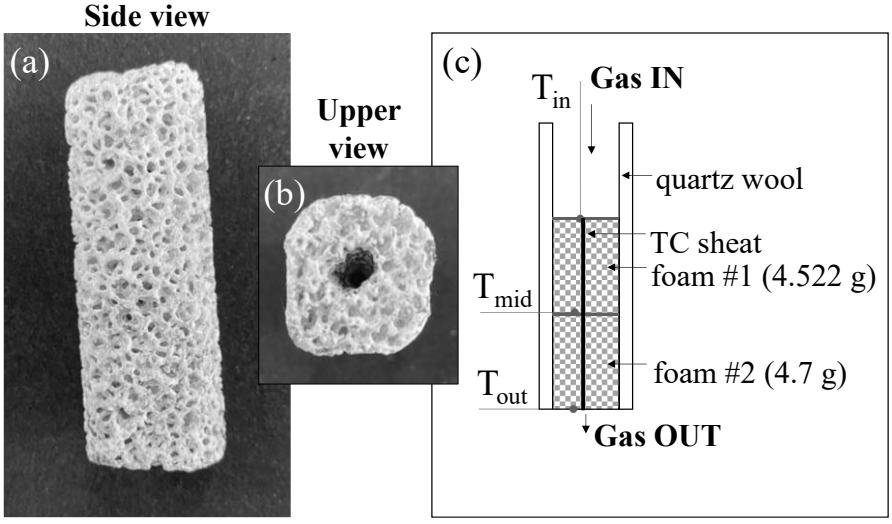

Fig. VIII-7: (a) and (b) views of the final structured catalyst; (c) scheme of the reactor loading.

The performances of the structured catalysts were evaluated through a screening at different operating temperatures and contact times. The temperatures were varied in the range 40-90 °C, considering 40 °C as the minimum temperature at which the condensation of water is avoided, and 90 °C as the maximum process temperature, recalling the target of performing COS hydrolysis below 100 °C.

The whole temperature span was investigated in three contact time conditions – 1 s, 2 s, and 4 s – which corresponded to a wGHSV of 3.2, 6.4 and 10.8 $NL(hg)^{-1}$ respectively. Since the refinery tail gas streams are often processed in cooling towers, the typical water content is around 5 vol.%. Therefore, the experimental evaluations were conducted in presence of a feed composed of COS and a large excess of water (H_2O:COS=100:1, with 500 ppm COS). The outcomes are displayed in Fig. VIII-8.

For this system, the variation of the operating temperature within a span of almost 50 °C allowed to cover the whole activity range of the catalyst, as COS conversion varied from less than 10% up to 100%. This result is an outstanding achievement, since even at the less favorable contact time conditions the structured catalyst was able to achieve a total conversion below 100 °C, in perfect agreement with our target.

Furthermore, as expected, the decrease in contact time implied a drop in the catalytic activity resulting in the X-vs-T curves shifted to higher temperature. Despite the difference in operating conditions and kind of catalyst, this result is strongly coherent with previous literature findings, in which is clearly reported the remarkable kinetic limitations suffered by this system due to the low temperatures.

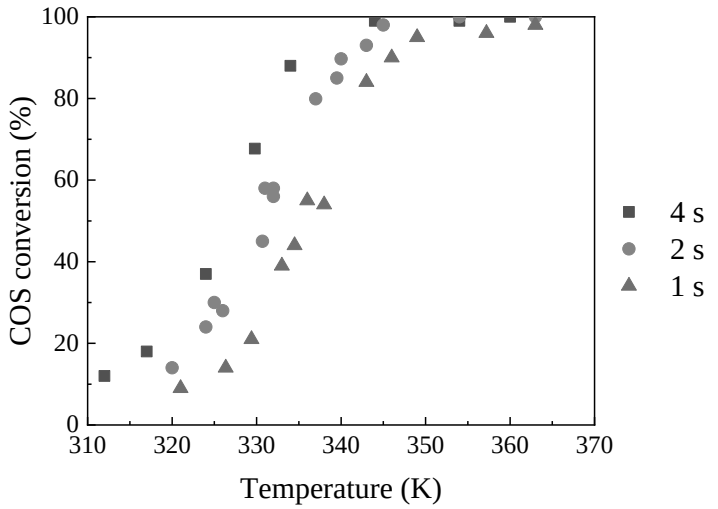

Fig. VIII-8: Experimental data of COS conversion for the whole set of operating conditions. (COS = 500 ppm, H_2O = 5 vol.%, N_2 bal.)

VIII.1.3 Influence of the components over the reaction

To the aim of applying this catalyst in an industrial plant, several other considerations are mandatory. To the best of our knowledge, the influence of a more complex composition of the feed stream on the performances of COS hydrolysis has not been reported so far. Poor attention has been paid to the presence of high concentrations of CO_2 in the feed stream, even though it is a product of most of the industrial processes, both in the sector of chemicals production and power generation. At the same time, the amount of water fed to the system is usually regulated by cooling towers, and therefore it depends on the plant location and atmospheric conditions and can suffer a certain variability.

For this reason, the effect on the activity of the concentration of CO_2 and water was lately evaluated, and the outcomes are reported in Fig. VIII-9 (a) and (b) respectively. Both water and CO_2 had a detrimental effect on the catalytic activity, but the decrease of COS conversion followed two remarkably different trends. In particular, the effect of water concentration was milder than the one of CO_2, with a gradual decrease in COS conversion in presence of H_2O, in opposition to the strong drop detected in presence of CO_2.

To understand the different dependencies of COS conversion on water and carbon dioxide concentration, it was necessary to consider the thermodynamic equilibrium of such a complex mixture, reported in Fig. VIII-10. Since a high-water contents theoretically promote the reaction, it was possible to exclude the effect of thermodynamic limitations on the reaction. On the other hand, CO_2 slightly impacts on the COS thermodynamic conversion, but the equilibrium value is above 99.98% at 393 K and 20 vol.% of CO_2, therefore the equilibrium limitation did not apply to the experimental results. Hence, the decrease in COS conversion could only be ascribed to adsorption phenomena, in which the behavior of COS, H_2O and CO_2 is competitive and, in particular, COS has the lowest affinity to the active sites.

Based on the discussed results, the different trends in COS conversion reduction observed in presence of either water or carbon dioxide could only be attributed to the dissimilar interactions with the catalyst surface, i.e. COS, water and carbon dioxide have different adsorption behavior. However, this aspect will be further evaluated through the mathematical modeling of the system.

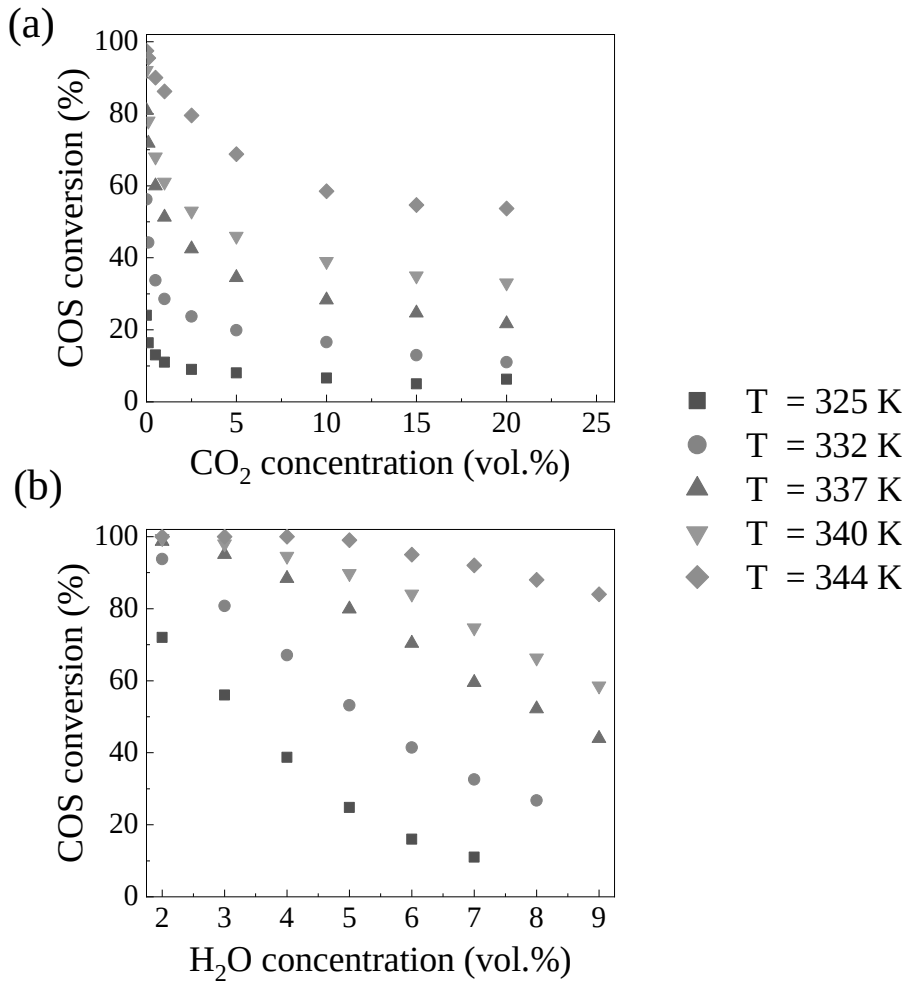

Fig. VIII-9: COS conversion as a function of (a) CO_2 concentration and (b) H_2O concentration. Operating conditions: (a) tc = 2 s, COS = 500 ppm, H_2O = 5 vol.%, N_2 bal.; (b) tc = 2 s, COS = 500 ppm, N_2 bal.

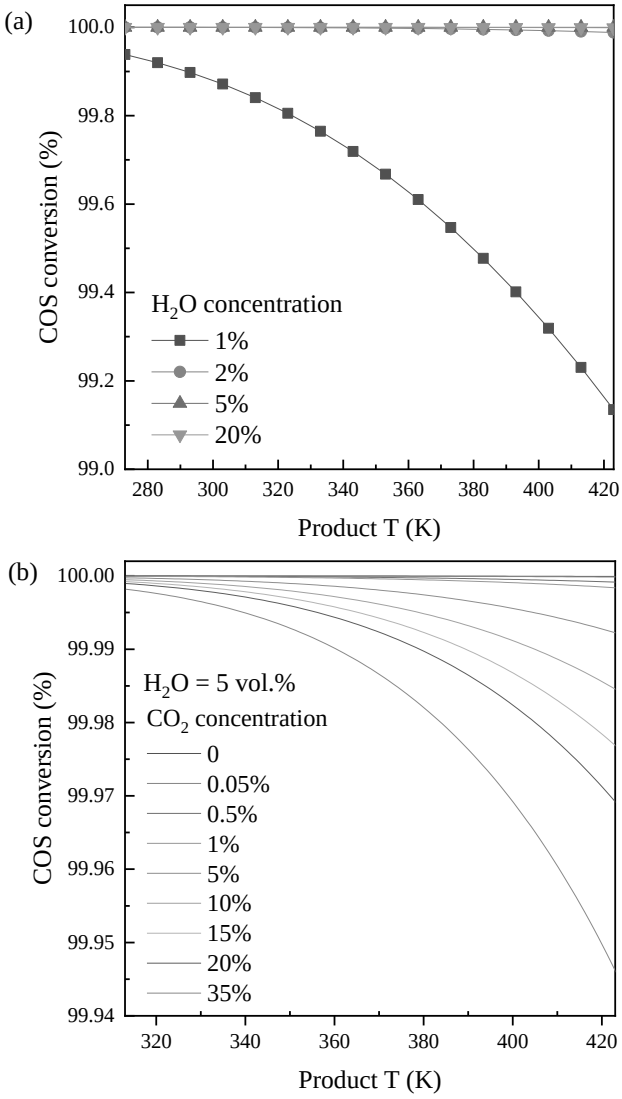

Fig. VIII-10: Thermodynamic COS conversion as a function of temperature, H_2O concentration and CO_2 concentration

VIII.1.4 Evaluation of the stability

Stability is a key issue in the development of a catalyst for processes involving sulfur compounds. Despite the K-doped formulation was already observed to be stable for a considerable amount of time (50 h, as shown in Fig. VI-8), the result achieved on the pellet catalysts could not be reproducible on the structured sample. Therefore, the foams were tested in a time-on-stream experiment at a contact time of 2 s and a temperature of about 60 °C. Temperature and COS conversion were monitored for 170 h. In addition, to further stress the catalyst, more than 100 hours of stability test were conducted in presence of a stream containing 20 vol.% of CO_2. Indeed, it has been reported that deactivation can be caused by two different mechanisms: (i) sulfidation of the catalyst caused by H_2S (Huang *et al.*, 2005) and (ii) formation of sulfur oxidized species on the catalyst surface, which are able to deactivate the catalysts (Li *et al.*, 2017). According to the second mechanism, the presence of oxidizing species such as CO_2 could determine the deactivation.

The results of the study are reported in Fig. VIII-11. As it can be observed, there is a slight decrease in COS conversion in the first 24 hours of test, which however corresponds to the slight decrease in temperature. As it was observed through the screening of the catalytic activity, the system has a high dependency on the operating temperature, and in particular between 50 and 60 °C a small temperature variation induces a sensible variation in the COS conversion. When CO_2 was added to the feed stream the conversion dropped, as expected, but it remained constant for almost 120 h. To evaluate any possible deactivation effect, CO_2 was removed from the feed stream and the initial conditions were restored. COS conversion was found to be slightly lower, but again its variation is coherent with the variation in temperature.

To further corroborate that the variation in COS conversion is only ascribable to temperature and not to deactivation phenomena, the initial and final conversion values and temperatures were overlapped to the first screening of the catalyst activity. In Fig. VIII-12, the red dots represent the initial and final COS conversion of the stability test. They are perfectly coherent with the shape of the conversion curve, corroborating the absence of deactivation of the catalyst within 170 h of time-on-stream test.

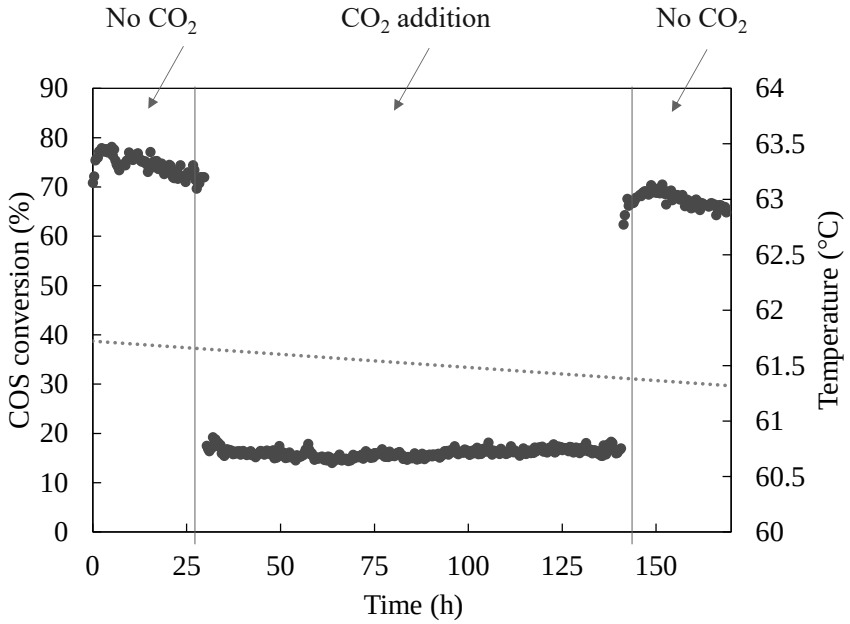

Fig. VIII-11: Stability test on the foam catalyst

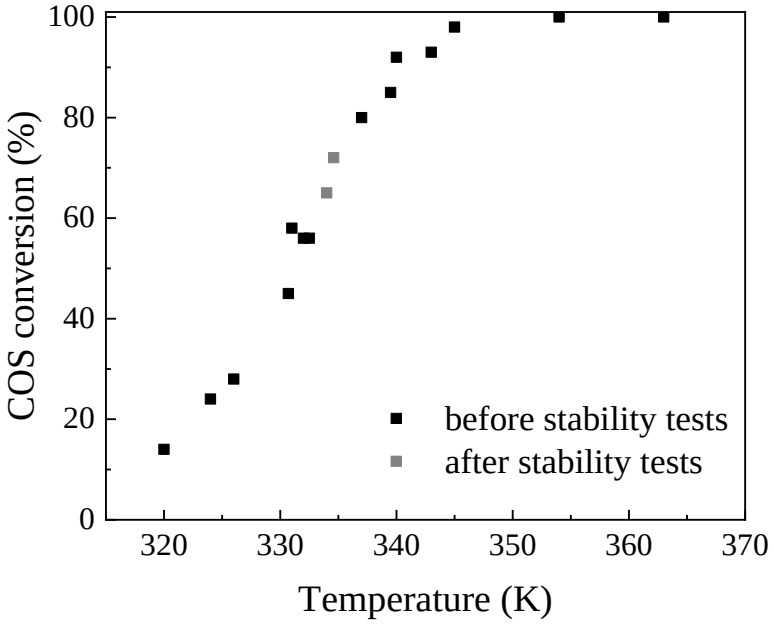

Fig. VIII-12: Comparison between the activity test results and the initial and final activity of the catalyst measured during the stability test

VIII.1.5 Characterization of the spent catalyst

Since during the tests performed on structured catalysts no deactivation was observed, neither during the activity test nor at the end of the stability test, the foams were occasionally analyzed to evaluate the surface modification. The characterization chosen to this aim was the Raman analysis, since the sulfur compounds are easily detectable under visible-light radiation.

The foams were analyzed in different conditions (fresh, spent, spent and calcined) and in different axial positions, according to Table VIII-1.

Table VIII-1: Resume of the labels for the samples characterized with Raman analysis

Label	Sample condition	Foam	Distance from inlet section (cm)
A	Fresh	1-2	1 – 4 – 7 – 9 (overlapped)
B1	Spent	1	1 – 4 (overlapped)
B2	Spent	2	7 – 9 (overlapped)
C1	Spent + calcined	1	1 – 4 (overlapped)
C2	Spent + calcined	2	7 – 9 (overlapped)
D1	Spent	1	1
D2	Spent	1	3
D3	Spent	1	5
D4	Spent	2	7
D5	Spent	2	9
E	Spent	1-2	1 – 4 – 7 – 9 (overlapped)

Samples B and C were obtained at the end of the activity tests. After the characterization of sample B, due to the observed spectra, the foams were calcined obtaining the sample C. The results are displayed in Fig. VIII-13. As can be observed from the comparison of the fresh sample A and the spent sample B, there is a complete disappearance of the peak corresponding to the potassium carbonate at 1063 cm^{-1}. Meanwhile, a peak at 1097 cm^{-1} arose, which can be attributed to the formation of $KAl(OH)_2CO_3$ in the humid atmosphere (Wang *et al.*, 2001). Indeed, once calcined in air (and consequently in presence of atmospheric CO_2), the peaks of K_2CO_3 at 1063 and 1026 cm^{-1} reappeared, even though it was still existent the signal of the presence of $KAl(OH)_2CO_3$. In addition, a peak at 450 cm^{-1} was detected on samples B which disappeared after calcination. This signal could be attributed to K_2SO_4 (Qiu *et al.*, 2019), which formation could be due to the large presence of CO_2 in some tests. Indeed, it has been reported that the presence of an oxidant in the reaction system induces the formation of metal sulfates, which usually are responsible for the deactivation of the catalyst (Li *et al.*,

2017). However, no other signals related to K_2SO_4 are clearly distinguishable, and the activity was not observed to decay.

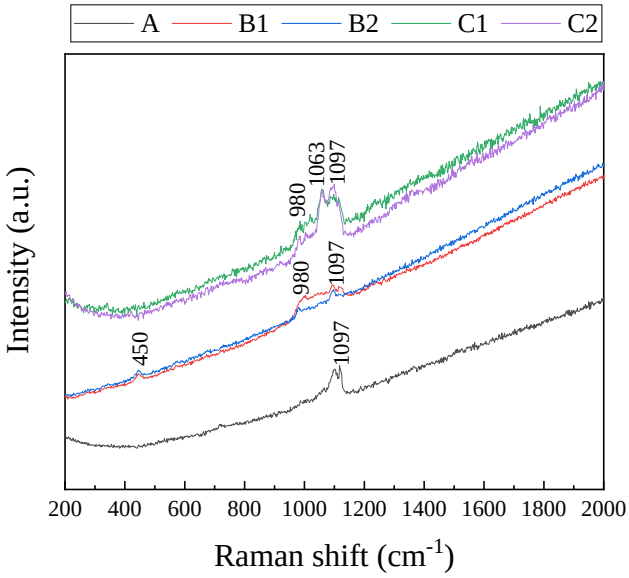

Fig. VIII-13: Raman spectra of NiFe_KWC foams at the end of the activity tests

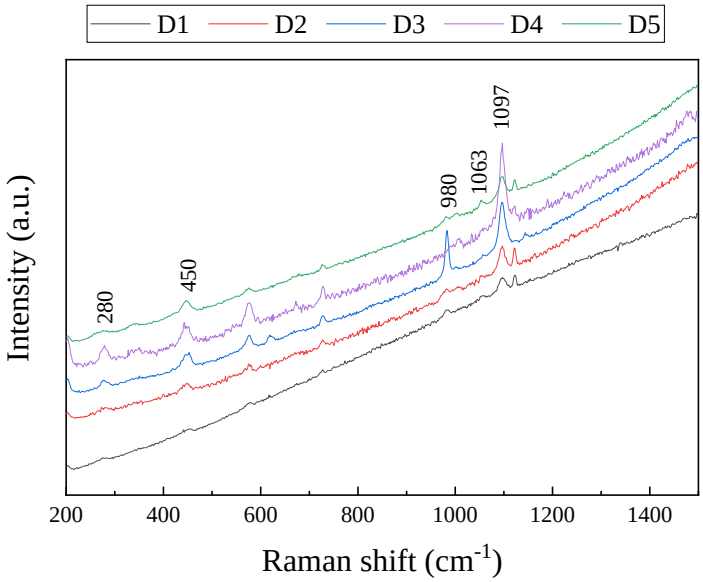

Fig. VIII-14: Raman spectra of NiFe_KWC foams at the end of the stability tests

The samples D (Fig. VIII-14) were obtained at the end of the stability test and of the overall experimental campaign, which lasted approximately six months. Also in this case, no deactivation was observed based on the performances of the catalyst. However, looking at the spectra obtained in different points of the samples, several observations can be made. Firstly, there is an evolution in the peaks, moving from the inlet to the outlet section of the catalytic bed. The peak ascribable to the presence of $KAl(OH)_2CO_3$ is visible in correspondence of the inlet and the outlet section, but it is particularly sharp in positions that correspond to the middle part of the catalytic bed (spectra of the position D3 and D4). In position D2, there are two small peaks at 450 and 980 cm^{-1} which become more evident in positions D3 and D4, and can be attributed without a doubt to the presence of K_2SO_4 over the surface. In addition, in positions D2 and D3, but more clearly in position D4, there is a peak at 280 cm^{-1} that can be related to the presence of sulfides on the surface, and in particular to the presence of K_2S.

Hence, it is possible to conclude that the presence of H_2S produced by the reaction and the co-existence of a large amount of CO_2 imply the formation of potassium sulfides and sulfates over the catalyst. However, this did not have an impact on the catalytic activity, which remained unvaried all over the tests period.

To further stress the catalyst, it was left in a more concentrated hydrolysis stream (1 vol.% COS) for 24 h. At the end of the test, the initial activity dropped remarkably (COS conversion around 10%), and the foams showed a distinguish layer of sulfur deposited onto the surface. The results of the analysis are in line with the previous observation on spent catalysts and with the visible sulfur deposition. In addition, a peak ascribable to α-S_8 appeared in the spent spectrum at 155, 223 and 474 cm^{-1} (Fig. VIII-15), coherently with the macroscopic sulfur observation (Fig. VIII-16). The resume of the peaks attribution in this section is given in Table VIII-2.

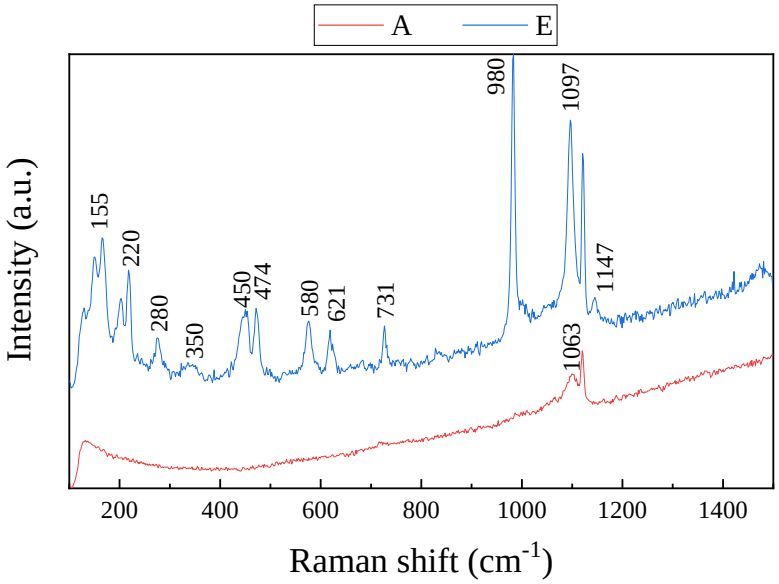

Fig. VIII-15: Raman spectra of the fresh and spent (after stress test) NiFe_KWC sample

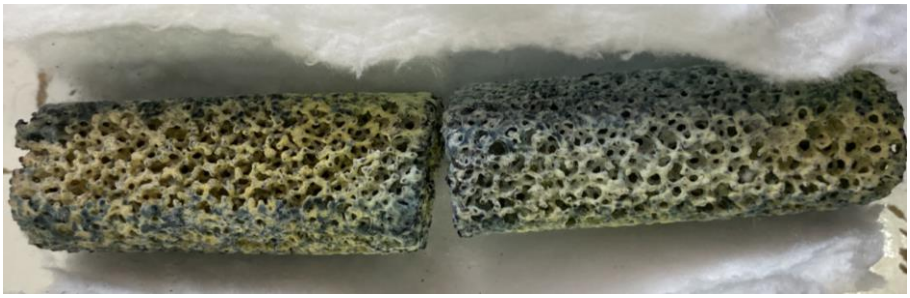

Fig. VIII-16: Foams at the end of the concentrated COS stream stability test

Table VIII-2: Raman peaks attribution for the spectra in this work

Peak position (cm^{-1})	Attribution	Ref.
155	α-S_8	(Remazeilles *et al.*, 2011)[1]
206	FeS	[1]
220	α-S_8	[1]
222	ß-NiS	(Bishop *et al.*, 1998)[2]
280	K_2S/FeS	[1]
350	ß-NiS	[2]
450	K_2SO_4	(Qiu *et al.*, 2019)[3]
474	α-S_8	[1]
621	K_2SO_4	[3]
980	K_2SO_4	[3]
1063	K_2CO_3	(Wang *et al.*, 2001)[4]
1097	$KAl(OH)_2CO_3$	[4]
1147	K_2SO_4	[3]

VIII.2 Hydrolysis and absorption integration

VIII.2.1 The idea

As discussed, the integration of two or more process units is one of the main tools of process intensification. In the case of COS abatement, the idea at the basis of the integration of the hydrolysis and absorption units can be explained as follows.

As proven in the first part of this PhD thesis, it is possible to find a condition in which the hydrolysis and the absorption can work at the same operating conditions. This is already a solution to lower the overall equipment and processing costs. Once achieved the temperature coupling, the process could be further intensified. The industrial columns are equipped with packing materials, to enhance the mass transfer between phases. In the hypothesis of substituting this packing material with a catalyst, different interphase surfaces can be created:

- A solid/gas/liquid (S/G/L) interphase is created. A fraction of the overall COS entering the system is converted over the catalyst via the heterogeneous gas-phase reaction at the interphase S/G, while another aliquot is absorbed at the interphase G/L (Scheme A in Fig. VIII-17). In this case, the COS concentration at the solid surface is at its maximum (only depends on the diffusion phenomena of COS in the gas bulk) and the reaction can be performed at its maximum extent. In addition, the gas phase hydrolysis over the catalyst could be further enhanced by the continuous absorption of H2S by the amine solution.
- A solid/liquid/gas (S/L/G) interphase is created. COS has to be absorbed in the liquid phase at the interphase G/L, and then transferred at the L/S interphase where it can react (Scheme B in Fig. VIII-17). In this second case, the resistance to mass transfer is due to the concentration gradient in the gas and liquid film, and also to the limitation of the gas/liquid equilibrium regulated by the Henry's low. Hence, the COS concentration at the solid surface is inevitably lower than case A, then a lower COS conversion is expectable.

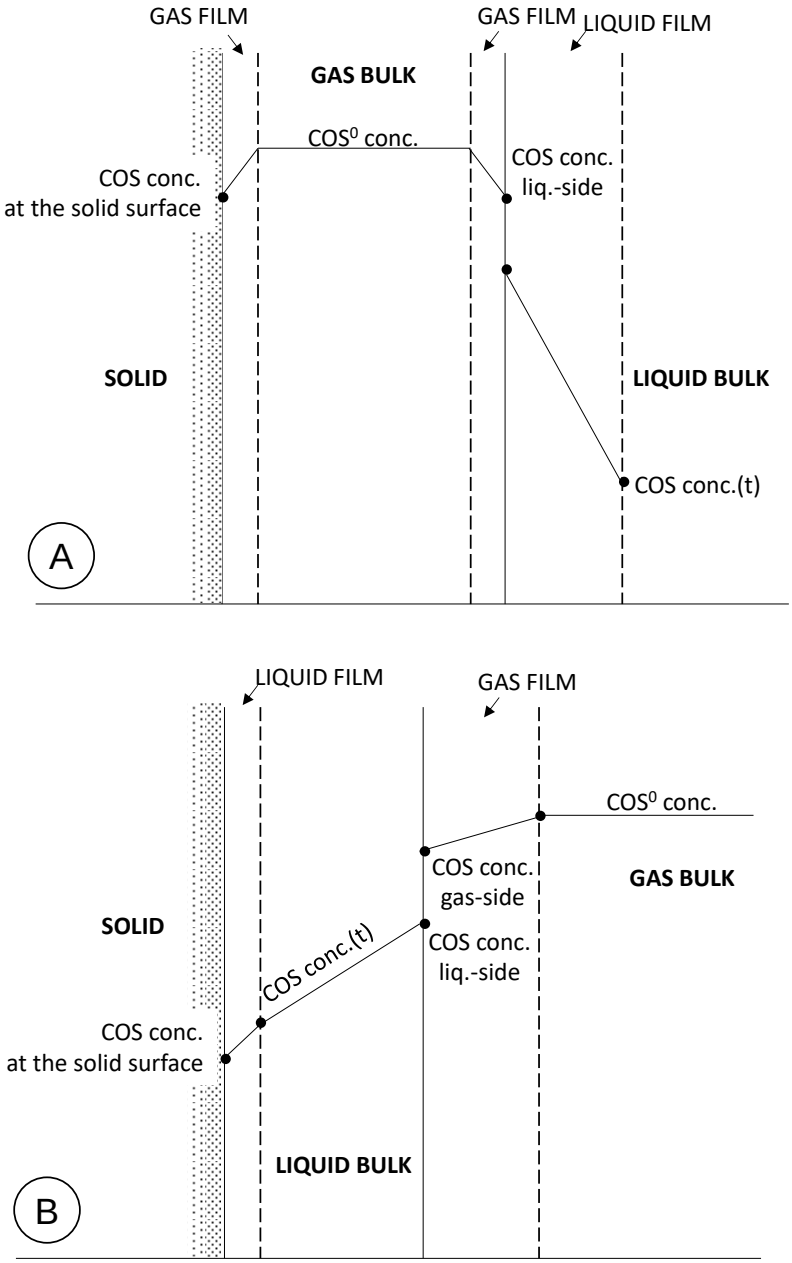

Fig. VIII-17: Schematic representation of the three-phase system's possible interphase surfaces.

The possibility of substituting the optimized packings already present in an absorption column with a conventional pellet is slightly appealing: the pellets

would never allow to achieve the same interphase surfaces, and the overall mass transfer would be penalized.

Nevertheless, this work demonstrated that it is possible to employ structured catalysts for the gas-phase hydrolysis. Furthermore, their application resulted in an enhancement of the catalytic performances of the process, thanks to the existence of a micrometric layer of catalyst deposed on the carrier which offer an inferior mass transport resistance, boosting the overall reaction rate.

Structured catalysts can be of any shape and any material; eventually, the coating procedure is adjusted to reach the desired adherence. Hence, it is possible to hypothesize a substitution of the non-catalytic packing material with a catalyzed packing material, to investigate the possibility of a three-phase reaction system. Naturally, this study must be preceded by the optimization of the reactor configuration, to approach the industrial fluid dynamic conditions. Furthermore, a comprehensive evaluation of the behavior of the system in several conditions, to discriminate the absorbing capacity and the influence of the packing material must be conducted prior to the evaluation of the effect of the catalyst presence within the system.

VIII.2.2 Reactor design

As discussed in Chapter VII, the hydrolysis and the absorption stage can be performed as a closed box kept at the same temperature. Nevertheless, the results achieved with the customized absorber cMDEA were discouraging, with only the 4.7% of COS removed from the gaseous stream at 60 °C and 36 s. As already observed, the geometry of the reactor is not able to represent sufficiently the highly turbulent conditions realized in an industrial absorber, and in particular the gas linear velocity is extremely limited.

Therefore, the design of a new lab-scale absorber was performed. In order to reach a gas linear velocity as near as possible to the industrial process, the aspect ratio of the reactor was completely overturned. The diameter was shrunk from 32 mm up to 10 mm. Therefore, to ensure a sufficient contact time considering the limitation on the flowrate, the length of the reactor was increased to 110 cm. Because of the high gas linear velocity produced by this configuration, the possibility of entrainment of liquid droplets was taken into account. Hence, the reactor designed comprehended a conic section at the head, in correspondence to the outlet of the gas stream, to avoid the liquid to reach the sampling line, which could induce problems to the analyzer and possible plugging of the capillary.

In addition, considering the reduced dimensions of this reactor, it was designed to be modular. This choice had the purpose of solving two issues: in the first instance, to have user-friendly charge/discharge operations; secondly,

to moderate as much as possible the damage to the structured catalysts, which are particularly fragile, since the diameter is remarkably small.

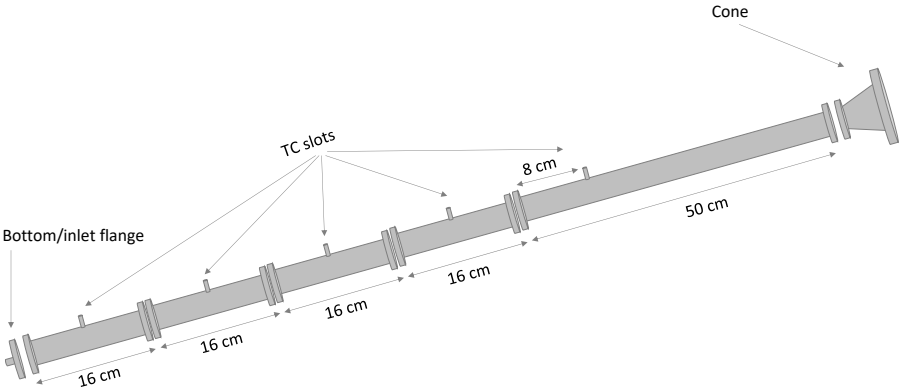

Fig. VIII-18: Scheme of the designed reactor configuration

The scheme of the reactor was provided in Fig. IV-3 (a).

A preliminary test to evaluate the fluid dynamic was performed with a colored solution, to trace eventual entraining to the outlet, and indeed even when using half of the total height of the reactor some droplets of solution were dragged to the outlet. To overcome the problem, it was decided to work with a maximum solution volume of 50 cm^3 and to add a coarse filter before the conic section to disrupt the droplets. This solution allowed to establish an adequate condition to operate the reactor.

VIII.2.3 Absorption test in liquid phase

To evaluate the absorption ability of the cMDEA solution in the new designed reactor, several tests were performed. The contact time was varied in the range 4-14 s, since higher contact time were not achievable in this configuration, and the temperature was kept at 60 °C for sake of comparison.

Since the liquid phase in the designed configuration is batch, to avoid a possible deterioration of the solution due to deactivation or changes in liquid/gas interphase equilibrium conditions, each condition has been tested with a fresh amine solution. The COS absorption was evaluated as average of the value acquired over a one-hour test.

The results are outstanding, when compared to the one obtained in the previous reactor configuration, as reported in Table VIII-3. As can be easily observed, even with a contact time of approximately one-half of the previously evaluated one, the system was able to ensure a COS removal efficiency of about 28%, compared to the 4.6% reached in the saturator-like configuration. This outcome confirmed the theory of mass transfer limitation, and further

highlighted the importance of having a high gas linear velocity within the system.

Table VIII-3: Comparison of COS removal efficiency at 60 °C in the two configurations employed for absorption in cMDEA

Configuration	Total flowrate ($Ncm^3\ min^{-1}$)	Contact time (s)	Gas linear velocity ($cm\ s^{-1}$)	COS removal efficiency (%)
Saturator-like reactor (Ø 30 mm)	200	36	0.5	4.6
Tubular reactor (Ø 9 mm)	180	14	5	28.1
	400	6	10	21.6
	600	5	16	17.3

Furthermore, it was also observed that with the decrease of the contact time and the increase in gas linear velocity, a reduction in COS removal efficiency occurred, but it was not particularly effective, with the lower value obtained of 17.3% of COS removed. Despite the contact time approximately 1/6 of the initial value, thanks to the improved transport in the gaseous bulk the efficiency was still significantly higher than the one measured in the first attempt. Therefore, also the absorption temperature was progressively reduced to 33 °C, the lowest condition which was possible to achieve. The absorption ability of the cMEDA solution was evaluated in each contact time condition and the results are shown in Fig. VIII-19.

As can be observed, the temperature reduction produces a drop in the COS removal efficiency. Nevertheless, even in the most disadvantageous operating condition, almost the 10% of initial COS is removed from the gas stream. Furthermore, the obtained results are conservative, with respect to the industrial conditions. Indeed, the condition at 33 °C and 14 s, with a gas linear velocity of 5 cm s^{-1}, allows to achieve a 15% COS removal efficiency, which is a value comparable to the industrial abatement, performed at ~ 25 s and with a gas linear velocity of ~ 13 cm s^{-1}.

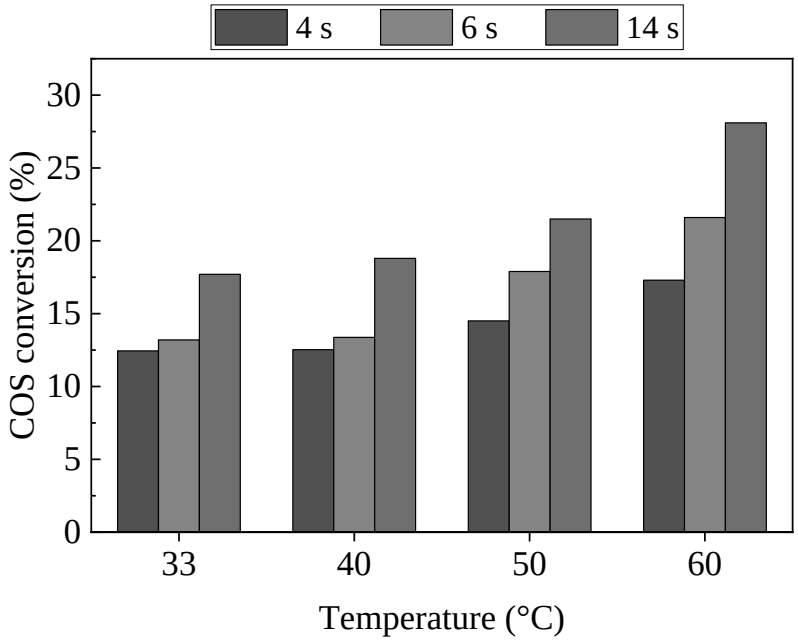

Fig. VIII-19: COS removal in cMDEA aqueous solution as a function of T and contact time. COS^{in} = 500 ppm. No packing material in the absorber.

After these preliminary evaluations, several investigations were conducted to test the amine solution absorption capacity. Indeed, it is likely that, in a batch configuration, the solution is saturated with all the compounds in the system. The time and the saturation capacity are significant for the forthcoming evaluation of the three-phase system performances.

Hence, a stability test on COS absorption was conducted in presence of 40 cm^3 of cMDEA solution, at the temperature of 33 °C and the contact time of 14 s, and the outcomes are reported in Fig. VIII-20. The test was conducted both in the absence and in presence of a non-catalytic packing, in particular NiFe foams.

The first consideration that can be made observing the outcomes is that the absorption behavior is different depending on the presence of the packing material. In particular, when the removal is realized only in presence of the cMDEA solution, the COS concentration plateau is reached after almost 4 h, while with the system containing also the NiFe foams the plateau is reached after almost 12 h. This observation is quite strange if considering that in presence of physical absorption, the capacity of the solution should be the same; the only difference between the two configurations is the absorption velocity (higher for the system with packing) and thus the breakthrough time (lower for the system with packing, consequently). The other particularity is that the COS concentration reached at the plateau is not consistent with the fed COS.

In the present literature, the absorption of COS in tertiary amine solutions has been described as a stepwise process that needs the hydrolysis reaction in liquid phase to occur first. Coupling this consideration with the present results, it can be hypothesized that the total amount of COS absorbed in cMDEA solution is the sum of two contributions: a part of COS is physically absorbed by the solution, while another part reacts in liquid phase forming H_2S and CO_2, both absorbed by the cMDEA and then not observed during the test.

Hence, the liquid phase reaction is enhanced by the presence of packing, subtracting COS to the physical absorption aliquot, and increasing the time to reach the plateau value. In addition, once that the COS absorption capacity is reached, the liquid phase hydrolysis continues since that the H_2S absorption capacity is apparently higher.

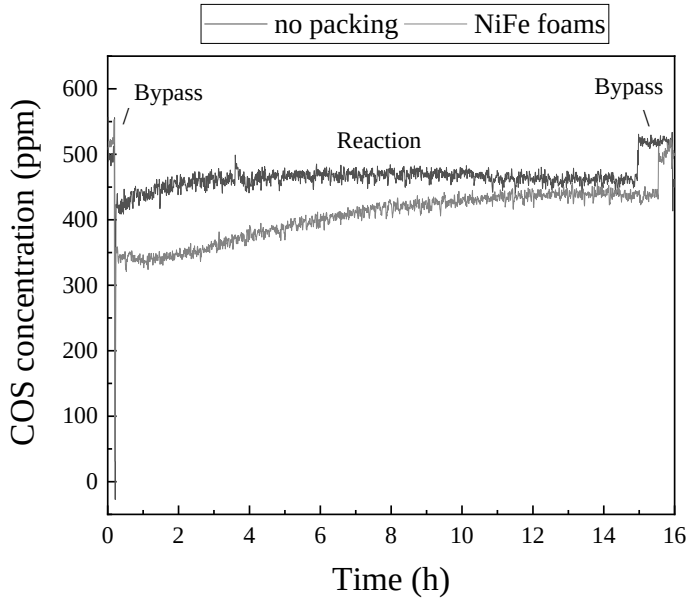

Fig. VIII-20: COS absorption in cMDEA solution: stability test. Operating conditions: t = 14 s, T = 33 °C, COS 500 ppm, H_2O 5 vol.%, N_2 bal.

To prove that in the time of COS absorption test it was impossible to see any H_2S leaving the cMDEA solution, also the H_2S absorption capacity of the sorbent was tested, in presence and in the absence of NiFe foams as packing material. The outcomes are reported in Fig. VIII-21.

As can be observed, the H_2S absorption capacity is outstanding, compared to the COS absorption capacity. The H_2S concentration instantaneously went to zero when the feed stream was kept in contact with the solution, and the removal was total in the first hours of test. The time of breakthrough was of almost 5 h in case of no packing and almost 6 h in case of NiFe foams presence. Accordingly, the H_2S concentration at the outlet of the absorber

returned to 500 ppm after 45 h for the NiFe foams system and after 60 h for the no packing system.

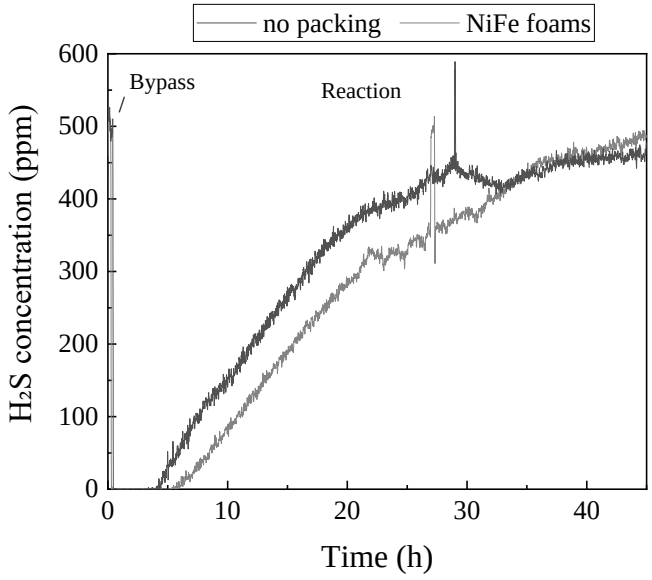

Fig. VIII-21: H_2S absorption in cMDEA solution: stability test. Operating conditions: t = 14 s, T = 33 °C, H_2S 500 ppm, H_2O 5 vol.%, N_2 bal.

This result is consistent with the hypothesis of chemical reaction in liquid phase, since that in presence of 500 ppm of H_2S the solution is able to absorb the whole hydrogen sulfide for almost 5-6 h, thus a higher time can be expected for a much lower concentration (closing the balances of Fig. VIII-20, no more than 100 ppm of H_2S).

To further corroborate the initial hypothesis, the cMDEA solution absorption was tested in presence of 5000 ppm of COS: the higher concentration is expected to allow to observe the hydrogen sulfide breakthrough. The outcomes, reported in Fig. VIII-22, completely upheld the hypotheses of this section.

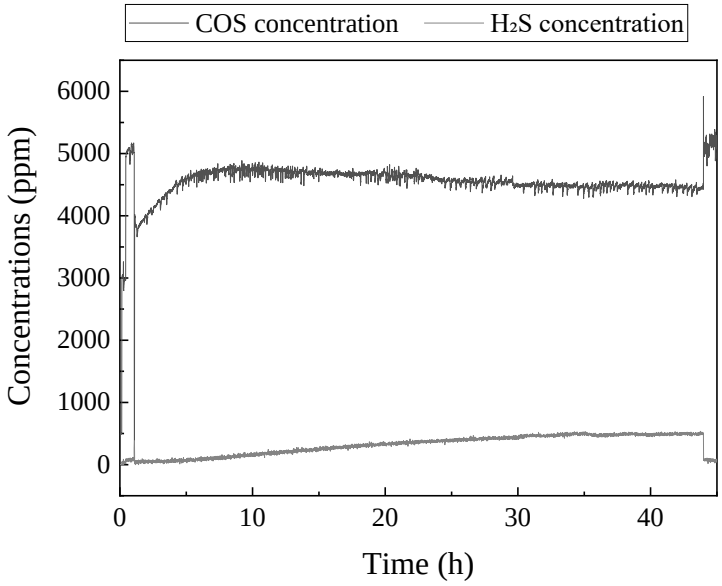

Fig. VIII-22: COS absorption in cMDEA solution: stability test. Operating conditions: t = 14 s, T = 33 °C, COS 5000 ppm, H_2O 5 vol.%, N_2 bal.

At the beginning of the absorption test, the COS removal was consistent with the one observed in the 500 ppm test: the removal is order 1 with respect to COS. Then, a fast increase in COS conversion was observed, while the H_2S concentration at the outlet remained zero until 6 h of test. Afterward, a slight increase in H_2S concentration was observed, fixing again the breakthrough time to 6 h. Considering that, except for the COS concentration, none of the other operating conditions was changed, this would suggest that almost 500 ppm of H_2S are produced. The reaction was interrupted at 45 h, when the plateau in H_2S concentration seemed to be reached.

At the end of the reaction, the balance closure was verified by calculating the average concentration of COS and H_2S in the time span 40-44 h. As can be observed from Table VIII-4, the sulfur balance is closed within an error of 1%. In addition, the H_2S concentration at the end of the test corresponds to 492 ppm, coherently with the time of breakthrough.

Table VIII-4: Sulfur balance verification at the end of 5000 ppm COS hydrolysis in liquid phase stability test

Time span (h)	COS (ppm)	H_2S (ppm)	Error (%)
40-44 h	4454	492	1%

VIII.2.4 Absorption test with a non-catalytic packed column

A general solution adopted in the industrial absorption column to enhance the transport phenomena between two different phases is to fill the column with a packing material. This allows to expand the interphase contact surface, and to increase the mass transfer coefficient. Due to the modest dimension of the lab-scale reactor, common packing material such as rasching ring are not applicable. To the aim of the process integration, packing materials having the same shape of the catalysts employed in this work were tested in a first instance. The pellets catalysts have been represented by glass spheres having a 3 mm diameter, as Fig. VIII-23 (a), while the foam catalysts are substituted with the foam carrier, without any catalytic phase deposited, a detail of the geometry is given in Fig. VIII-23 (b). To fit within the reactor, the foams were manually shaped in a cylindrical form with a diameter of 8 mm and a length of 160 mm, and then wrapped in a Teflon tape (Fig. VIII-24), to avoid eventual gas bypass phenomena between the packing and the reactor wall, and to help them sliding along the reactor length in the loading procedure.

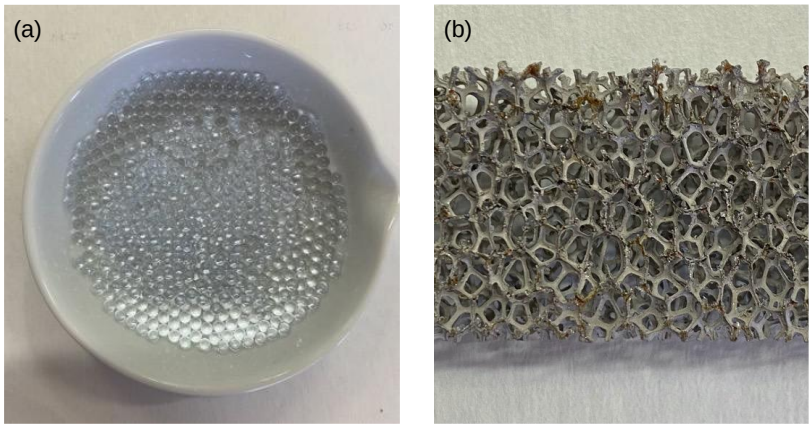

Fig. VIII-23: (a) glass spheres; (b) Ni-Fe mesh detail

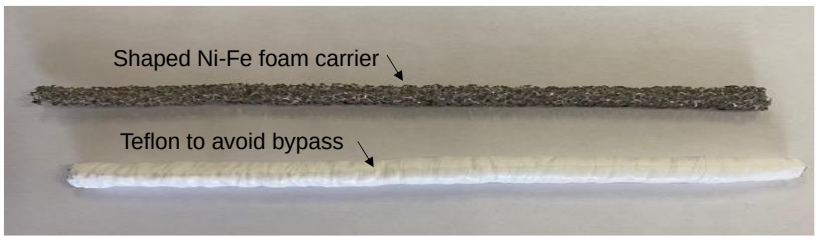

Fig. VIII-24: Shaped foam inserted in the reactor as a packing for COS absorption in cMDEA

To test the influence of the packing material, a total volume of 40 cm^3 of packing was set, corresponding to 4 stacked foams. The tests were conducted at a contact time of 4 and 14 s, and varying the temperature between 33 and 60 °C, to be comparable to the previous evaluations. The results are reported in Fig. VIII-25 (a) and (b).

As can be observed, the presence of a packing material is always beneficial to the absorption efficiency. This was expected, since the packing material has the explicit function of improving the mass transport and the interphase surface. Nevertheless, it is worth noting that in every operating condition, the foam structure is able to ensure better performances, thanks to its peculiar structure which increases the turbulence of the fluids. This is particularly visible at 14 s, since in this condition it is possible to observe the benefit of both the higher contact time and the higher turbulence which increase the local gas velocity, and thus the K_G coefficient.

Hence, the foams can be considered a good approximation of the conventional column packing.

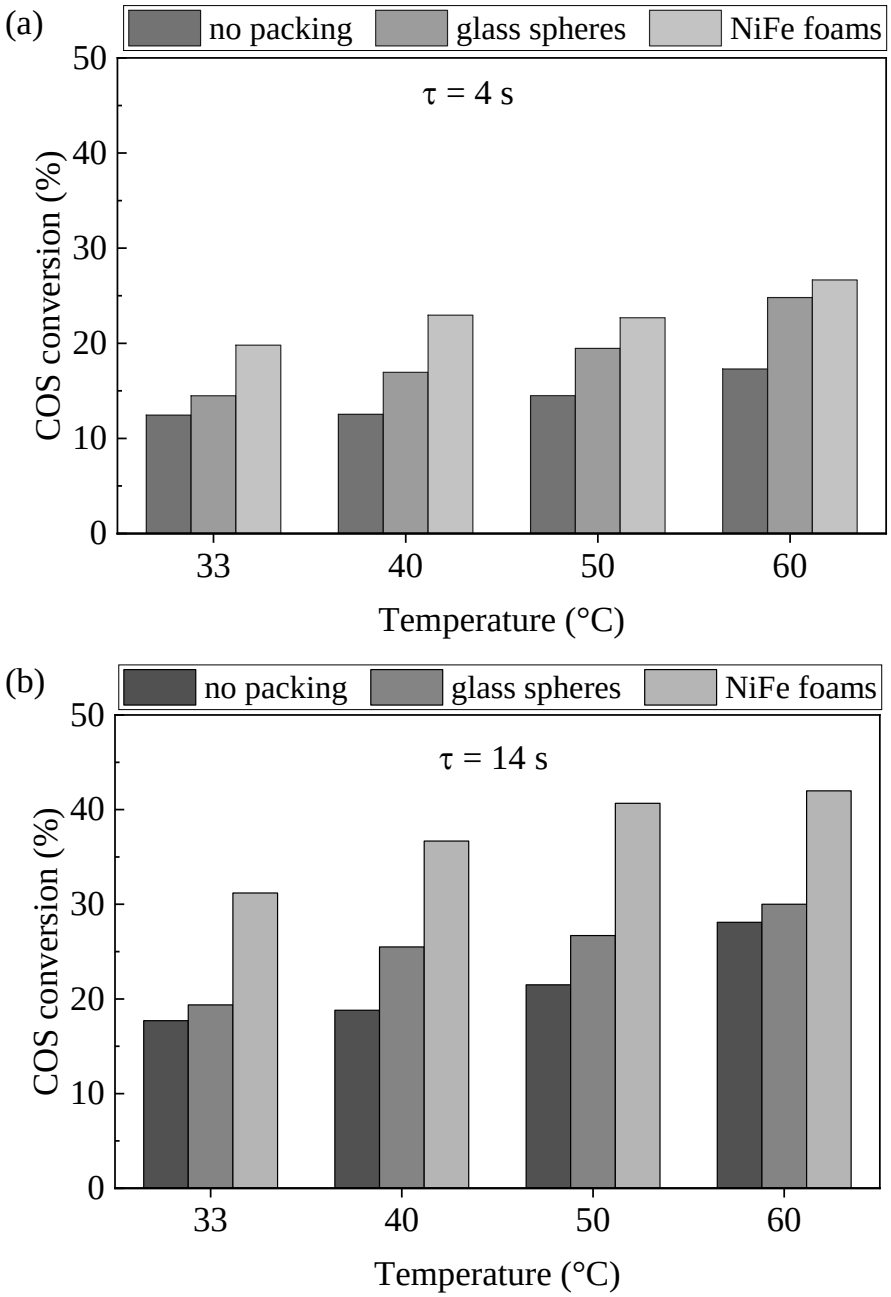

Fig. VIII-25: COS removal in cMDEA aqueous solution as a function of T and type of packing material. Operating conditions: 5 s, 500 ppm COS; (a) τ = 4 s, (b) τ = 14 s.

VIII.2.5 Absorption with a catalytic packing: three-phase system

To evaluate the effect of a catalytic packing within the absorption system, and to compare the efficiency of different catalysts in the liquid phase, both the pellet catalysts and the foams were tested. The foam catalysts were re-prepared following the procedure described in section IV.4, using the carriers shaped as in Fig. VIII-24. The tests were carried out in agreement with the previous ones, using temperatures in the range 33-60 °C and contact times of 5 and 17 s.

For sake of comparison, the COS efficiency obtained for both the catalysts was compared to the absorption in cMDEA (gas/liquid system) and in the corresponding cMDEA+packing system.

For the pellet catalysts, the results of the evaluation are reported in Fig. VIII-26. As it can be observed from Fig. VIII-26 (a), when the contact time is 4 s, it seems that the substitution of an inert packing material with a catalyst is not effective. The removal efficiency remained almost unvaried at all the temperatures evaluated. This may be ascribed to the fact that the catalyst pellets are soaking in the cMDEA solution, and the pores – which are responsible for the catalytic activity – are filled of liquid phase. Therefore, the mechanism followed by COS to arrive on the catalyst surface is probably the one displayed in Scheme B of Fig. VIII-17. The mass transport is limited by several resistances (diffusion in the gas bulk, absorption in the liquid solution, diffusion in the liquid bulk), and the contact time ensured is not enough for the COS to arrive on the solid surface. In good agreement with this hypothesis, as shown in Fig. VIII-26 (b), an improvement in the removal efficiency was observed at 14 s, in particular in condition of low operating temperatures. Despite the lower gas linear velocity, the higher contact time allows some of the COS in the feed to reach the catalyst surface and react. The advantageous effect of having a catalyst within the solution is observed especially at low temperatures because, as it was already observed (section VI.2), the pellet catalyst suffers of the problem of internal diffusion within the pores, already perceptible at 60 °C. Hence, at this temperature, the COS diffusion in porosities controls the overall reaction rate, and the presence of the catalyst is only slightly appreciable, compared to the effect of the glass spheres.

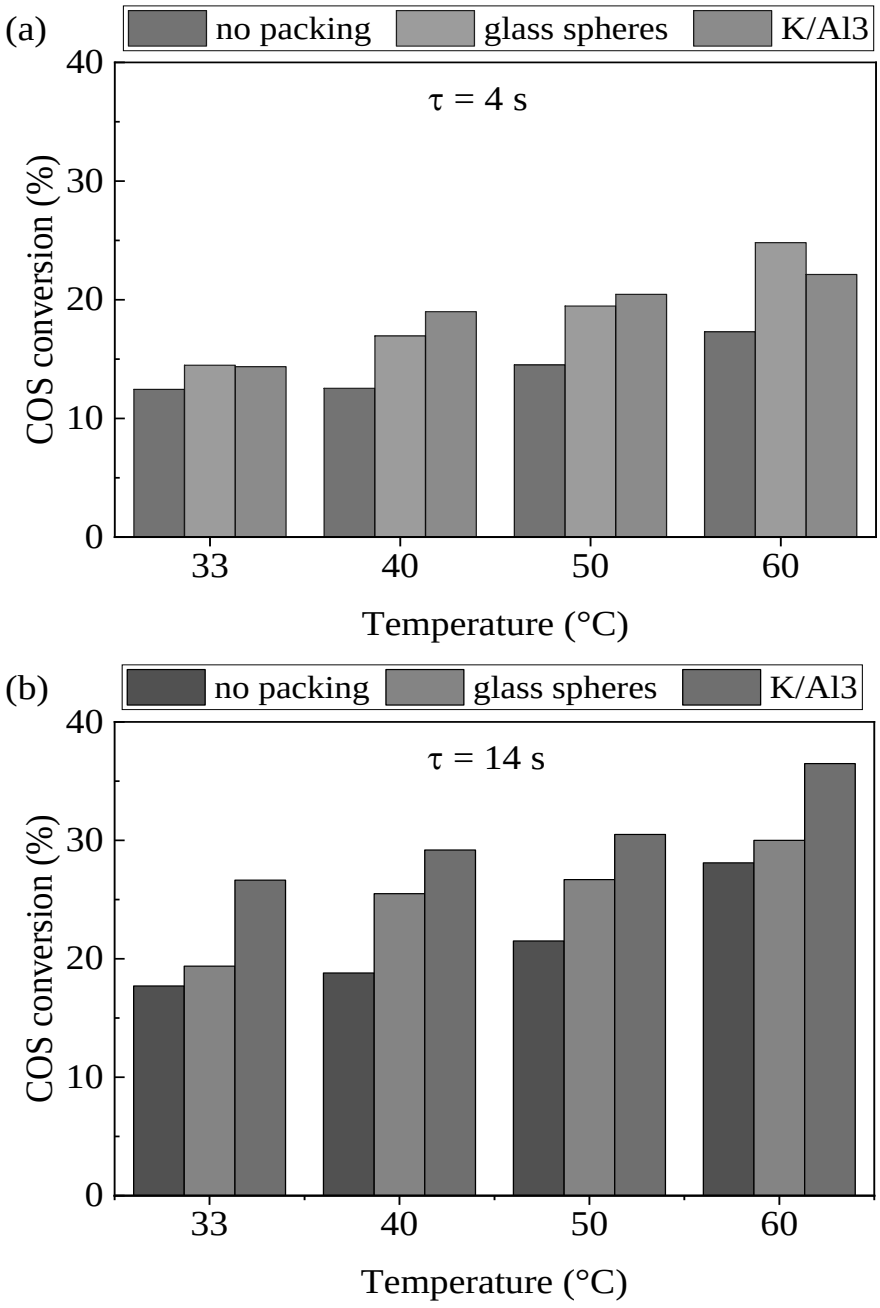

Fig. VIII-26: COS removal in cMDEA aqueous solution as a function of T and type of packing material. Operating conditions: 500 ppm COS; (a) τ = 4 s, (b) τ = 14 s.

As demonstrated in the first part of this chapter, the diffusion limitations due to the porous structure of the pellets can be overcome through the employment of structured catalysts. Furthermore, it has been observed that the complex structure of the foams employed as a carrier particularly enhances the mass transport, improving the COS removal also in presence of the ammine solution only. Hence, four foams shaped as Fig. VIII-24 were coated with the alumina washcoat and loaded with potassium, repeating the procedure followed for the Ø25 mm samples formerly tested, obtaining the samples shown in Fig. VIII-27. Then, the catalytic foams were wrapped with the Teflon tape as it was done for the non-catalytic ones, and stacked in the reactor. In line with all the previous experimental evaluations, the samples were activated in a 20% CO_2 stream for 1 h.

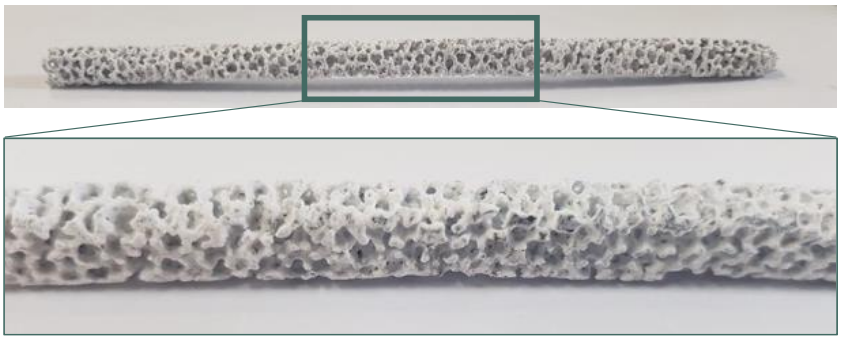

Fig. VIII-27: Catalytic foam (whole length and detail of the coating)

The foams were tested in the gas-phase reaction at first, to quantify the ability to convert COS when no liquid phase is present, and to discern the effect of the heterogeneous reaction and of the absorption in the three-phase system. For sake of comparison, the same flowrate employed in the previous tests with the cMDEA solution (which ensured the contact time of 4 and 14 s with respect to the liquid phase) were used for the catalytic activity tests. The results are reported in Table VIII-5. As can be observed, the catalytic activity is always outstanding, even in low-temperature conditions, thanks to the high contact time and the favorable fluid dynamic conditions.

Table VIII-5: COS conversion in the heterogeneous gas-phase reaction over the Ø9 mm foams

Total flowrate (Ncc min^{-1})	Contact time (s)	COS conversion (%)			
		33 °C	40 °C	50 °C	60 °C
180	14	25%	53%	99%	100%
600	4	5%	35%	90%	100%

Afterwards, to the catalytic foams stacked in the reactor, the cMDEA solution was added, to test the heterogeneous system. Since the effect of the heterogeneous reaction was observed with pellets in particular at high contact time, for the preliminary investigation a total flowrate of 180 Ncc min^{-1} was chosen, setting a contact time of 14 s.

The three-phase system was tested in two operating temperature conditions; the results obtained from the test are reported in Fig. VIII-28.

At 40 °C, comparing the three-phase system with catalytic packing material with non-catalytic absorption, only a slight increase in COS removal was observed. Nevertheless, if the achieved removal efficiency is compared to the conversion obtained with the same catalyst and in the same reactor (thus same fluid dynamic conditions), it can be noticed that the values are corresponding. This could suggest that the actual limitation in this three-phase system is the conversion on COS on the catalyst surface. Therefore, the operating condition was modified by setting the temperature at 60 °C, a condition in which the catalyst already ensured a total COS conversion (Table VIII-5) in order to not have limitations on the catalyst side.

As it can be observed from the second data set of Fig. VIII-28, the three-phase system achieved an almost total removal of COS. Hence, the previous hypothesis was confirmed to be valid: the limitation of the three-phase system in presence of structured catalysts is the COS conversion operated by the catalyst, since no other limitations to mass transport seemed to be present. For this reason, it can be supposed that the situation prospected by Scheme A in Fig. VIII-17 is the multiphase condition of the system. The micrometric layer of catalytic phase has its own porosities, but it behaves like a flat surface with respect to the liquid, probably promoting the direct contact between the structured catalyst and the gas phase.

These evaluations allowed to draw the following conclusions:

- It is feasible to perform a catalyst-assisted absorption of COS in a single three-phase reactor, with an enhancement of COS removal with respect to the absorption only
- The three-phase system removal efficiency is only limited by the COS conversion over the catalyst, thus from the catalyst activation threshold
- There is no beneficial effect due to H_2S removal through the amine solution on the hydrolysis, hence the three-phase system has no thermodynamic limitations.

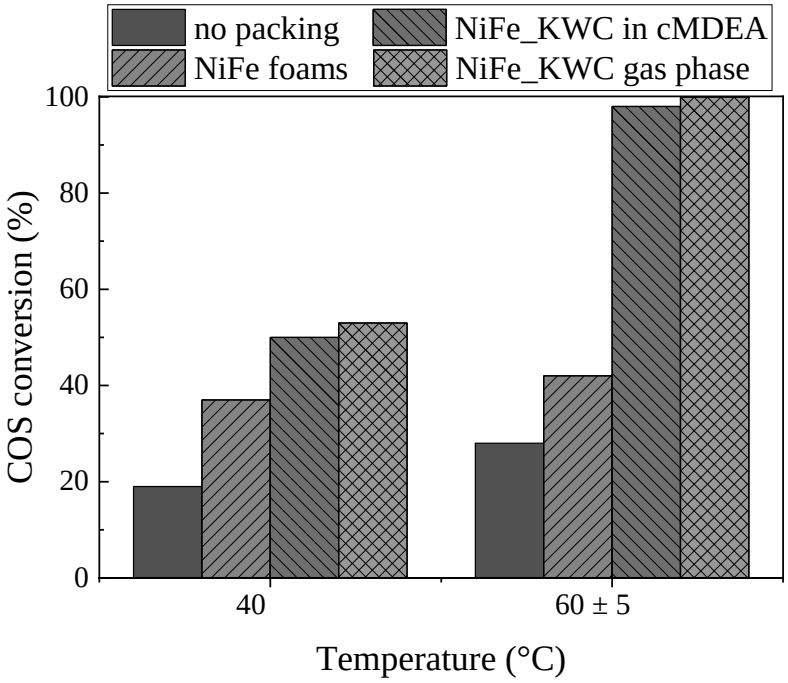

Fig. VIII-28: COS removal in three-phase system using catalytic foams as packing material in comparison with non-catalytic absorption and gas phase hydrolysis. Operating conditions: COS 500 ppm, H_2O 5 vol.%, N_2 bal.; contact time of 14 s.

The results of a short-term stability test on the three-phase system at 60 °C are displayed in Fig. VIII-29. As can be observed, for the first 20 minutes of test, the COS removal offered by the solution was total. Then, a slight decrease in the removal capacity up to the discussed 98% was observed, and this performance was maintained for the whole time of the test, which was more than 1 h. Hence, the catalyst was considered stable observing this time-on-stream test, with a COS emission of 9 ppm offered by the entire system. In addition, it is also possible to appreciate the role of the selected sorbent cMDEA, specifically designed to have a total selectivity toward H_2S. Indeed, no hydrogen sulfide was detected by the mass spectrometer during the whole test.

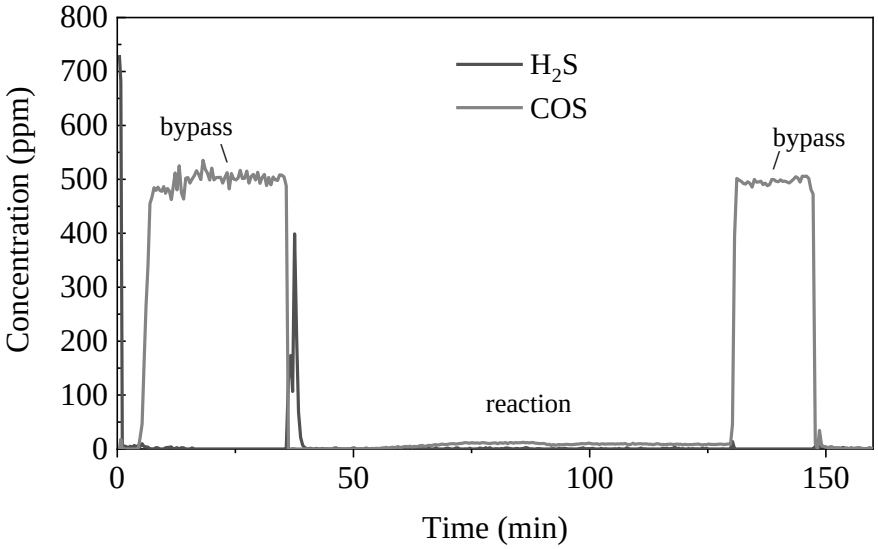

Fig. VIII-29: Time-on-stream stability test over the catalytic foam

Concluding, the designed three-phase system allow to treat a COS stream in a single process unit achieving an almost-total removal of sulfur compounds.

This achievement results particularly promising for industrial applications from several points of view.

In a first instance, the feasibility of a three-phase system means that it is possible to convert COS with the hydrolysis reaction without adding reactors and auxiliary units to pre-existent systems.

Secondly, it means that the COS removal obtained industrially in a single step can be enhanced without so much effort.

Then, the H_2S produced by the hydrolysis is no longer to be further removed, since that it is absorbed by the amine as it is produced, during the hydrolysis.

Concluding, this technology allows to enhance the COS removal even up to 100% with a change in the conventional operating conditions, without any modification of the industrial systems. The substitution of the column packings with a packing material coated with a suitable catalyst would simply do.

Chapter IX.
Modelling Results

IX.1 Preliminary kinetic model over pellet catalyst

During the first year of PhD, preliminary kinetic evaluations were performed on the optimized formulation. The knowledge of the kinetic parameters which are characteristic for each catalyst is particularly important for several calculations: dimensioning of reactors, scale-up considerations and further modeling of a reacting system. For what concerns previously reported kinetic models for COS hydrolysis, it is important to remind that, as above discussed, the reaction conditions strictly influence the driving phenomena and the reaction mechanism. For this reason, a model already present in literature could not be suitable to be applied in different conditions. The operating conditions employed in this work are scarcely investigated in literature, due to the remarkable disadvantage in using such high-water concentrations, therefore it is reasonable to find a poor agreement between the model available in literature and the present work. Hence, no assumption was made based on the literature in order to retrieve a kinetic description of the present catalytic system.

As a first step, the reaction order in COS and H_2O was evaluated, considering a power-law-type expression for the reaction rate.

Since the water concentration was found to be relevantly impacting on COS conversion, the reaction order in COS was evaluated on the optimized catalyst K/Al3 under two water concentrations (2 vol.% and 10 vol.%). In a first analysis, as reported in Fig. IX-1, the amount of reacted COS was found to be linear with the COS concentration in the feed stream, thus it was possible to conclude that the reaction rate is first order in COS. The same conclusion could be drawn with a different evaluation performed using the second feed condition (H_2O 10 vol.%): the COS concentration in the feed was kept unvaried, while the contact time was modified. The tests were conducted both on the catalyst K/Al3 and on the support Al3, obtaining the results shown in Fig. IX-2.

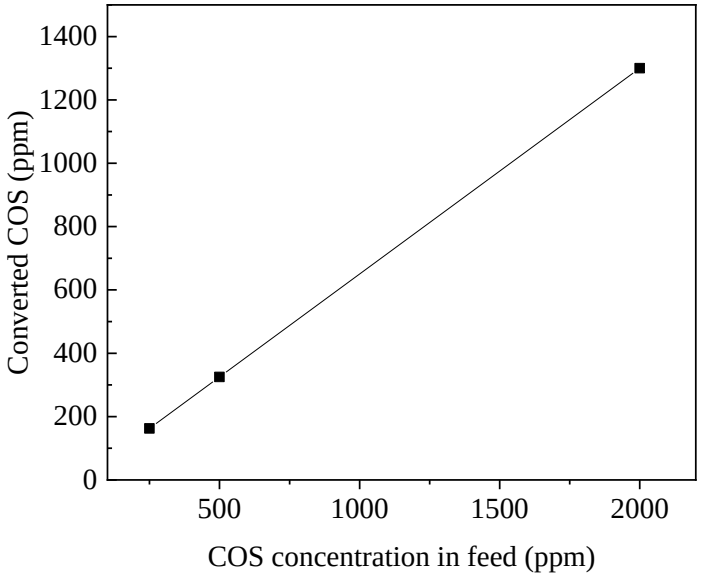

Fig. IX-1: Determination of COS reaction order. Operating conditions: H_2O 2 vol.%, T = 60 °C.

The Fig. IX-2 (a) shows the variation of COS conversion on contact time, and it is possible to see that, for both the catalysts, it is well approximated by a decreasing exponential function, approaching the total conversion in a long contact time. According to the integral analysis method and following eq. IV-4, it is possible to solve the equation in the hypothesis of any reaction order *n*. The results of the linear regression for the reaction order investigated were expressed in term of the statistic coefficient of determination, R^2, for both samples and are reported in Table IX-1.

Table IX-1: R^2 valued obtained for the linear regressions

	Al3	K/Al3
$n = 0$	0.987	0.9619
$n = 1$	0.9998	0.9976
$n = 2$	0.990	0.9861

The R^2 value is remarkably high in each case (> 0.95), and this is due to the relatively small number of experimental points; however, it is still possible to individuate a best fitting in the reaction order equal to 1, as shown in Fig. IX-2 (b).

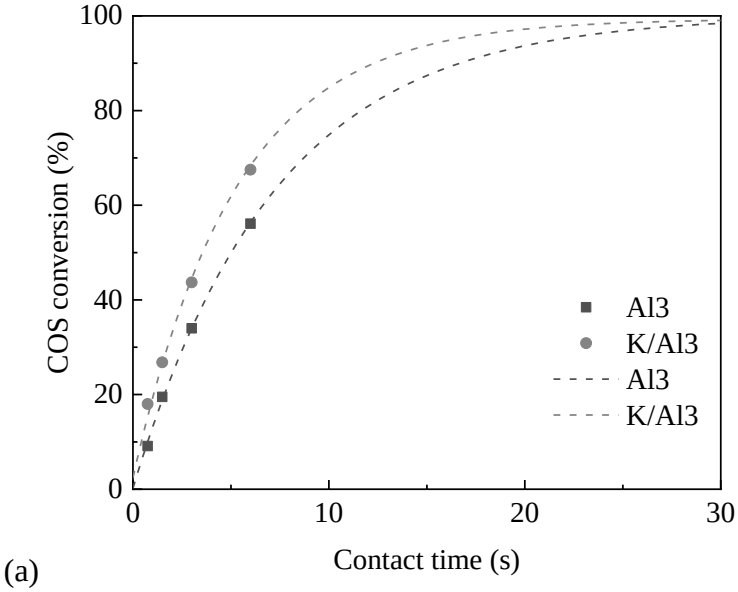

(a)

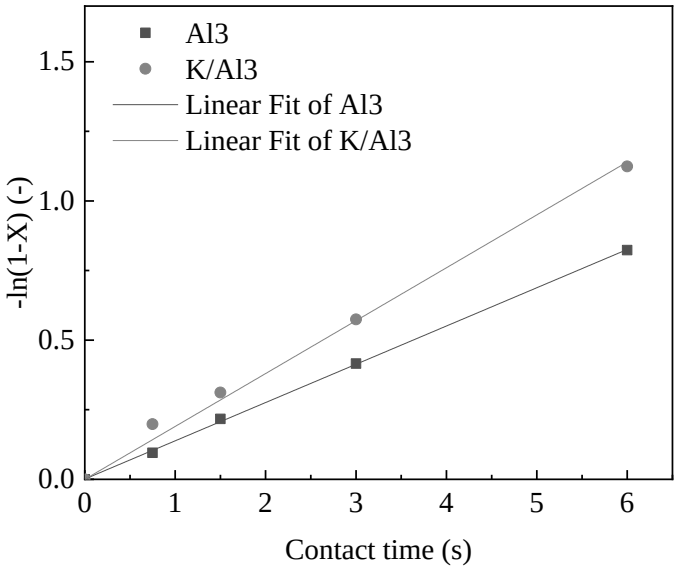

(b)

Fig. IX-2: (a) COS conversion dependency on contact time at T = 60°C and H_2O = 10 vol.%; (b) linear fit assuming an order-one kinetic in COS

Since the same conclusion was obtained adopting two different methods and two different operating conditions to establish the apparent reaction order in COS, it was assumed to be 1 from now on. Different were the conclusions drawn for the reaction order in water.

With the same methodology previously adopted, it was observed the amount of COS converted as a function of water concentration in feed, obtaining the results reported in IX-3). As it can be observed, there is a quasi-

linear trend in water concentration effect on COS conversion with a reaction order of -1 in water. Nevertheless, the approximation is poor. Therefore, a power-law expression for the reaction rate would be poor as well.

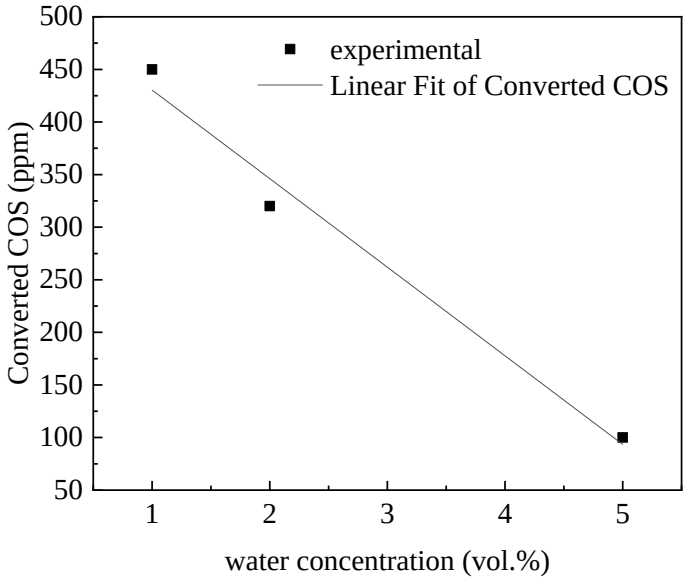

Fig. IX-3: Determination of H_2O reaction order. Operating conditions: COS 500 ppm, T = 60 °C.

The best option to describe the model is to select another reaction rate expression. Despite most of the kinetic model available in the present literature utilize a power-law expression, some more detailed works describe the COS hydrolysis using a Langmuir-Hinshelwood type reaction kinetic. This kinetic expression considers the adsorption on the catalyst surface of all the species which characterize a reacting system. In a system with *n* components, the total number of active sites (θ_{TOT}) can be occupied by the *i* species in different ways, depending on the tendency of each species to adsorb on the catalysts surface and on the species concentration within the system. In general, the adsorption of a component *i* can be expressed as eq. IX-1, with its adsorption equation given as eq. IX-2 and $\theta*$ being the number of free active sites. When more than one species is present, the adsorption is defined competitive, and the Langmuir equation for adsorption is generalized according to eq. IX-3. These considerations represent the basis for most of the kinetic models available in the open literature, and in particular have been widely applied to the COS hydrolysis case, leading to the expression for the reaction rate that has been reported the most, eq. IX-4 (Chiche and Schweitzer, 2017; Tong *et al.*, 1993; Zhao *et al.*, 2020a).

$$\theta_i = \frac{KP_i}{1+KP_i} \quad \text{IX-1}$$

$$i + \theta^* \rightleftarrows \theta_i \quad \text{IX-2}$$

$$\theta_i = \frac{KP_i}{\sum_{i=1}^{n} 1+KP_i} \quad \text{IX-3}$$

$$r_{COS} = k_c \frac{K_{COS} p_{COS} \cdot K_{H2O} p_{H2O}}{1+K_{COS} p_{COS}+K_{H2O} p_{H2O}} \quad \text{IX-4}$$

Using the Langmuir-Hinshelwood equation reported in literature, the kinetic and adsorption parameters can be obtained through the fitting of a set of experimental data. This has been done using fixed feed conditions, and changing the operating temperature and contact time. The parameters derived by the fitting are reported in Table IX-2, while the results of the fitting are displayed in Fig. IX-4.

Table IX-2: Kinetic and adsorption parameters obtained for the preliminary kinetic evaluation

	COS	**H_2O**
k^0 ($Torr^{-1}$)	$1.31 \cdot 10^{-15}$	$1.406 \cdot 10^{-3}$
ΔH (kJ mol^{-1})	-79	-99
K^0 ($Torr^2$ s^{-1})		**E_a** (kJ mol^{-1})
~ 33		~ 91

The model demonstrated a good representability of the experimental data for the higher temperatures, while a bad agreement was obtained for the condition of 43 °C (Fig. IX-4 a). In addition, it was evaluated the predictivity of the model by increasing the COS volumetric fraction in the feed stream from the initial 500 ppm up to 1500 ppm. As shown in Fig. IX-4 (b), only the 53 °C experimental set was well represented by the kinetic expression found. Besides, this preliminary result highlighted that the LH expression can be suitable for the representation of the kinetic behavior of COS hydrolysis.

Naturally, in order to obtain a fully-descriptive and predictive kinetic model, further considerations need to be made, and a wider range of experimental conditions must be considered.

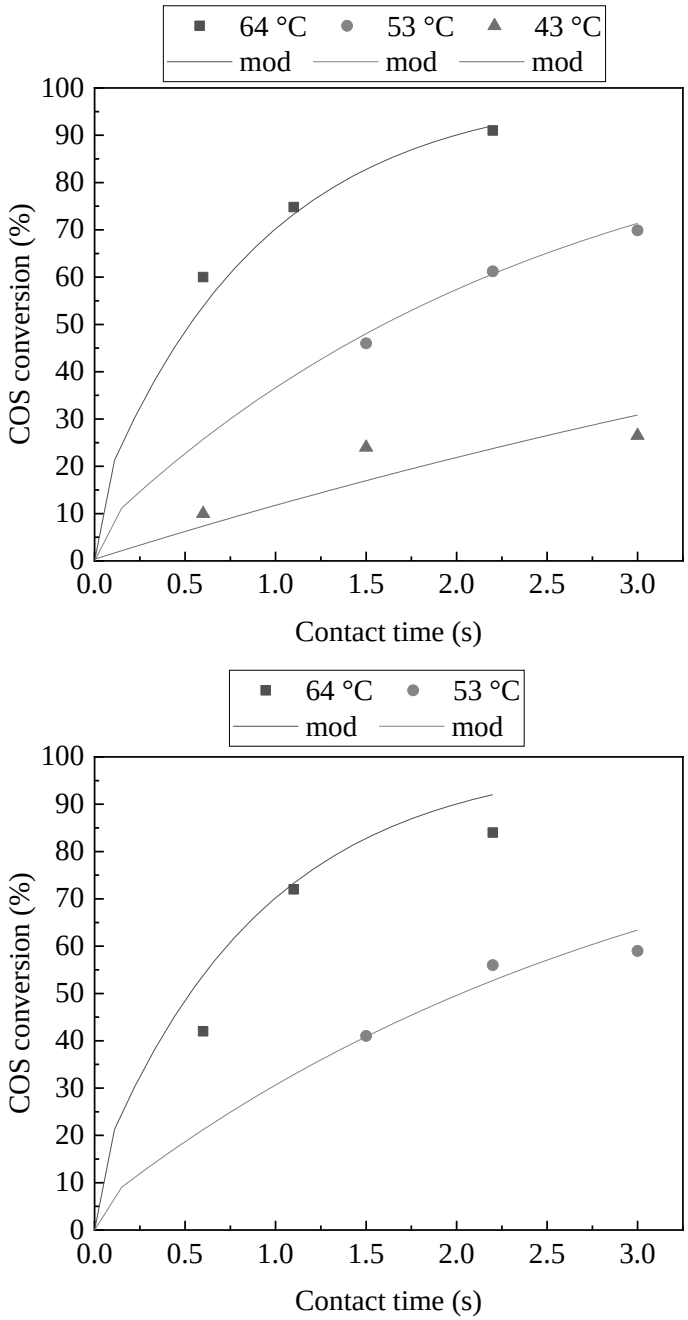

Fig. IX-4: (a) fitting of the experimental data using the LH model for the parameters estimation; (b) predictivity of the constructed model

IX.2 Kinetic model over structured catalyst

As stated in the Introduction and discussed in the previous section, the most credited model to describe the reaction kinetic of COS hydrolysis is the Langmuir-Hinshelwood theory.

The Langmuir-Hinshelwood expression given as eq. IX-4, which will be from now on addressed as Langmuir-Hinshelwood model 1 (LH1), is derived from the adsorption eqs. IX-5 and IX-6, from the hypothesis of superficial reaction according to eq. IX-7 and considering a first order reaction in COS and H_2O sites respectively, as eq. IV-11. The physical meaning of the two adsorption equations is that both water and COS adsorb on the catalysts surface following the single-site approach, and therefore the reaction occurs between two adsorbed molecules.

$$COS + \theta^* \rightleftarrows \theta_{COS} \qquad \text{IX-5}$$

$$H_2O + \theta^* \rightleftarrows \theta_{H_2O} \qquad \text{IX-6}$$

$$\theta_{H_2O} + \theta_{COS} \rightleftarrows \theta_{H_2S} + \theta_{CO_2} \qquad \text{IX-7}$$

LH1 cannot represent satisfactorily the COS hydrolysis reaction. This can be easily demonstrated by considering the dependence of COS conversion on CO_2 concentration in the feed stream. Since the model does not contain any dependence on CO_2 concentration, it is impossible to describe the experimental results. Hence, CO_2 must be deemed in the model.

Considering the equilibrium constant in the operating range of this work, the reaction can be assumed irreversible. For this reason, the only way to introduce CO_2 in the LH equation is to consider its competitive adsorption, leading to the expression of the total number of occupied active sites as eq. IX-8. In a first instance, the CO_2 adsorption can be approached as single-site adsorption, likewise COS and H_2O, given by eq. IX-9. Substituting eq. IX-8 in eq. IX-7, one can obtain the expression for LH2, gave in eq. IX-10.

$$\theta_{TOT} = \theta_{H_2O} + \theta_{COS} + \theta^* + \theta_{CO_2} \qquad \text{IX-8}$$

$$CO_2 + \theta^* \rightleftarrows \theta_{CO_2} \qquad \text{IX-9}$$

$$r_{COS} = k_c \frac{K_{COS} p_{COS} \cdot K_{H2O} p_{H2O}}{1 + K_{COS} p_{COS} + K_{H2O} p_{H2O} + K_{CO2} p_{CO2}} \qquad \text{IX-10}$$

The kinetic and adsorption parameters for the LH2 model, have been optimized through the minimization of the objective function defined in eq. IV-12. Since the solver (non-linear GRG) provides for a local solution, the initial values have been modified to obtain a global minimum for the system. The functionality of COS conversion on temperature, contact time, CO_2 and

H_2O concentration predicted by the model is compared to the experimental results in Fig. IX-5. As can be observed from the graphics, the LH2 model cannot fit the actual COS conversion dependency on CO_2 and H_2O concentration.

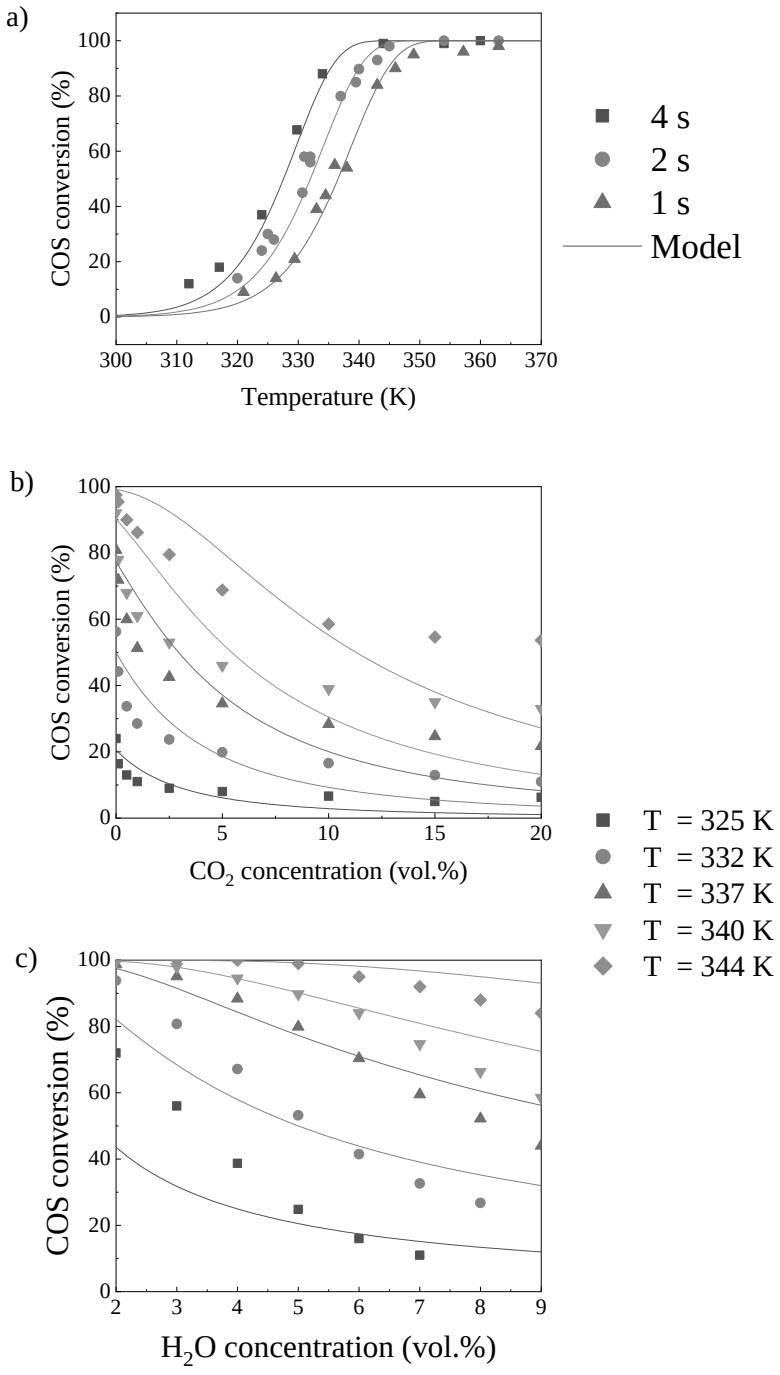

Fig. IX-5: Comparison of LH2 model and the experimental data. Fig. a) COS = 500 ppm, H_2O = 5 vol.%, N_2 bal.; Fig. b) tc = 2 s, COS = 500 ppm, H_2O = 5 vol.%, N_2 bal.; Fig. c) tc = 2 s, COS = 500 ppm, N_2 bal.

Based on the above, the hypotheses considered for this model are not satisfied, since it was impossible to find a set of parameters which fulfilled the representation of the experimental data. Therefore, as guessed in the former evaluation of the experimental results, it was necessary to distinguish for the contribution of each species. Of course, this must find a mathematical representation in the kinetic expression. Following the Langmuir theory of adsorption (Swenson and Stadie, 2019), it is possible to discriminate among six different adsorption mechanisms:

- Single-site
- Multi-site
- Generalized
- Cooperative
- Dissociative
- Multi-layer

Despite the single-site approach is by far the most employed for the description of adsorption phenomena, there are cases in which this assumption fails, as in the present study. This can be due to the low temperatures, the low concentration of the main reactant and the strong competition among the species for the adsorption on the active site, together with the reaction mechanism itself. Carbon dioxide adsorption mechanism was frequently reported in other literature systems as dissociative (Chen *et al.*, 2010; D'Evelyn *et al.*, 1986; Weatherbee and Bartholomew, 1982). Considering this hypothesis, the adsorption of CO_2 becomes described by eq. IX-11, and the number of sites consequently occupied depends on $p_{CO2}^{1/2}$ IX-12.

$$CO_2 + 2\theta^* \rightleftarrows \theta_{CO_2} \qquad \text{IX-11}$$

$$\theta_{CO2} = \frac{KP_{CO2}^{1/2}}{1+KP_{CO2}^{1/2}} \qquad \text{IX-12}$$

On the other hand, water is usually considered in literature with the approach of single-site adsorption. Nevertheless, COS hydrolysis has a peculiar mechanism, which is strictly dependent on water concentration. Indeed, DFT studies report that a single COS molecule could coordinate with one up to eight water molecules, and that the coordination of COS with two molecules of H_2O occurs with the higher probability (Deng *et al.*, 2007; Li *et al.*, 2014). Therefore, one can speculate that the need for this interaction could induce the cooperative adsorption of two water molecules on a single active site. Then, the adsorption equation is given by eq. IX-13 and the number of active sites occupied by water molecules is expressed as eq. IX-14, with a quadratic functionality in p_{H2O}.

Since no particular observations regarding the COS adsorption behavior could be found in literature, it was assumed that this could be described by a single-site mechanism. Considering the hypotheses of adsorption mechanism (i) single-site for COS, (ii) dissociative for CO_2, (iii) cooperative for H_2O, by

substituting the number of sites occupied by each species in eq. IX-8, the reaction rate (LH3) can be expressed as eq.IX-15.

$$2H_2O + \theta^* \rightleftarrows \theta_{H_2O} \qquad \text{IX-13}$$

$$\theta_{H2O} = \frac{KP_{H2O}^2}{1+KP_{H2O}^2} \qquad \text{IX-14}$$

$$r_{COS} = k_c \frac{K_{COS}p_{COS} \cdot K_{H2O}p_{H2O}^2}{1+K_{COS}p_{COS}+K_{H2O}p_{H2O}^2+K_{CO2}p_{CO2}^{1/2}} \qquad \text{IX-15}$$

The optimization of the kinetic and adsorption parameters following the LH3 expression are finally reported in Table IX-3, and the comparison with the experimental data is given by Fig. IX-6.

The fitting of the experimental results obtained with LH3 model is outstanding, particularly in view of the high number of tests and conditions which are represented, and also considering that a non-neglectable experimental error affects the measurements.

Comparing the fitting obtained with LH2 and LH3 models, it can be observed that it is always possible to extrapolate values for kinetic and adsorption parameters which could fit a number of experimental data obtained at fixed feed ratio, varying temperature and contact time (cases -a- in Figs. IX-5 and IX-6). When the variations also interest the concentration of reactants and products in the feed stream, the addition of other constraints to the resolution narrows the range in which the optimum can be found, and the fitting cannot be obtained without an adequate kinetic expression. In the case of COS hydrolysis, it was necessary to consider other possibilities for the adsorption equations to guarantee an adequate representation of the experimental data.

Based on the above, it is possible to speculate a reaction mechanism according to Fig. IX-7, in which an active site can potentially adsorb one molecule of COS and two of H_2O, while a single molecule of CO_2 can adsorb following a dissociative mechanism, occupying two active sites.

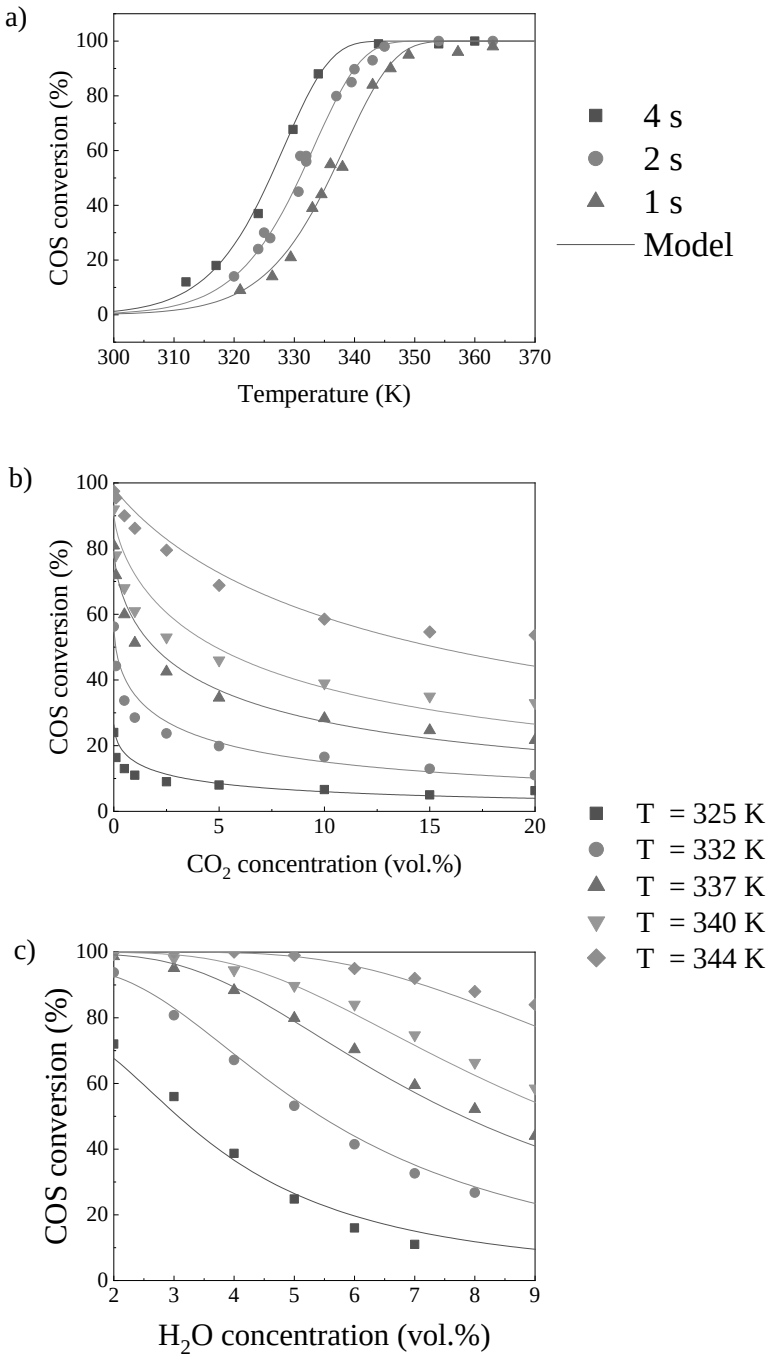

Fig. IX-6: Comparison of LH3 model and the experimental data. Fig. a) COS = 500 ppm, H_2O = 5 vol.%, N_2 bal.; Fig. b) tc = 2 s, COS = 500 ppm, H_2O = 5 vol.%, N_2 bal.; Fig. c) tc = 2 s, COS = 500 ppm, N_2 bal.

Table IX-3: Resume of the kinetic and adsorption parameters of this study

	LH1	LH2	LH3
k_c^0	33 ($Torr^2\ s^{-1}$)	$9.14 \cdot 10^{17}$ ($mol\ m^{-3}\ min^{-1}$)	$1.57 \cdot 10^{17}$ ($mol\ m^{-3}\ min^{-1}$)
E_a ($kJ\ mol^{-1}$)	91	98.4	86.5
k_{COS}^0 ($Torr^{-1}$)	$1.31 \cdot 10^{-15}$	$1.59 \cdot 10^{-5}$	$4.85 \cdot 10^{-8}$
ΔH_{COS} ($kJ\ mol^{-1}$)	-79	-54.7	-40.8
k_{H2O}^0	$1.406 \cdot 10^{-3}$ ($Torr^{-1}$)	$1.59 \cdot 10^{-5}$ ($Torr^{-2}$)	$3.42 \cdot 10^{-8}$ ($Torr^{-2}$)
ΔH_{H2O} ($kJ\ mol^{-1}$)	-99	-98.0	-81.4
k_{CO2}^0 ($Torr^{-0.5}$)	-	$2.79 \cdot 10^{-7}$	$1.59 \cdot 10^{-5}$
ΔH_{CO2} ($kJ\ mol^{-1}$)	-	-108.7	-79.4

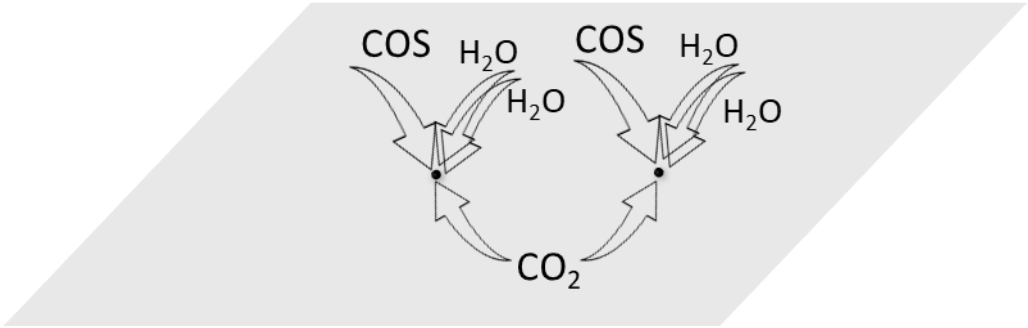

Fig. IX-7: Proposed mechanism for COS hydrolysis

IX.3 Evaluation of the predictivity of the model

The knowledge of a kinetic expression describing a catalytic system is a powerful tool, especially when applied to the industrial sector. Most of the processes undergo frequent changes in the feed stream conditions, based on

the kind of raw materials employed and other factors. This often defines limitations in the operating ranges, and on the equipment. The knowledge of the effect that a specific change would have on the process has the potential of solving impending issues prior to their manifestation. Using as a starting point a reliable kinetic model, a complete mapping of the reaction extent can be provided, in almost every condition.

Crossing the H_2O and CO_2 concentration, a matrix of over 26000 points for each temperature and contact time couple can be obtained. The 3D plots were obtained for four temperature conditions, up to 353 K, and the results are displayed in Fig. IX-8. The results confirm the strong detrimental effect of CO_2 presence in the system, which can be observed to be almost independent on the water concentration. On the other hand, a slight increase in temperature would significantly boost the COS conversion in a system in which a possible change in the feedstock would force the CO_2 concentration to increase.

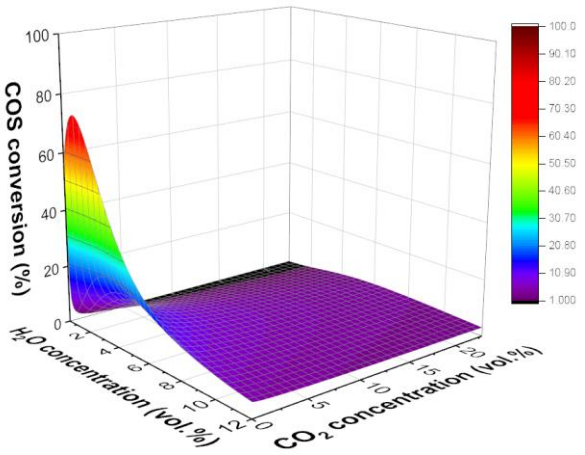

325 K

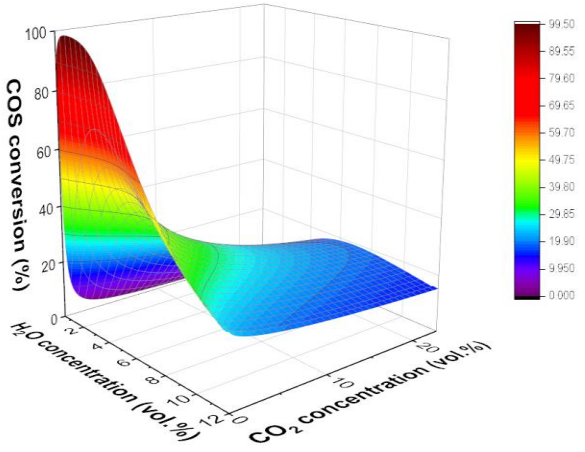

333 K

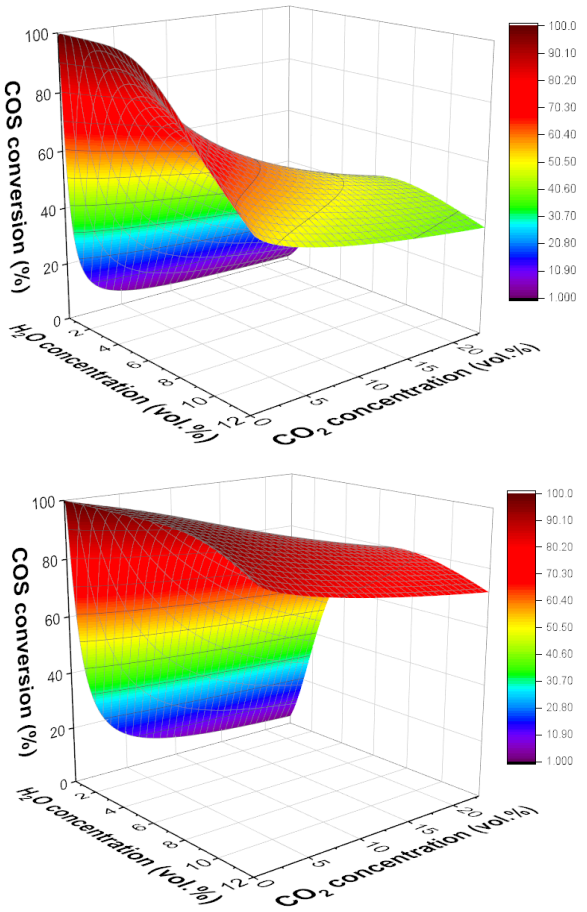

Fig. IX-8: Projection of COS conversion in several operating conditions using LH3 model.

To further corroborate the obtained model through the study of its predictivity, some experimental tests were performed crossing the H_2O and CO_2 concentration to obtain points of COS conversion within the XY-area, using as operating conditions T = 345 K and tc = 2 s. The experimental points and the modelled surface were overlaid, and the outcomes are displayed in Fig. IX-9. As can be observed, within the experimental error the model finds a noteworthy agreement with the experimental data. This achievement additionally validates the hypotheses of the adsorption type for each species, and the kinetic and adsorption parameters mathematically optimized.

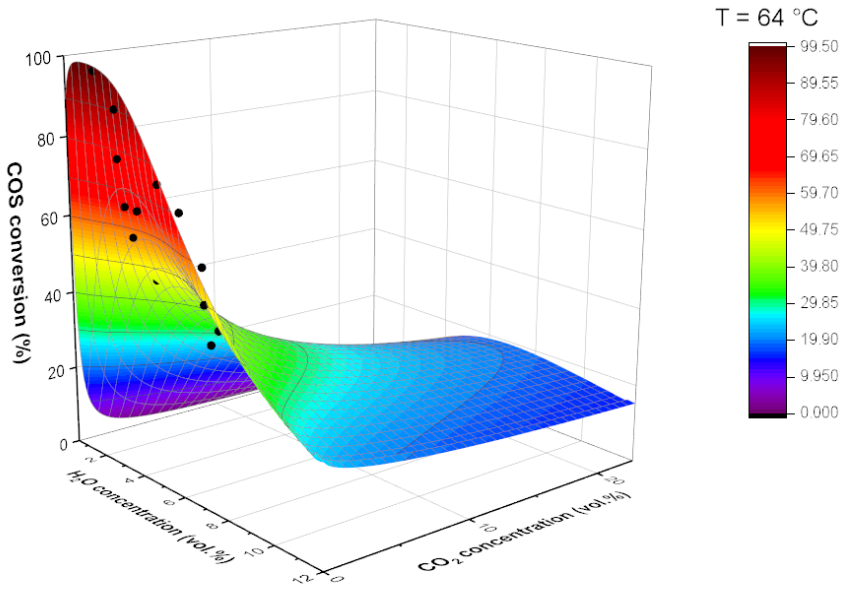

Fig. IX-9: Evaluation of the predictivity of the model. Comparison between experimental data and modelled surface.

Conclusions

As widely discussed in this final thesis, this PhD project arose from the shared interest of our laboratory, the ProCeed lab of the University of Salerno, and the company KT – Kinetic Technology of Rome, in depollution and new technologies.

The primary aim of this project was to put a step forward in the knowledge of carbonyl sulfide hydrolysis and in the transition of this technology between the research scale and the industrial sector.

Considering the nowadays gap that prevents its large-scale application, a first state-of-the-art analysis was performed in order to correctly address this research.

Two main issues were observed to affect the catalysts reported in literature: the complexity of the formulations, scarcely suitable from an industrial point of view, and the lifetime of the catalyst. The first achievement of the present study was then the finding of a relatively simple formulation, which demonstrated to be remarkably active in COS hydrolysis at low temperatures, reaching a complete COS abatement below 80 °C. Although the existence of limiting mass transfer phenomena was demonstrated during this work, the catalyst was designed to be in pellet shape, in order to faithfully resemble the ones commonly adopted by the industry. Further investigations on this catalyst allowed the stabilization of the active phase in a carbonate form, realizing a formulation able to resist to the S-rich atmosphere for several hours. Despite the deposition of elemental sulfur on the catalyst surface, no deactivation was detected during the time-on-stream stability tests.

Once identified the catalyst able to satisfactorily perform the hydrolysis of carbonyl sulfide at low temperatures, the feasibility of coupling the hydrolysis stage with the sweetening unit typical of the tail-gas treatment plants seemed not so far. A complete lab-scale setup was designed and realized in an open architecture configuration, with the hydrolysis reactor and the absorber operating at the same temperature in a closed box. Preliminary evaluations performed using DEA as sorbent allowed to reach an overall COS removal at 60 °C of about 60%, which is a competitive result compared to the abatement nowadays achieved by industrial applications. In addition, this solution would allow to reduce the equivalent SO_2 emissions of about 36% with respect to the stand-alone hydrolysis unit and of about 25% with respect to the conventional sweetening units. Considering that, in these results, the DEA solution did not allow to absorb completely the H_2S produced by the hydrolysis stage, a switch to a more selective absorber would provide for a better H_2S removal. On the other hand, the COS absorption would be penalized, hence for this kind of configuration would be preferable to have a better-performing hydrolysis

stage. Briefly, the units coupling in an open architecture configuration was highly promising, but still needed further optimization.

The achievement reported so far are two milestones in the COS hydrolysis process intensification, even though the actual research to this aim starts from the basis laid up to this point.

To enhance the COS hydrolysis by overcoming the mass diffusion limitations without losing the advantage of a shape applicable to industrial processes, it was decided to transfer the optimized formulation on a structured catalyst. These have a wide application in several processes, but they had not been tested, so far, in COS hydrolysis. Discriminating among several possible carriers, a 20 ppi Ni-Fe foam was selected, washcoated with an alumina-based slurry and in the end treated in KOH for the active phase deposition. Applied to COS hydrolysis, the structured catalyst demonstrated outstanding performances compared to the pellets, remarkably lowering the application range. This result has been addressed to the presence of a micrometric layer of doped-alumina, which clearly reduced the limitation to the diffusion of the reactants into the pores, compared to pellets. The obtainment of a system working in kinetic regime also allowed to redefine the kinetic model representing the reaction rate, switching from a Langmuir-Hinshelwood type expression with simplified hypothesis to a detailed LH type expression which accounted for the presence of the reaction products and considering three different adsorption mechanism. The developed model demonstrated to have a faithful predictivity of operating conditions remarkably different from the ones that allowed the parameters optimization. This achievement has a high industrial interest, since the knowledge of the predictivity of a system allows the tuning of the operating parameters in order to constantly ensure to reach the abatement target.

Going toward the end of the project, a final goal was set: the integration of catalytic COS hydrolysis and H_2S absorption in sweetening unit, in a single three-phase reactor. To fulfill this aim, a new reactor was designed and realized in order to ensure fluid dynamic conditions and contact time comparable to the industrial ones, and to accommodate structured catalyst in a user-friendly configuration. The results obtained from this study undoubtedly represent the most consistent step toward the industrial application. It was demonstrated that it is possible to perform a catalytic-assisted absorption of sulfur compounds in a sweetening unit, where COS is converted at the solid/gas interphase in H_2S, which is furtherly removed by a highly selective tertiary amine. The system has been tested both at 40 °C and 60 °C, allowing to assess that the actual limitation in COS abatement of this technology is the catalytic conversion: once the catalyst is able to ensure a complete COS conversion, then the abatement of sulfur compound in the integrated reactor is almost total.

The incalculable potential that this result has for the industrial sector can be easily discussed. It was demonstrated that is possible to achieve the total

removal of COS in Claus tail gas streams without any changes in existing plants configuration. It would be sufficient to substitute the conventional inert packing of the absorber column with a suitable catalytic packing, to have the COS hydrolyzed to more easily removable H_2S.

References

Al-Ghawas, H.A., Ruiz-Ibanez, G., Sandall, O.C., 1989. Absorption of carbonyl sulfide in aqueous methyldiethanolamine. Chem. Eng. Sci. 44, 631–639. https://doi.org/10.1016/0009-2509(89)85039-0

Alhashimi, H.A., Aktas, C.B., 2017. Life cycle environmental and economic performance of biochar compared with activated carbon: A meta-analysis. Resour. Conserv. Recycl. 118, 13–26. https://doi.org/10.1016/j.resconrec.2016.11.016

Amararene, F., Bouallou, C., 2004. Kinetics of carbonyl sulfide (COS) absorption with aqueous solutions of diethanolamine and methyldiethanolamine. Ind. Eng. Chem. Res. 43, 6136–6141. https://doi.org/10.1021/ie030540f

Bachelier, J., Aboulayt, A., Lavalley, J.C., Legendre, O., Luck, F., 1993. Activity of different metal oxides towards COS hydrolysis. Effect of SO2 and sulfation. Catal. Today 17, 55–62. https://doi.org/10.1016/0920-5861(93)80007-N

Bishop, D.W., Thomas, P.S., Ray, A.S., 1998. Raman spectra of nickel(II) sulfide. Mater. Res. Bull. 33, 1303–1306. https://doi.org/10.1016/S0025-5408(98)00121-4

Boffito, D.C., Van Gerven, T., 2019. Process Intensification and Catalysis, Chemistry Molecular Sciences and Chemical Engineering. Elsevier Inc. https://doi.org/10.1016/b978-0-12-409547-2.14343-4

Caplow, M., 1968. Kinetics of Carbamate Formation and Breakdown. J. Am. Chem. Soc. 90, 6795–6803. https://doi.org/10.1021/ja01026a041

Chen, H.L., Chen, H.T., Ho, J.J., 2010. Density functional studies of the adsorption and dissociation of CO2 molecule on Fe(111) surface. Langmuir 26, 775–781. https://doi.org/10.1021/la9021646

Chiche, D., Schweitzer, J.M., 2017. Investigation of competitive COS and HCN hydrolysis reactions upon an industrial catalyst: Langmuir-Hinshelwood kinetics modeling. Appl. Catal. B Environ. 205, 189–200. https://doi.org/10.1016/j.apcatb.2016.12.002

Clark, P.D., Dowling, N.I., Huang, M., Svrcek, W.Y., Monnery, W.D., 2001. Mechanisms of CO and COS formation in the Claus furnace. Ind. Eng. Chem. Res. 40, 497–508. https://doi.org/10.1021/ie990871l

Crutzen, P.J., 1976. The possible importance of CSO for the sulfate layer of the stratosphere. Geophys. Res. Lett. 3, 73.

D'Evelyn, M.P., Hamza, A. V., Gdowski, G.E., Madix, R.J., 1986. Dynamics of the dissociative adsorption of CO2 on Ni(100). Surf. Sci. 167, 451–473. https://doi.org/10.1016/0039-6028(86)90717-X

Deng, C., Li, Q.-G., Ren, Y., Wong, N.-B., Chu, S.-Y., Zhu, H.-J., 2007. A Comprehensive Theoretical Study on the Hydrolysis of Carbonyl Sulfide

in the Neutral Water. J. Comput. Chem. 29, 466–480. https://doi.org/10.1002/jcc

Di Stasi, C., Alvira, D., Greco, G., González, B., Manyà, J.J., 2019. Physically activated wheat straw-derived biochar for biomass pyrolysis vapors upgrading with high resistance against coke deactivation. Fuel 255, 115807. https://doi.org/10.1016/j.fuel.2019.115807

Di Stasi, C., Cortese, M., Greco, G., Renda, S., González, B., Palma, V., Manyà, J.J., 2021a. Optimization of the operating conditions for steam reforming of slow pyrolysis oil over an activated biochar-supported Ni e Co catalyst. Int. J. Hydrog. Energy. https://doi.org/10.1016/j.ijhydene.2021.05.193

Di Stasi, C., Renda, S., Greco, G., González, B., Palma, V., Manyà, J.J., 2021b. Wheat-straw-derived activated biochar as a renewable support of Ni-CeO2 catalysts for CO2 methanation. Sustain. 13. https://doi.org/10.3390/su13168939

EPA, 2018. Reporton the Environment: Sulfur dioxide emissions. https://doi.org/10.1126/science.228.4698.390

Ernst, W.R., Chen, M.S.K., Mitchell, D.L., 1990. Hydrolysis of carbonyl sulfide: Comparison to reactions of isocyanates. Can. J. Chem. Eng. 68, 319–323. https://doi.org/10.1002/cjce.5450680218

Feng, W., Kwon, S., Borguet, E., Vidic, R., 2005. Adsorption of hydrogen sulfide onto activated carbon fibers: Effect of pore structure and surface chemistry. Environ. Sci. Technol. 39, 9744–9749. https://doi.org/10.1021/es0507158

Fenton, D.M., Gowdy, H.W., 1979. The chemistry of the Beavon sulfur removal process. Environ. Int. 2, 183–186. https://doi.org/10.1016/0160-4120(79)90077-1

Ferm, R.J., 1957. The Chemistry of Carbonyl Sulfide. Chem. Rev. 57, 621–640. https://doi.org/10.1021/cr50016a002

Fioletov, V.E., McLinden, C.A., Krotkov, N., Li, C., Joiner, J., Theys, N., Carn, S., Moran, M.D., 2016. A global catalogue of large SO2 sources and emissions derived from the Ozone Monitoring Instrument. Atmos. Chem. Phys. 16, 11497–11519. https://doi.org/10.5194/acp-16-11497-2016

Frey, M., Édouard, D., Roger, A.C., 2015. Optimization of structured cellular foam-based catalysts for low-temperature carbon dioxide methanation in a platelet milli-reactor. Comptes Rendus Chim. 18, 283–292. https://doi.org/10.1016/j.crci.2015.01.002

Guo, F., Li, S., Hou, Y., Xu, J., Lin, S., Wang, X., 2019. Metalated carbon nitrides as base catalysts for efficient catalytic hydrolysis of carbonyl sulfide. Chem. Commun. 55, 11259–11262. https://doi.org/10.1039/c9cc06246g

Guo, H., Tang, L., Li, K., Ning, P., Peng, J., Lu, F., Gu, J., Bao, S., Liu, Y., Zhu, T., Duan, Z., 2015. Influence of the preparation conditions of

MgAlCe catalysts on the catalytic hydrolysis of carbonyl sulfide at low temperature. RSC Adv. 5, 20530–20537. https://doi.org/10.1039/c5ra00463b

He, E., Huang, G., Fan, H., Yang, C., Wang, H., Tian, Z., Wang, L., Zhao, Y., 2019. Macroporous alumina- and titania-based catalyst for carbonyl sulfide hydrolysis at ambient temperature. Fuel 246, 277–284. https://doi.org/10.1016/j.fuel.2019.02.097

Hinderaker, G., Sandall, O.C., 2000. Absorption of carbonyl sulfide in aqueous diethanolamine. Chem. Eng. Sci. 55, 5813–5818. https://doi.org/10.1016/S0009-2509(00)00420-6

Homann, V.K.H., Krome, G., Wagner, H.G., 1969. Schwefelkohlenstoffoxydation II. Zur Oxydation von Carbonylsulfid. Berichte der Bunsengesellschaft für Phys. Chemie 73, 967–971.

Huang, H., Young, N., Williams, B.P., Taylor, S.H., Hutchings, G., 2006a. High temperature COS hydrolysis catalysed by γ-Al2O3. Catal. Letters 110, 243–246. https://doi.org/10.1007/s10562-006-0115-x

Huang, H., Young, N., Williams, B.P., Taylor, S.H., Hutchings, G., 2006b. High temperature COS hydrolysis catalysed by γ-Al2O 3. Catal. Letters 110, 243–246. https://doi.org/10.1007/s10562-006-0115-x

Huang, H., Young, N., Williams, B.P., Taylor, S.H., Hutchings, G., 2005. COS hydrolysis using zinc-promoted alumina catalysts. Catal. Letters 104, 17–21. https://doi.org/10.1007/s10562-005-7430-5

Huttenhuis, P.J.., Mohan, A., van Loo, S., Versteeg, G.F., 2006. Absorption of Carbonyl Sulphide in Aqueous Piperazine. IchemE Symp. Ser. 152, 581–589.

Inn, E.C.Y., Vedder, J.F., Tyson, B.J., 1979. COS in the stratosphere. Geophys. Res. Lett. 6, 191–193.

Islam, M.S., Yusoff, R., Ali, B.S., Islam, M.N., Chakrabarti, M.H., 2011. Degradation studies of amines and alkanolamines during sour gas treatment process. Int. J. Phys. Sci. 6, 5883–5896. https://doi.org/10.5897/IJPS11.237

Jin, H., An, Z., Li, Q., Duan, Y., Zhou, Z., Sun, Z., Duan, L., 2021. Catalysts of Ordered Mesoporous Alumina with a Large Pore Size for Low-Temperature Hydrolysis of Carbonyl Sulfide. Energy and Fuels 35, 8895–8908. https://doi.org/10.1021/acs.energyfuels.1c00475

Karan, K., Mehrotra, A.K., Behie, L.A., 1998. COS-forming reaction between CO and sulfur: A high-temperature intrinsic kinetics study. Ind. Eng. Chem. Res. 37, 4609–4616. https://doi.org/10.1021/ie9802966

Kato, Y., Nakamura, K., 2017. Gas purification apparatus and Gas purification method. US 9845438B2.

Kohl, A., Nielsen, R., 1997a. Sulfur Recovery Processes, in: Gas Purification 5th Edition. Gulf Publishing Company, Houston, Texas, p. 670.

Kohl, A., Nielsen, R., 1997b. Alkanolamines for Hydrogen Sulfide and Carbon Dioxide Removal, in: Gas Purification 5th Edition. Gulf

Publishing Company, Houston, Texas, p. 40.
Lee, S.C., Snodgrass, M.J., Park, M.K., Sandall, O.C., 2001. Kinetics of removal of carbonyl sulfide by aqueous monoethanolamine. Environ. Sci. Technol. 35, 2352–2357. https://doi.org/10.1021/es0017312
Levenspiel, O., 2001. Chemical Reaction Engineering, Third ed. ed. Wiley.
Li, K., Song, X., Wang, C., Mei, Y., Sun, X., Ning, P., 2017. Deactivation mechanism of the simultaneous removal of carbonyl sulphide and carbon disulphide over Fe–Cu–Ni/MCSAC catalysts. J. Chem. Sci. 129, 1893–1903. https://doi.org/10.1007/s12039-017-1397-9
Li, W., Shudong, W., Quan, Y., 2010. Removal of carbonyl sulfide at low temperature: Experiment and modeling. Fuel Process. Technol. 91, 777–782. https://doi.org/10.1016/j.fuproc.2010.02.013
Li, X.H., Ren, S.J., Wei, X.G., Zeng, Y., Gao, G.W., Ren, Y., Zhu, J., Lau, K.C., Li, W.K., 2014. Concerted or stepwise mechanism? New insight into the water-mediated neutral hydrolysis of carbonyl sulfide. J. Phys. Chem. A 118, 3503–3513. https://doi.org/10.1021/jp5021559
Littel, R. J., Versteeg, G.F., van Swaaij, W.P.M., 1992. Kinetics of COS with primary and secondary amines in aqueous solutions. AIChE J. 38, 244–250. https://doi.org/10.1002/aic.690380210
Littel, Rob J., Versteeg, G.F., van Swaaij, W.P.M., 1992a. Kinetic Study of COS with Tertiary Alkanolamine Solutions. 1. Experiments in an Intensely Stirred Batch Reactor. Ind. Eng. Chem. Res. 31, 1262–1269. https://doi.org/10.1021/ie00005a004
Littel, Rob J., Versteeg, G.F., van Swaaij, W.P.M., 1992b. Kinetic Study of COS with Tertiary Alkanolamine Solutions. 2. Modeling and Experiments in a Stirred Cell Reactor. Ind. Eng. Chem. Res. 31, 1269–1274. https://doi.org/10.1021/ie00005a005
Magné-Drisch, J., Gazarian, J., Gonnard, S., Schweitzer, J.M., Chiche, D., Laborie, G., Perdu, G., 2016. COSWEET^{TM}: A New Process to Reach Very High COS Specification on Natural Gas Treatment Combined with Selective H2S Removal. Oil Gas Sci. Technol. 71. https://doi.org/10.2516/ogst/2015038
Martijn, V.H.R., Herold, R.H.M., Kodde, A.J., Last, T., Smit, C.J., 2010. Process for the removal of cos and H2S from a synthesis gas stream Comprising H2S and COS. US 7846325B2.
Mi, J., Chen, X., Zhang, Q., Zheng, Y., Xiao, Y., Liu, F., Au, C.T., Jiang, L., 2019. Mechanochemically synthesized MgAl layered double hydroxide nanosheets for efficient catalytic removal of carbonyl sulfide and H2S. Chem. Commun. 55, 9375–9378. https://doi.org/10.1039/c9cc03637g
Mikhonin, A. V., Dando, N.R., Gershenzon, M., 2013. Hydrolysis of Carbonyl Sulfide (COS) on smelting grade alumina, in: Sadler, B. (Ed.), Light Metals. Jon Wiley & Sons, Inc., San Antonio, Texas, USA, pp. 905–908.
Miura, K., Mae, K., Inoue, T., Yoshimi, T., Nakagawa, H., Hashimoto, K.,

1992. Simultaneous Removal of COS and H2S from Coke Oven Gas at Low Temperature by Use of an Iron Oxide. Ind. Eng. Chem. Res. 31, 415–419. https://doi.org/10.1021/ie00001a056

Montebelli, A., Visconti, C.G., Groppi, G., Tronconi, E., Kohler, S., Venvik, H.J., Myrstad, R., 2014. Washcoating and chemical testing of a commercial Cu/ZnO/Al2O3 catalyst for the methanol synthesis over copper open-cell foams. Appl. Catal. A Gen. 481, 96–103. https://doi.org/10.1016/j.apcata.2014.05.005

Nimthuphariyha, K., Usmani, A., Grisdanurak, N., Kanchanatip, E., Yan, M., Suthirakun, S., Tulaphol, S., 2019. Hydrolysis of carbonyl sulfide over modified Al2O3 by platinum and barium in a packed-bed reactor. Chem. Eng. Commun. 208, 1–10. https://doi.org/10.1080/00986445.2019.1705794

Nochi, K., Yasutake, T., Yoshida, K., 2020. Catalyst for use in hydrolysis of carbonyl sulfide, and method of producing same. US 2020/0398256A1.

Ojala, S., Pitkäaho, S., Laitinen, T., Niskala Koivikko, N., Brahmi, R., Gaálová, J., Matejova, L., Kucherov, A., Päivärinta, S., Hirschmann, C., Nevanperä, T., Riihimäki, M., Pirilä, M., Keiski, R.L., 2011. Catalysis in VOC abatement. Top. Catal. 54, 1224–1256. https://doi.org/10.1007/s11244-011-9747-1

Palma, V., Meloni, E., Renda, S., Martino, M., 2020. Catalysts for Methane Steam Reforming Reaction: Evaluation of CeO2 Addition to Alumina-Based Washcoat Slurry Formulation. C — J. Carbon Res. 6, 52. https://doi.org/10.3390/c6030052

Palma, V., Pisano, D., Martino, M., 2018. Comparative study between aluminum monolith and foam as carriers for the intensification of the CO water gas shift process. Catalysts 8. https://doi.org/10.3390/catal8110489

Palma, V., Pisano, D., Martino, M., Ciambelli, P., 2016. Structured catalysts with high thermoconductive properties for the intensification of Water Gas Shift process. Chem. Eng. J. 304, 544–551. https://doi.org/10.1016/j.cej.2016.06.117

Palma, V., Vaiano, V., Barba, D., Colozzi, M., Palo, E., Barbato, L., Cortese, S., Miccio, M., 2019. Study of the carbonyl sulphide hydrolysis reaction in liquid phase. Chem. Eng. Trans. 73, 247–252. https://doi.org/10.3303/CET1973042

Partington, J.R., Neville, H.H., 1951. The thermal decomposition of carbonyl sulphide 1230–1237.

Qiu, J., Li, X., Qi, X., 2019. Raman Spectroscopic Investigation of Sulfates Using Mosaic Grating Spatial Heterodyne Raman Spectrometer. IEEE Photonics J. 11, 1. https://doi.org/10.1109/JPHOT.2019.2939222

Radford-Knęry, J., Cutter, G.A., 1994. Biogeochemistry of dissolved hydrogen sulfide species and carbonyl sulfide in the western North Atlantic Ocean. Geochim. Cosmochim. Acta 58, 5421–5431.

https://doi.org/10.1016/0016-7037(94)90239-9
Remazeilles, C., Tran, K., Guilminot, E., Conforto, E., Refait, P., 2011. Study of Iron(Ii) Sulphides By Environmental Scanning Electron Microscopy (Esem) and Micro-Raman Spectroscopy in Waterlogged Archaeological Woods. Researchgate.Net 2. https://doi.org/10.13140/2.1.3740.1282
Renda, S., Di Stasi, C., Manyà, J.J., Palma, V., 2021. Biochar as support in catalytic CO2 methanation : Enhancing effect of CeO2 addition. J. CO2 Util. 53, 101740. https://doi.org/10.1016/j.jcou.2021.101740
Rhodes, C., Riddel, S.A., West, J., Williams, B.P., Hutchings, G.J., 2000. Low-temperature hydrolysis of carbonyl sulfide and carbon disulfide: a review. Catal. Today 59, 443–464. https://doi.org/10.1016/S0920-5861(00)00309-6
Rivera-Tinoco, R., Bouallou, C., 2008. Reaction kinetics of carbonyl sulfide (COS) with diethanolamine in methanolic solutions. Ind. Eng. Chem. Res. 47, 7375–7380. https://doi.org/10.1021/ie8002649
Rivera-Tinoco, R., Bouallou, C., 2007. Kinetic study of carbonyl sulfide (COS) absorption by methyldiethanolamine aqueous solutions from 415 mol/m3 to 4250 mol/m3 and 313 K to 353 K. Ind. Eng. Chem. Res. 46, 6430–6434. https://doi.org/10.1021/ie070516s
Roddaeng, S., Promvonge, P., Anuwattana, R., 2018. Behaviors of hydrogen sulfide removal using granular activated carbon and modified granular activated carbon. MATEC web Conf. 192, 1–4.
Sandalls, F.J., Penkett, S.A., 1977. Measurements of carbonyl sulphide and carbon disulphide in the atmosphere. Atmos. Environ. 11, 197–199. https://doi.org/10.1016/0004-6981(77)90227-x
Sander, R., 2015. Compilation of Henry's law constants (version 4.0) for water as solvent. Atmos. Chem. Phys. 15, 4399–4981. https://doi.org/10.5194/acp-15-4399-2015
Sato, F., Ogino, S., Aihara, M., Kato, Y., Ishida, K., Kakesako, S., 2016. System for recovering high-purity CO2, from gasification gas containing CO, CO2, COS and H2S. US 9278312B2.
Shangguan, J., Liu, Y., Wang, Z., Xu, Y., 2019. The Synthesis of Magnesium-aluminium Spinel for Catalytic Hydrolysis of Carbonyl Sulphur at the Middle Temperature. IOP Conf. Ser. Mater. Sci. Eng. 585, 1–8. https://doi.org/10.1088/1757-899X/585/1/012039
Sharma, M.M., 1965. Kinetics of reactions of carbonyl sulphide and carbon dioxide with amines and catalysis by Brönsted bases of the hydrolysis of COS. Trans. Faraday Soc. 61, 681–688. https://doi.org/10.1039/TF9656100681
Song, X., Chen, X., Sun, L., Li, K., Sun, X., Wang, C., Ning, P., 2020. Synergistic effect of Fe2O3 and CuO on simultaneous catalytic hydrolysis of COS and CS2: Experimental and theoretical studies. Chem. Eng. J. 399, 125764. https://doi.org/10.1016/j.cej.2020.125764
Song, X., Ning, P., Wang, C., Li, K., Tang, L., Sun, X., Ruan, H., 2017.

Research on the low temperature catalytic hydrolysis of COS and CS2 over walnut shell biochar modified by Fe–Cu mixed metal oxides and basic functional groups. Chem. Eng. J. 314, 418–433. https://doi.org/10.1016/j.cej.2016.11.162

Speight, J.G., 2018. Gas cleaning processes, in: Natural Gas: A Basic Handbook. Gulf Publishing Company, Wyoming, USA, pp. 277–324. https://doi.org/10.1017/CBO9781107415324.004

Sui, R., Lavery, C.B., Deering, C.E., Prinsloo, R., Li, D., Chou, N., Lesage, K.L., Marriott, R.A., 2020. Improved carbon disulfide conversion: Modification of an alumina Claus catalyst by deposition of transition metal oxides. Appl. Catal. A Gen. 604. https://doi.org/10.1016/j.apcata.2020.117773

Sun, X., Ning, P., Tang, X., Yi, H., Li, K., He, D., Xu, X., Huang, B., Lai, R., 2014. Simultaneous catalytic hydrolysis of carbonyl sulfide and carbon disulfide over Al2O3-K/CAC catalyst at low temperature. J. Energy Chem. 23, 221–226. https://doi.org/10.1016/S2095-4956(14)60139-X

Svoronost, P.D.N., Bruno, T.J., 2002. Carbonyl sulfide: A review of its chemistry and properties. Ind. Eng. Chem. Res. 41, 5321–5336. https://doi.org/10.1021/ie020365n

Swenson, H., Stadie, N.P., 2019. Langmuir's Theory of Adsorption: A Centennial Review. Langmuir 35, 5409–5426. https://doi.org/10.1021/acs.langmuir.9b00154

Taniguchi, K., Hirano, S., Uddin, M.A., Kasaoka, S., Sakata, Y., 1995. Catalytic Activity of ZnS Formed from Desulfurization Sorbent ZnO for Conversion of COS to H2S. Ind. Eng. Chem. Res. 34, 1102–1106. https://doi.org/10.1021/ie00043a011

Thomas, B., Williams, B.P., Young, N., Rhodes, C., Hutchings, G.J., 2003. Ambient temperature hydrolysis of carbonyl sulfide using γ-alumina catalysts: Effect of calcination temperature and alkali doping. Catal. Letters 86, 201–205. https://doi.org/10.1023/A:1022611901253

Thompson, K.A., Shimabuku, K.K., Kearns, J.P., Knappe, D.R.U., Summers, R.S., Cook, S.M., 2016. Environmental Comparison of Biochar and Activated Carbon for Tertiary Wastewater Treatment. Environ. Sci. Technol. 50, 11253–11262. https://doi.org/10.1021/acs.est.6b03239

Tong, S., Dalla Lana, I.G., Chuang, K.T., 1993. Kinetic modeling of the hydrolysis of carbon disulfide catalyzed by either titania or alumina. Can. J. Chem. Eng. 71, 392–400. https://doi.org/10.1002/cjce.5450730208

Tong, S., Dalla Lana, I.G., Chuang, K.T., 1992. Appraisal of catalysts for the hydrolysis of carbon disulfide. Can. J. Chem. Eng. 70, 516–522. https://doi.org/10.1002/cjce.5450700315

Trucko, J.E., Forest, L., Tertel, J.A., Laricchia, L., Rios, J., 2016. Process for removing carbonyl sulfide froma hydrocarbon stream. US 9394490B2.

Vaidya, P.D., Kenig, E.Y., 2009. Kinetics of carbonyl sulfide reaction with

alkanolamines: A review. Chem. Eng. J. 148, 207–211. https://doi.org/10.1016/j.cej.2008.08.009
Visconti, C.G., 2012. Alumina: A key-component of structured catalysts for process intensification. Trans. Indian Ceram. Soc. 71, 123–136. https://doi.org/10.1080/0371750X.2012.738481
Wang, H., Yi, H., Ning, P., Tang, X., Yu, L., He, D., Zhao, S., 2011. Calcined hydrotalcite-like compounds as catalysts for hydrolysis carbonyl sulfide at low temperature. Chem. Eng. J. 166, 99–104. https://doi.org/10.1016/j.cej.2010.10.025
Wang, H., Yi, H., Tang, X., Ning, P., Yu, L., He, D., Zhao, S., Li, K., 2012. Catalytic hydrolysis of COS over calcined CoNiAl hydrotalcite-like compounds modified by cerium. Appl. Clay Sci. 70, 8–13. https://doi.org/10.1016/j.clay.2012.09.008
Wang, L., Wang, S., Yuan, Q., Lu, G., 2008. COS hydrolysis in the presence of oxygen: Experiment and modeling. J. Nat. Gas Chem. 17, 93–97. https://doi.org/10.1016/S1003-9953(08)60032-8
Wang, Y., Jian Hua Zhu, Wen Yu Huang, 2001. Synthesis and characterization of potassium-modified alumina superbases. Phys. Chem. Chem. Phys. 3, 2537–2543. https://doi.org/10.1039/b100084p
Weatherbee, G.D., Bartholomew, C.H., 1982. Hydrogenation of CO2 on group VIII metals II. Kinetics and mechanism of CO2 hydrogenation on nickel. J. Catal. 77, 460–472. https://doi.org/10.1016/0021-9517(82)90186-5
Wei, Z., Zhang, X., Zhang, F., Xie, Q., Zhao, S., Hao, Z., 2021a. Boosting carbonyl sulfide catalytic hydrolysis performance over N-doped Mg-Al oxide derived from MgAl-layered double hydroxide. J. Hazard. Mater. 407, 124546. https://doi.org/10.1016/j.jhazmat.2020.124546
Wei, Z., Zhang, X., Zhang, F., Xie, Q., Zhao, S., Hao, Z., 2021b. Boosting carbonyl sulfide catalytic hydrolysis performance over N-doped Mg-Al oxide derived from MgAl-layered double hydroxide. J. Hazard. Mater. 407, 124546. https://doi.org/10.1016/j.jhazmat.2020.124546
West, J., Williams, B.P., Young, N., Rhodes, C., Hutchings, G.J., 2001. Ni- and Zn-promotion of γ-Al2O3 for the hydrolysis of COS under mild conditions. Catal. Commun. 2, 135–138. https://doi.org/10.1016/S1566-7367(01)00021-8
Williams, B.P., Young, N.C., West, J., Rhodes, C., Hutchings, G.J., 1999. Carbonyl sulphide hydrolysis using alumina catalysts. Catal. Today 49, 99–104. https://doi.org/10.1016/s0920-5861(98)00413-1
Xu, Y., Ju, S., Wang, Z., Liu, Y., 2018. The Study of the Preparation of Catalysts for Carbonyl Sulfide Hydrolysis under Moderate Temperature. J. Mater. Sci. Chem. Eng. 6, 31–38. https://doi.org/10.4236/msce.2018.64005
Yan, R., Liang, D.T., Tsen, L., Tay, J.H., 2002. Kinetics and mechanisms of H2S adsorption by alkaline activated carbon. Environ. Sci. Technol. 36,

4460–4466. https://doi.org/10.1021/es0205840
Yang, Y., Shi, Y., Cai, N., 2016. Simultaneous removal of COS and H2S from hot syngas by rare earth metal-doped SnO2 sobents. Fuel 181, 1020–1026. https://doi.org/https://doi.org/10.1016/j.fuel.2016.05.007
Yi, H., Li, K., Tang, X., Ning, P., Peng, J., Wang, C., He, D., 2013. Simultaneous catalytic hydrolysis of low concentration of carbonyl sulfide and carbon disulfide by impregnated microwave activated carbon at low temperatures. Chem. Eng. J. 230, 220–226. https://doi.org/10.1016/j.cej.2013.06.082
Yonemura, M., Sawata, A., Tanaka, Y., Yoshioka, H., Yasutake, T., 2017. Method for regenerating cos hydrolysis catalyst. US 9604206B2.
Zhang, Y., Xiao, Z., Ma, J., 2004. Hydrolysis of carbonyl sulfide over rare earth oxysulfides. Appl. Catal. B Environ. 48, 57–63. https://doi.org/10.1016/j.apcatb.2003.09.015
Zhao, S., Kang, D., Liu, Y., Wen, Y., Xie, X., Yi, H., Tang, X., 2020a. Spontaneous Formation of Asymmetric Oxygen Vacancies in Transition-Metal-Doped CeO2 Nanorods with Improved Activity for Carbonyl Sulfide Hydrolysis. ACS Catal. 10, 11739–11750. https://doi.org/10.1021/acscatal.0c02832
Zhao, S., Kang, D., Liu, Y., Wen, Y., Xie, X., Yi, H., Tang, X., 2020b. Spontaneous Formation of Asymmetric Oxygen Vacancies in Transition-Metal-Doped CeO2Nanorods with Improved Activity for Carbonyl Sulfide Hydrolysis. ACS Catal. 10, 11739–11750. https://doi.org/10.1021/acscatal.0c02832
Zhao, S., Tang, X., He, M., Yi, H., Gao, F., Wang, J., Huang, Y., Yang, Z., 2018. The potential mechanism of potassium promoting effect in the removal of COS over K/NiAlO mixed oxides. Sep. Purif. Technol. 194, 33–39. https://doi.org/10.1016/j.seppur.2017.10.032
Zhao, S., Yi, H., Tang, X., Gao, F., Yu, Q., Wang, J., Huang, Y., Yang, Z., 2019a. The regulatory effect of Al atomic-scale doping in NiAlO for COS removal. Catal. Today. https://doi.org/10.1016/j.cattod.2019.07.035
Zhao, S., Yi, H., Tang, X., Gao, F., Yu, Q., Zhou, Y., Wang, J., Huang, Y., Yang, Z., 2016. Enhancement effects of ultrasound assisted in the synthesis of NiAl hydrotalcite for carbonyl sulfide removal. Ultrason. Sonochem. 32, 336–342. https://doi.org/10.1016/j.ultsonch.2016.04.001
Zhao, S., Yi, H., Tang, X., Jiang, S., Gao, F., Zhang, B., Zuo, Y., Wang, Z., 2013. The hydrolysis of carbonyl sulfide at low temperature: A review. Sci. World J. https://doi.org/10.1155/2013/739501
Zhao, S., Yi, H., Tang, X., Kang, D., Gao, F., Wang, J., Huang, Y., Yang, Z., 2019b. Calcined ZnNiAl hydrotalcite-like compounds as bifunctional catalysts for carbonyl sulfide removal. Catal. Today 327, 161–167. https://doi.org/10.1016/j.cattod.2018.05.011
Zhao, S., Yi, H., Tang, X., Kang, D., Wang, H., Li, K., Duan, K., 2012.

Characterization of Zn-Ni-Fe hydrotalcite-derived oxides and their application in the hydrolysis of carbonyl sulfide. Appl. Clay Sci. 56, 84–89. https://doi.org/10.1016/j.clay.2011.11.026

Zhao, S., Yi, H., Tang, X., Ning, P., Wang, H., He, D., 2010. Effect of Ce-doping on catalysts derived from hydrotalcite-like precursors for COS hydrolysis. J. Rare Earths 28, 329–333. https://doi.org/10.1016/S1002-0721(10)60341-9

List of symbols

List of acronyms used in the text, in alphabetical order.

cMDEA	Customized MDEA solution
DEA	Diethanol ammine
GHSV	Gas Hourly Space Velocity
HTH	High-temperature hydrolysis
K_G	Mass transfer coefficient – gas side
LTH	Low-temperature hydrolysis
MDEA	Methyl-diethanol ammine
PM	Particulate matter
SEM-EDS	Scanning Electron Microscope with Energy Dispersive Spectrometer
SEM-EDX	Scanning Electron Microscopy with Energy Dispersive X-ray Spectroscopy analysis
SRU	Sulfur recovery unit
SSA	Specific Surface Area
TGA	Thermo-Gravimetric Analysis
TGT	Tail gas treatment
VOCs	Volatile organic compounds
wGHSV	Weight-basis Gas Hourly Space Velocity
XRD	X-Ray Diffraction

Appendix

Table A-I: Resume of the catalysts reported in this work

Label	Sample details	Discussed in:
Promoted	Promoted alumina Claus catalyst (commercial, pellets)	Chapter VI
Al3	γ-Al_2O_3 (commercial, spheres, 3 mm)	Chapter VI
K/Al3	K_2CO_3/γ-Al_2O_3 (laboratory, spheres, 3 mm)	Chapter VI
Al5	γ-Al_2O_3 (commercial, spheres, 5 mm)	Chapter VI
K/Al5	K_2CO_3/γ-Al_2O_3 (laboratory, spheres, 5 mm)	Chapter VI
NiFe_WC450	γ-Al_2O_3(wc)/NiFe foam (structured catalyst, laboratory) Carrier: NiFe foam Washcoat: calcined @450 °C	Chapter VIII
NiFe_KWC	K_2CO_3/γ-Al_2O_3(wc)/NiFe foam (structured catalyst, laboratory) Carrier: NiFe foam Washcoat: calcined @450 °C Active phase: K_2CO_3	Chapter VIII

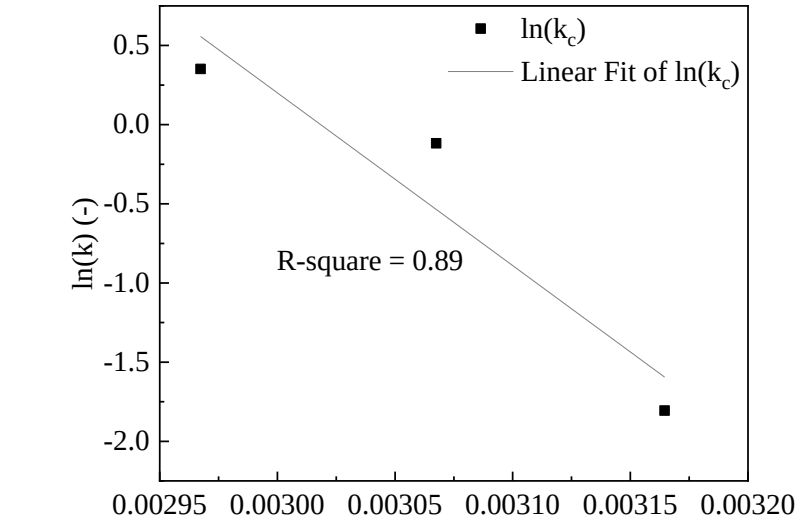

(a)

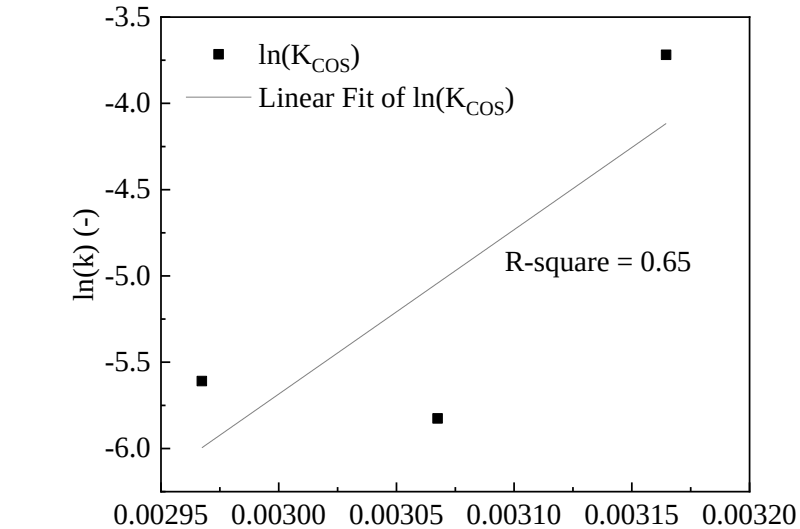

(b)

Fig. A-1: Determination of the values reported in Table IX-2: (a) kinetic parameters; (b) COS adsorption parameters.